Elsevier Editorial System(tm) for Lithos
Manuscript Draft

Manuscript Number: LITHOS6474R3

Title: Refertilized mantle keel below the Southern Alps domain (North-East Italy): Evidence from Marosticano refractory mantle peridotites

Article Type: Regular Article

Keywords: Veneto Volcanic Province, cratonic mantle xenoliths, carbonatite metasomatism, rejuvenation.

Corresponding Author: Miss Valentina Brombin,

Corresponding Author's Institution: University of Ferrara

First Author: Valentina Brombin

Order of Authors: Valentina Brombin; Costanza Bonadiman; Massimo Coltorti; Maria Florencia Fahnestock; Julia Bryce; Andrea Marzoli

Abstract: The Veneto Volcanic Province (VVP), a Cenozoic magmatic province in northeastern Italy, is one of the widest volcanic areas of the Adria plate. It consists of five main volcanic districts, and its most primitive products common host mantle xenoliths. In this study, we present a newly discovered xenolith suite from the Marosticano district that contains peridotites with compositional characteristics of mineral assemblages that provide insight into an unexpected nature for the sub-continental lithospheric mantle (SCLM) of the Adria plate. In contrast to xenoliths from other VVP sites previously studied (i.e.: Val d'Adige and Lessini Mts.), Marosticano xenoliths exhibit highly refractory compositions typical of on-craton peridotites. In particular, high olivine forsteritic contents (Fo: 91-93) indicate high degrees of partial melting (>25%) that should lead to the complete consumption of clinopyroxene. Major and trace element compositions further link these peridotite fragments to early Proterozoic cratonic mantle, and the juxtaposition of clinopyroxene within these rocks suggests like most on-craton clinopyroxene, Marosticano clinopyroxene have a metasomatic legacy. The i) LREE-enrichments of Marosticano clinopyroxene and ii) the dissolved CO_2 mole fractions (up to 1.0) for the inferred clinopyroxene-forming melt are consistent with carbonatite/CO_2-rich silicatic melts as metasomatic agents. The latter could be responsible for the equilibrium temperatures (1033-1117 °C) and oxidizing conditions ($\Delta \log fO_2$ (FMQ)=-0.6 - +1.1), anomalously high for a cratonic environment but similar to the off-craton VVP xenoliths.
The cratonic signature and carbonatite/CO_2-rich silicate metasomatism found together in the Marosticano mantle xenoliths reveal that ancient features can be preserved in SCLM in a young, active geodynamic setting as the Adria plate boundary. In this framework Lessini Mts. and Val d'Adige xenoliths could be interpreted as the typical features of circumcratonic reminiscent domains affected by refertilization due to infiltration of asthenosphere-derived melts, rather than newly accreted "off-craton" SCLM. These new interpretations could be useful for completing the reconstruction of the Africa/Eurasia interplay during the Alpine collision.

Dear Editor,

Please find enclosed our manuscript (LITHOS6474R2- favourably received and recommended for publication with minor revision): "**Refertilized mantle keel below the Southern Alps domain (North-East Italy): Evidence from Marosticano refractory mantle peridotites**" by Valentina Brombin, Costanza Bonadiman, Massimo Coltorti, M. Florencia Fahnestock, Julia G. Bryce and Andrea Marzoli, revised with additional English corrections.

The final version of this text was reviewed and corrected by an English-native and an English-fluent co-author. We hope that you will find this version now suitable for publication in *Lithos*.

Regards,

for the authors,

Valentina Brombin

*Abstract
Click here to download Abstract: Brombin et al.-REVISION 3- Abstract.docx

Refertilized mantle keel below the Southern Alps domain (North-East Italy): Evidence from Marosticano refractory mantle peridotites

Valentina Brombin[a]*, Costanza Bonadiman[a], Massimo Coltorti[a], M. Florencia Fahnestock[b], Julia G. Bryce[b], Andrea Marzoli[c]

[a] *Dipartimento di Fisica e di Scienze della Terra, Università di Ferrara, Italy; brmvnt@unife.it*

[b] *Department of Earth Science, University of New Hampshire, USA; julie.bryce@unh.edu; florencia.fahnestock@unh.edu*

[c] *Dipartimento di Geoscienze e IGG-CNR, Università di Padova, Italy; andrea.marzoli@unipd.it*

ABSTRACT

The Veneto Volcanic Province (VVP), a Cenozoic magmatic province in northeastern Italy, is one of the widest volcanic areas of the Adria plate. It consists of five main volcanic districts, and its most primitive products common host mantle xenoliths. In this study, we present a newly discovered xenolith suite from the Marosticano district that contains peridotites with compositional characteristics of mineral assemblages that provide insight into an unexpected nature for the sub-continental lithospheric mantle (SCLM) of the Adria plate. In contrast to xenoliths from other VVP sites previously studied (i.e.: Val d'Adige and Lessini Mts.), Marosticano xenoliths exhibit highly refractory compositions typical of on-craton peridotites. In particular, high olivine forsteritic contents (Fo: 91-93) indicate high degrees of partial melting (>25%) that should lead to the complete consumption of clinopyroxene. Major and trace element compositions further link these peridotite fragments to early Proterozoic cratonic mantle, and the juxtaposition of clinopyroxene within these rocks suggests like ~~most on-craton clinopyroxene,~~ Marosticano clinopyroxene have a metasomatic legacy. The i) LREE-enrichments of Marosticano clinopyroxene and ii) the dissolved CO_2 mole fractions (up to 1.0) for the inferred clinopyroxene-forming melt are consistent with

carbonatite/CO_2-rich silicatic melts as metasomatic agents. The latter could be responsible for the equilibrium temperatures (1033-1117 °C) and oxidizing conditions ($\Delta\log fO_2$ (FMQ)=-0.6 - +1.1), anomalously high for a cratonic environment but similar to the off-craton VVP xenoliths.

The cratonic signature and carbonatite/CO_2-rich silicate metasomatism found together in the Marosticano mantle xenoliths reveal that ancient features can be preserved in SCLM in a young, active geodynamic setting as the Adria plate boundary. In this framework Lessini Mts. and Val d'Adige xenoliths could be interpreted as the typical features of circumcratonic reminiscent domains affected by refertilization due to infiltration of asthenosphere-derived melts, rather than newly accreted "off-craton" SCLM. These new interpretations could be useful for completing the reconstruction of the Africa/Eurasia interplay during the Alpine collision.

HIGHLIGHTS

Petrology and geochemistry of newly discovered Adria plate mantle xenoliths present unexpected cratonic features.

Xenolith clinopyroxene record metasomatic overprinting of restitic peridotite from carbonatite/CO_2-rich silicate melts.

Cratonic keel is preserved only in the Marosticano district, while the rest of VVP mantle domains are interpreted as circumcratonic portions subject to rejuvenation from asthenospheric-derived melts.

Refertilized mantle keel below the Southern Alps domain (North-East Italy): Evidence from Marosticano refractory mantle peridotites

Valentina Brombin[a]*, Costanza Bonadiman[a], Massimo Coltorti[a], M. Florencia Fahnestock[b], Julia G. Bryce[b], Andrea Marzoli[c]

[a] *Dipartimento di Fisica e di Scienze della Terra, Università di Ferrara, Italy;* brmvnt@unife.it

[b] *Department of Earth Science, University of New Hampshire, USA;* julie.bryce@unh.edu; *florencia.fahnestock@unh.edu*

[c] *Dipartimento di Geoscienze e IGG-CNR, Università di Padova, Italy;* andrea.marzoli@unipd.it

ABSTRACT

The Veneto Volcanic Province (VVP), a Cenozoic magmatic province in northeastern Italy, is one of the widest volcanic areas of the Adria plate. It consists of five main volcanic districts, and its most primitive products common host mantle xenoliths. In this study, we present a newly discovered xenolith suite from the Marosticano district that contains peridotites with compositional characteristics of mineral assemblages that provide insight into an unexpected nature for the sub-continental lithospheric mantle (SCLM) of the Adria plate. In contrast to xenoliths from other VVP sites previously studied (i.e.: Val d'Adige and Lessini Mts.), Marosticano xenoliths exhibit highly refractory compositions typical of on-craton peridotites. In particular, high olivine forsteritic contents (Fo: 91-93) indicate high degrees of partial melting (>25%) that should lead to the complete consumption of clinopyroxene. Major and trace element compositions further link these peridotite fragments to early Proterozoic cratonic mantle, and the juxtaposition of clinopyroxene within these rocks suggests like most on-craton clinopyroxene, Marosticano clinopyroxene have a metasomatic legacy. The i) LREE-enrichments of Marosticano clinopyroxene and ii) the dissolved CO_2 mole fractions (up to 1.0) for the inferred clinopyroxene-forming melt are consistent with carbonatite/CO_2-rich silicatic melts as metasomatic agents. The latter could be responsible for the equilibrium temperatures (1033-1117 °C) and oxidizing conditions ($\Delta \log fO_2$ (FMQ)=-0.6 - +1.1), anomalously high for a cratonic environment but similar to the off-craton VVP xenoliths.

The cratonic signature and carbonatite/CO_2-rich silicate metasomatism found together in the Marosticano mantle xenoliths reveal that ancient features can be preserved in SCLM in a young, active geodynamic setting as the Adria plate boundary. In this framework Lessini Mts. and Val d'Adige xenoliths could be interpreted as the typical features of circumcratonic reminiscent domains affected by refertilization due to infiltration of asthenosphere-derived melts, rather than newly accreted "off-craton" SCLM. These new interpretations could be useful for completing the reconstruction of the Africa/Eurasia interplay during the Alpine collision.

HIGHLIGHTS

Petrology and geochemistry of newly discovered Adria plate mantle xenoliths present unexpected cratonic features.

Xenolith clinopyroxene record metasomatic overprinting of restitic peridotite from carbonatite/CO_2-rich silicate melts.

Cratonic keel is preserved only in the Marosticano district, while the rest of VVP mantle domains are interpreted as circumcratonic portions subject to rejuvenation from asthenospheric-derived melts.

KEYWORDS

Veneto Volcanic Province, cratonic mantle xenoliths, carbonatite metasomatism, rejuvenation.

1. Introduction

The stability of continents is intimately linked to the underlying sub-continental lithospheric mantle (SCLM). Peridotite xenoliths hosted in intraplate basaltic rocks provide a useful way to evaluate the petrological features and evolution of the SCLM in terms of mineral compositions, modal abundance and to fluid modification (Liu et al., 2015).

The mantle xenoliths occurring in Veneto Volcanic Province (VVP; SE Alps, NE Italy, Fig. 1) depict the "big" picture of the SCLM beneath the Adria plate, the African promontory of the central-western Mediterranean area. In the Cretaceous the VVP region was involved in a convergence between Africa and Eurasia plates, inducing subduction processes of the latter southeastward (Schmid et al., 1997; von Blanckenburg and Davies, 1995). In spite of the immense quantity of seismic, structural, petrologic, and geochemical data compiled over at least five decades, the Adria microplate (Fig. 1, inset) remains an enigmatic aspect in the geodynamic evolution of the Africa-Eurasia collision system (Carminati and Doglioni, 2012; Lustrino, et al., 2011). It has been considered either to be in crustal continuity with the African mainland or separated from the latter by an oceanic plate (Catalano et al., 2000; Lustrino et al., 2011; Muttoni et al., 2001; Schmid et al., 2008).

Mantle xenoliths from a few VVP localities previously investigated (Lessini Mts. and Val d'Adige localities; Fig. 1) reveal variably depleted mantle domains, which were subsequently enriched by one or more episodes of metasomatism as recorded by widespread interstitial recrystallized glassy patches (Beccaluva et al., 2001; Gasperini et al., 2006; Morten et al., 1989; Siena and Coltorti, 1989). In this paper, we describe results from a petrological and geochemical study of a newly discovered occurrence of mantle xenoliths from the Marostica Hills, in the Marosticano district of the VVP. We then interpret our findings to constrain the mantle domain underlying the northern (continental) sector of the Adria plate, with the ultimate goal of shedding insight dynamic processes at work during plate boundary interaction (Carminati and Doglioni, 2012).

2. Geological setting

The Central-Western Mediterranean area is a geologically young area, mostly developed during the last 30 Ma. Geological structures and the igneous activity within this region are intimately linked with the relative movements of two large plates (Africa and Europe) plus a number of smaller continental and oceanic plates (e.g., Lustrino et al., 2011). A key smaller plate, likely an African promontory, is the Adria (or Apulia) plate in which the VVP (Fig. 1) constitutes one of the largest and most important magmatic provinces. During the Cenozoic, the Veneto and Trentino regions were affected by extensive volcanic activity, mainly basic-ultrabasic in composition that took place intermittently from the late Paleocene to the late Oligocene (Barbieri et al., 1982, 1991; De Vecchi et al., 1976; De Vecchi and Sedea, 1995; Piccoli, 1966). Most of the VVP products are spread over a NNW to SSE elongated area of about 1,500 km^2. Five main volcanic districts can be defined from west to east (Fig. 1): (1) the Val d'Adige district, between Arco and Rovereto; (2) the Lessini Mts. district between Val d'Adige and the Schio-Vicenza tectonic line; (3) the Marosticano district, east of the Schio-Vicenza line; (4) the Berici Hills district, which is separated from (5) the Euganean Hills, the southernmost district, by the Riviera dei Berici line (Beccaluva et al., 2007). Most VVP volcanic products are relatively undifferentiated lavas, and range in composition from nephelinites to quartz (Qz)-normative tholeiitic basalts. They tend to be spatially and temporally distributed, becoming gradually younger and less alkaline toward SE. Differentiated products only occur in the Euganean district, where quartz-trachytes and rhyolites predominate (Milani et al., 1999, and references therein). Nephelinites and basanites commonly carry spinel-peridotite mantle xenoliths (Beccaluva et al., 2001; 2007).

The mafic volcanism in the VVP is thought to be related to extensional tectonics in the Southern Alps foreland as response to Alpine orogenesis (De Vecchi and Sedea, 1995; Milani et al., 1999; Zampieri, 1995). Geophysical data (Ansorge et al., 1992; Giese and Buness, 1992) indicate a rather normal thickness of the continental crust under the VVP, with a NW-SE elliptical mantle dome culminating at about 28 km beneath the Lessini Mts., while the lithosphere-asthenosphere boundary has been detected at ~~a~~ depth of ~100 km (Panza and Suhadolc, 1990).

Isotopic signatures, notably $^{206}Pb/^{204}Pb$ and $^{87}Sr/^{86}Sr$ ratios (18.8-19.8 and 0.703-0.704, respectively) led Beccaluva et al. (2001, 2007) to argue that the SCLM beneath the Adria plate has been enriched by metasomatizing agents, likely including FOZO or HIMU components. This signature may be related to the European Asthenospheric Reservoir (EAR; Hoernle et al., 1995), a large mantle upwelling extending from the eastern Atlantic to Europe and the Mediterranean area.

Alternatively, Wilson and Patterson (2001), and more recently Lustrino and Wilson (2007) argued that this Tertiary-Quaternary volcanism is related to diapiric upwelling of small-scale, finger-like~~,~~ convective instabilities from the base of the upper mantle.

3. Petrography

The Marosticano xenoliths were sampled in the quarry of Monte Gloso (MG), a few kilometers east of Marostica (Fig. 1). The basanitic host lavas show ~~a~~ porphyritic texture with phenocrysts of olivine, clinopyroxene, and magnetite set in a fine-grained groundmass composed of clinopyroxene, plagioclase, and oxides. The xenoliths are generally subrounded or (more rarely) angular, ranging in size from a few centimeters up to 10 cm. Heavy fracturing and alteration are present throughout of the suite. Only five samples were sufficiently fresh to permit a complete petrological characterization. These samples also showed no evidence of host magma infiltration.

The Marosticano xenoliths are peridotites with complete spinel-facies equilibration. They display a coarse-grained protogranular texture following the nomenclature of Mercier and Nicholas (1975). Two of the five investigated xenoliths are harzburgites with 4% clinopyroxene ~~(cpx)~~, one is low-~~cpx~~ (6%) lherzolite and two are lherzolites with 9-13% ~~cpx~~ (Table 1). In two out of three lherzolites, orthopyroxene ~~(opx)~~ is modally scarce (12-14%) as compared to typical peridotites (e.g., Streckeisen, 1974). All Marosticano peridotites are characterized by large crystals of olivine ~~(ol)~~

and ~~opx~~, (up to 2 mm across) with smaller grains of ~~cpx~~, (0.5-1 mm in size) and spinel ~~(sp)~~ (up to 1 mm across). These latter show ~~a~~ typical holly-leaf or lobate shape, while ~~ol~~ and pyroxene crystals display curvilinear grain boundaries. Kinking is common in ~~ol~~, while ~~opx~~ display exsolution lamellae and, rarely, show sieved rims. ~~Cpx~~ are always smaller in size with respect to ~~opx~~ and show large cloudy portions ~~(spongy cpx)~~.

Several types of pyrometamorphic textures are superimposed on these features. They consist of (1) cloudy, spongy ~~cpx~~ crystals: the recrystallized portion generally replaces the whole crystal, in rare cases it covers only the rim zones (Fig. ~~2a, b)~~; (2) reaction areas ~~involving primary opx, cpx and sp, with a secondary assemblage~~ made up of small crystals of ~~ol, cpx~~, vermicular ~~sp~~ and rare glass (Fig. 2c, d); (3) brown to pale yellow glassy patches containing secondary crystals of ~~ol, cpx and sp~~; The secondary paragenesis is generally too small to be analyzed by Electron MicroProbe (EMP) and therefore was not considered for *in-situ* analysis.

4. Analytical methods

The modal composition of Marosticano samples was estimated by point counting with more than 1000 points for each thin section. Major element compositions of minerals from xenoliths and host lavas were determined by ~~Electron Microprobe~~ (EMP), using a Cameca SX50 instrument at the Istituto di Geoscienze e Georisorse, CNR, Padova (Italy). Trace element concentrations in ~~cpx and opx~~, were obtained by Laser Ablation Inductively Coupled Plasma Mass Spectrometry (LA-ICP-MS) at the Department of Earth Sciences, University of New Hampshire (USA) using an Analyte Excite 193 nm excimer laser plumbed into a Nu instruments AttoM high-resolution inductively coupled plasma mass spectrometer. Two out of five samples were sufficiently unaltered so as to be suitable for bulk rock analysis, which was performed on powder pellets using an ARL Advant-XP spectrometer at the Dipartimento di Fisica e di Scienze della Terra, Università di Ferrara (Italy).

More extensive descriptions of the analytical procedures, together with the standards supporting the analyses, are reported in the on-line Supplementary material.

5. Mineral Chemistry

Within each xenolith, minerals are generally homogeneous in composition with no significant chemical variation between core and rims of the same crystal. The latter is observed only for spongy crystals and grains close to reaction areas (Fig. 2). When these areas are near the contact with host basanites, ol and cpx core and rim analyses were performed and compared with ol and cpx phenocrysts in order to check if they could be the result of the host magma infiltration. Representative analyses of ol, opx, cpx, and sp are reported in Tables A-D of the Supplementary online material.

5.1 Major element composition

Olivine is chemically unzoned in Monte Gloso (MG) lherzolites and harzburgites. It shows a narrow compositional range with Fo content [=100 x $Mg/(Mg+Fe)_{mol}$] varying from 91.3 to 92.2 for lherzolites and from 90.5 to 92.5 for harzburgites (Fig. 3a), with high Ni contents (2600-3620 ppm and 2670-3540 ppm in lherzolites and harzburgites, respectively). Though conspicuous variability of Ni in ol within individual samples may suggest a potential interaction between MG xenoliths and the host magma, the invariant Fo contents for each sample are inconsistent with melt-xenolith reaction explaining the variable Ni contents. Specifically, it is noteworthy, that ol phenocrysts from the host lavas have Fo content ranging from 86.1 to 87.2 and Ni contents from 2240 to 2251 ppm, suggesting that melt-xenolith reaction may explain only a small component of the variable Ni contents found in the MG xenolith suite (Fig. 3b).

Opx from unreacted core to reacted rims is chemically unzoned and frequently contains elongate oriented rods of exsolved cpx. Opx mg# [=100 x Mg/(Mg+Fe)$_{mol}$] values vary from 91.2 to 92.8 for both lherzolites and harzburgites, like the coexisting ol grains. Contents of Al_2O_3 in opx are highly variable in lherzolite (1.68-4.18 wt.%) whereas a more restricted range is shown by harzburgites (1.78-2.60 wt.%), reflecting a common "harzburgitic" melting degree, or limited temperature-dependent subsolidus exchange with sp (Brey et al., 1999) (Fig. 3c). Contents of TiO_2 in lherzolites are more variable (0-0.07 wt.%) than those of harzburgites (0-0.03 wt.%).

By texture the most reactive phase, cpx bears evident compositional heterogeneity within each individual sample for most compositional features but mg#. Along with the coexisting ol and opx, mg#$_{cpx}$ ranges from 91.0 to 93.3 across all lithologies. By contrast, the Al_2O_3, Cr_2O_3 and to lesser extent Na_2O are highly variable in both lherzolite and harzburgite cpx. Lherzolites generally show a larger range in Al_2O_3 (1.73-4.53 wt.%), Cr_2O_3 (0.72-1.64 wt.%) and Na_2O (0.49-1.89 wt.%) compared to harzburgites (Al_2O_3= 0.63 to 3.79 wt.%; Cr_2O_3= 0.89-1.52 wt.%; Na_2O= 0.35-1.18 wt.%; Fig. 3). The high chromium contents classify these crystals as chromiferous cpx (Morimoto, 1988) with TiO_2 being always less than 0.60 wt.% (Fig. 3f). Mg# values in cpx for both lherzolite and harzburgite are not correlated with Al_2O_3, Na_2O, and TiO_2 distribution as would be expected for a mantle residual trend or, in turn, for alkaline basic-ultrabasic magma fractionation lines (Fig. 3d-f). Accordingly, we interpret negligible, if any interactions between peridotites and basanitic host lavas. Large compositional variations are exhibited in sp cr# [=100 x Cr /(Cr+Al)$_{mol}$] and mg#, with overlapping values for both lherzolite and harzburgite. However, cr# and mg# are homogenous within each individual sample with the exception of harzburgite MG13 (Fig. 3g). Across the samples, cr# and mg# vary from Cr-rich in harzburgite (cr#: 38.3-67.2; mg#: 56.2-69.6) to Al-rich types in lherzolite (cr#: 30.4-52.7; mg#: 62.2-75.9).

5.2 Pyroxene trace elements

Representative *in situ* (LA-ICP-MS) trace element analyses of pyroxenes are reported in Tables E-F of the on-line Supplementary material. The values are shown in chondrite-normalized incompatible trace elements (Fig. 4a, b; 5a, b) and rare earth element (REE) diagrams (Fig. 5c, d). In order to characterize the "original" features of the MG lithospheric domain prior to the metasomatic event trace element contents ~~of the cores~~ of both ~~opx~~ and unreacted ~~cpx~~ core were considered. One sample (harzburgite MG13) has only opx with rare cpx crystals occurring in reaction areas, ere their small size (<30 μm) prevent high resolved quantitative analysis.

Both lherzolite and harzburgite bear ~~opx~~ with heavy REE (HREE) contents in a narrow range ((Tb/Lu)$_N$ in lherzolites= 0.05-0.44; in harzburgites= 0.13-0.47) but large light (L)- middle (M)REE variability between ~~grains and samples~~ (e.g., Eu$_N$). MG16 lherzolite shows distinctive ~~opx~~ REE contents with nearly flat M-HREE ((Dy/Lu)$_N$=0.39-0.49) and LREE downward convex enrichments ((La/Nd)$_N$=0.27-0.79) (Fig. 4a). MG1, MG6 lherzolite and MG14 harzburgite preserve residual M-HREE signatures ((Dy/Lu)$_N$=0.18-0.37; Fig. 4a, b) typical of the ~~sp~~-stability field after melt extraction co-existing with an apparent LREE enrichment ((La/Nd)$_N$=1.05-13.1). In turn, ~~opx~~ of MG13 harzburgite shows an overall M-HREE enrichment ((Dy/Lu)$_N$=0.41-0.42; Fig. 4b). Finally, Ti shows both positive and negative anomalies in both xenolith rock types.

Across all lithologies MG ~~cpx~~ have an overall high REE content (ΣREE=185-621 ppm) and distinctive LREE enrichment relative to HREE (La$_N$ up to 100 times chondritic; (La/Yb)$_N$ in lherzolites = 9.58-26.68; (La/Yb)$_N$ in harzburgites = 13.88-19.24).

The geochemical data, taken together, allow for two groups of ~~cpx~~ compositions to be defined. Group-1 includes ~~cpx~~ of ~~lherzolites~~ MG1, MG6 and ~~harzburgit~~es MG13, MG14, which shows ~~an~~ almost flat M-HREE pattern ((Sm/Lu)$_N$= 1.31-4.76) with abrupt (more than one order of magnitude) LREE-enrichment ((La/Nd)$_N$= 1.53-6.18). Almost all these ~~cpx~~ display a positive Eu anomaly ({Eu$_N$/[(Sm+Gd)$_N$/2]}= 1.07-1.68) (Fig. 5c). In turn, group-2 is constituted by ~~cpx~~ of MG16 lherzolite only, which show distinctive convex upward REE pattern with a steep negative slope from Nd to Lu ((Nd/Lu)$_N$=14.0-18.0) and a maximum at Pr$_N$ (114-143) (Fig. 5d).

The entire MG ~~cpx~~ population has variable high Th and U content (Th and U up to 3.03 and 0.63 ppm, respectively) with negative ~~anomalies in~~ Ti and HFSE (e.g. Nb, Ta, Zr, and Hf), the most evident being the Zr anomaly in harzburgite with Zr* ~~(~~$Zr_N/[(Nd+Hf)_N/2]$~~)~~=0.09-0.24 (Fig. 5a, b). It should be noted that MG unreacted ~~cpx~~ have trace elements contents similar or even higher than those of primary and secondary ~~cpx~~ from mantle xenoliths of the Lessini Mts. (Beccaluva et al., 2001; Fig. 6).

6. Geothermobarometry

To estimate the temperature conditions under which the MG ~~sp~~ lherzolites and harzburgites were equilibrated, we used the two-pyroxene geothermometer based on Fe/Mg exchange of Brey and Köhler (1990) which we will denote as T_{BK}. ~~Ol-sp~~ geothermometers of Wells (1977) and Taylor (1998) were also applied for comparative purposes and are denoted as T_W and T_T, respectively. For the thermo-barometric calculations, we considered only cores of unreacted ~~opx and cpx~~ grains that were in close contact.

Though some studies provide barometry, mainly based on the Ca distribution ~~of ol and cpx~~ (e.g., Köhler and Brey, 1990), determining appropriate barometry in ~~sp~~-bearing peridotites (Medaris, 1999; O'Reilly et al., 1997) is challenging. Therefore, we assume the equilibrium pressure from experimental stability phase relationships (Caldeira and Munhá, 2002). Taking into account the absence of amphiboles (which could modify the peridotite mineral stability fields) and the presence of ~~sp~~ as the sole aluminum-bearing phase, an upper limit of 2.1 GPa and a lower limit of 0.9 GPa are set (Caldeira and Munhá, 2002; Green and Hibberson, 1970; Green and Ringwood, 1970; O'Neill and Wall, 1987; Siena and Coltorti, 1989). This pressure approximation agrees with the maximum depth of the local SCLM, constrained by seismic profiles (Carminati and Doglioni, 2012) to fall within the 1.5-2.0 GPa range. The pyroxene Fe/Mg exchange is largely dependent on temperature (Brey and Köhler, 1990; Wells, 1977; Wood and Banno, 1973) and is relatively insensitive to pressure; temperatures calculated at 1.0 GPa and 2.0 GPa show only minor variations (<10°C). Accordingly, primarily for comparative purposes, temperature calculations were made at a fixed pressure of 1.5 GPa.

6.1 Equilibration temperatures

MG sp-lherzolites record residual temperatures in the range of 923-1058°C. The highest value (MG16) is comparable with those recorded by the two MG harzburgites (MG13: 1117 ± 20°; MG14: 1033 ± 30°C; Table 2). This is in agreement with its low cpx content (6%), which could reflect a residual character analogous to harzburgites. We compared MG peridotites equilibration temperatures with those from the nearby districts of Lessini Mts. and Val d'Adige calculated with the Wells (1977) and Taylor (1998) geothermometers (Gasperini et al., 2006).

For comparison, equilibration temperature of a few Lessini Mts. and Val d'Adige peridotites were recalculated together with MG samples of this work applying the three thermobarometric models (Table 2). We observed that: i) as seen in other geothermobarometric studies (e.g., Greenfield et al., 2013), T_T values are always lower than T_{BK} and T_W; ii) with the exception of one sample from Lessini Mts., differences between T_{BK} and T_W within each sample are negligible (<20°C); iii) T_T diverges from T_{BK} by 2 to 78°C and diverges from T_W from by 19 to 78°C.

Taking this into account, the temperature range of 923-1117°C recorded by MG peridotites is higher than most of Val d'Adige (T_{BK}: 896-902°C) and of Lessini Mts. (T_{BK}: 885-975°C) xenoliths.

Looking at the entire VVP mantle domain, the high equilibration temperatures recorded for mantle xenoliths are only comparable to the highly metasomatized Lessini Mts. peridotites (1130 ± 60°C) studied by Siena and Coltorti (1989) (Fig. 7).

6.2 Oxygen fugacity

Oxygen fugacities ~~for~~ Marosticano peridotites were estimated using the method of Ballhaus et al. (1991) using temperatures provided by the Brey-Köhler thermometer (T_{BK}). Calculated fO_2 values are plotted in Fig. 7 in logarithmic units with respect to the fayalite-magnetite-quartz (FMQ) buffer ($\Delta \log fO_2$). Estimates for the two ~~sp-~~harzburgites range from +0.6 to +0.9, while for the ~~sp-~~lherzolites the range is wider (-0.6 to +1.1), with MG6 lherzolite being the most reduced sample. With the exception of the latter xenolith, MG peridotites are more oxidized than Val d'Adige lherzolites (~~Table 2 and Fig. 7,~~ $\Delta \log fO_2$ (FMQ) from +0.2 to +0.3 as calculated for compositions from Gasperini et al., 2006 and T_{BK} ~~from Table 2~~). The Lessini Mts. peridotites also yield more variability in the recorded redox conditions ($\Delta \log fO_2$ (FMQ) from -1 to +1, calculated from data of Gasperini et al., 2006 and Siena and Coltorti, 1993; Table 2) encompassing the entire range of Marosticano and Val d'Adige samples (Fig. 7).

7. Discussion

7.1. A cratonic origin?

The highly refractory bulk composition of lherzolites (Al_2O_3 <1.03 wt.%, mg# 90.3-91.6; Table 3), associated with low Al_2O_3 contents, high mg# values in both pyroxenes and ~~sp~~ of MG peridotites (Fig. 3c-d and Tables B-D ~~in~~ the on-line Supplementary material) testify for ~~a~~ large extraction of basaltic melts from the Marosticano mantle domain which appears the most residual of the entire VVP (e.g., Lessini Mts. lherzolites: Al_2O_3 >2.52 wt.% and mg# 85.8-89.9).

Peridotites with refractory composition are expected in Phanerozoic and Proterozoic off craton mantle and ophiolites. They generally follow the so-called "residual or oceanic trend", explained as an extraction of basaltic components, resulting in an increase of Fo content in ~~ol~~ accompanied by increased ~~ol~~ modal content (Boyd, 1989). Refractory peridotites characterize also the cratonic mantle, but they rarely follow the oceanic trend (Bernstein et al, 2007; Boyd, 1989; Boyd et al., 1997; Ionov et al., 2010). They are characterized by ~~ol~~ with ~~a range of~~ high Fo content (~91-94) at extremely variable modal ~~ol~~ content (~40-75%). In particular, the high Fo of ~~ol~~ in ~~sp~~-bearing (shallow) cratonic peridotites with relatively low ~~opx~~ modal content (<20%) (e.g., Tanzanian, Greenland, and Slave Cratons) are indicative of high degrees (~30 to 50%) of partial melting in thermal regime active only till Archean/early Proterozoic time (Ionov et al., 2010; Walter, 2003).

~~MG ol plotted (Fig. 3a)~~ in the Boyd diagram (Boyd, 1989; Boyd et al., 1997) plot off the oceanic trend, and follow the general behavior of cratonic ~~ol~~ (i.e. Kapvaal, Tanzanian, Greenland and Slave Cratons)~~. While~~ most of the Val d’Adige and Lessini Mts. exhibit lower ~~ol~~ modal contents at lower Fo following the oceanic trend (Fig. 3a). In addition Marosticano ~~ol~~ have also Ni values higher than those of Lessini Mts. but similar to those of Val d’Adige (Fig. 3b).

In association with high-Fo ~~ol~~, MG peridotites show high ~~Mg-opx~~ in the range of ~~30-12~~% modal contents (Table 1), out of any “ideal” Phanerozoic (abyssal, oceanic and continental) off-craton melting trend (Niu, 2004; Pelorosso et al., 2016). Instead, they recall a general ~~ol-opx~~ behavior recorded in "shallow" (garnet-free) cratonic mantle and interpreted as physical segregation of ~~ol~~ and ~~opx~~ in high-pressure melting residuum and polybaric re-equilibration (Bernstein et al., 2007; Ionov et al., 2010). In addition, trace element distributions in ~~opx~~ from MG16 lherzolite and MG13 harzburgite show almost flat M-HREE profiles ~~(~~i.e. $(Dy/Yb)_N$~~)~~, consistent with an original subsolidus equilibrium with garnet (Bonadiman et al., 2005). In garnet-bearing lherzolites at progressively decreasing sub-solidus T (1300-900°C), ~~opx~~ decrease~~s~~ the total REE contents with equal M-HREE solid-solid partition coefficient (Sun and Liang, 2014). In turn ~~opx~~ of MG1, MG6 and MG14 seem to be originally equilibrated in the ~~sp~~ stability field showing the typical steep slope for M-HREE at comparable subsolidus temperature (1000-900°C) (Sun and Liang, 2014) ~~(~~Fig. 4a, b).

Spinel, the distinctive phase of the great majority of off-craton mantle xenoliths, has cr# (30-67) which suggests a residual component neither coherent with the oceanic residual trend (i.e. “OSMA”; Arai, 1994a, 1994b) nor with the more fertile VVP-mantle fragment (cr# 9-12). On the other hand, Marosticano ~~sp~~ mimic the tendency observed for ~~sp~~ coexisting with ~~ol~~ in shallow on-craton (garnet-free) xenoliths (Bernstein et al., 2007).

In this refractory P-T system, ~~ol~~ Fo of 91.5 and ~~sp~~ cr# of 60.0 would suggest strong (or complete) ~~cpx~~ consumption by high degrees of partial melting (>25%; Bernstein et al., 2007; Bonadiman et al., 2005; Hellebrand et al., 2001; Scott et al., 2016; Walter, 2003) that are typical of the Archean or early Proterozoic mantle (Walter, 2003). Therefore, we suggest that the partial melting occurred at high melting T and thus more likely in an old mantle thermal regime. Subsequently, the Marosticano mantle was enriched, forming the observed ~~cpx (cpx~~ modal contents 4-13%) in MG xenolith. These are thus secondary in nature in accordance with several studies demonstrating that most ~~cpx~~ in on-craton mantle may have a metasomatic legacy (Grégoire et al., 2003; Pearson et al., 2003; Simon et al., 2003; 2007).

To sum up, Marosticano xenoliths are characterized by cratonic fingerprints ~~(Fig. 3a)~~, according to major and trace element compositions of the peridotite phases, and Re-Os geochronological modeling (T model age: 2.1-2.9; Brombin et al., in prep.). These geochemical characteristics are evident only for the Marosticano mantle fragment~~s~~, whereas the rest of the VVP mantle is, as expected, off-craton SCLM. The sole, intriguing link between on-craton and off-craton VVP mantle is the similarity of the Re-Os ages, ranging between 1.9 ~~to~~ 2.1 Ga, with a unique value at 3.1 Ga for the entire VVP domain. These results speak in favor for a continuum geodynamic set which includes on-craton and off-craton mantle portions, as more frequently reported.

Cratonic signatures in off-craton ~~sp~~-bearing mantle xenoliths derived from ~~intra-plate~~ volcanic areas are recognized in a few mantle xenolith populations, e.g. in the Massif Central (France; Lenoir et al., 2000), West Otago (New Zealand; Liu et al., 2015; Scott et al., 2014, 2016) and Cape Verde (Bonadiman et al., 2005; Coltorti et al., 2010).

In the Massif Central, two contrasting shallow lithospheric domains are faced. Relatively refractory (i.e., Al_2O_3 <2.0 wt.%) and highly fertile (i.e., Al_2O_3 >4.0 wt.%) ~~lherzolites and harzburgites~~ are interpreted as reminiscent of cratonic and circumcratonic SCLM domains, respectively (Lenoir, 2000). West Otago ~~sp-~~peridotites with high variable Re depletion Os model ages (0.5-2.7 Ga) would represent relicts of Archean depleted mantle residues recycled through the asthenosphere over Ga timescales along with more fertile convecting mantle ~~(Liu et al., 2015; McCoy-West et al., 2013)~~. Therefore, different remnants of shallow lithospheric domains are incorporated within the young (<300 Ma) Zealandia microplate.

It is important to note that "shallow" (garnet-free) cratonic mantle is not exclusive of continental setting. Cape Verde Islands lie in the Atlantic Ocean, in a clearly oceanic setting. Here Archean ~~sp-~~bearing mantle xenoliths~~,~~ record garnet precursor and K-rich metasomatism (Bonadiman et al., 2005), suggesting the involvement of ancient geochemical reservoir also for the genesis of oceanic basalts (Coltorti et al., 2010).

Although Archean cratons are considered ancient continental nuclei characterized by tectonic inactivity for at least the past 2 Ga and low heat flow, recent studies show that their highly refractory mantle roots are intensively modified over time by mechanical destructions (lithospheric thinning and incipient rifting) and by episodic rejuvenation events (Foley, 2008; Tang et al., 2013; Zhang et al., 2009a; Zhang et al., 2012).

The Wyoming Craton and North China Craton are well-known examples of complete chemical rejuvenation by varying degrees of refertilization (Eggler and Furlong, 1991; Fan and Menzies, 1992; Tang et al., 2008, 2012, 2013). In turn, other cratons might have not yet suffered large-scale removal of their ancient keels but they are in the early stages of disruption due to the efficiency of extensive regime (Foley, 2008). We recall that Lessini Mts. and Val d'Adige xenoliths are generally fertile lherzolites with ~~cpx and opx~~ coherently showing the typical LREE-depleted, M-REE flat and steep H-LREE fractionated patterns respectively (Beccaluva et al., 2001; Lenoir et al., 2000). These features are chemically contrasting with the refractory nature and the LREE enrichments of Marosticano xenolith population.

These differences could be interpreted in terms of compositional rejuvenation of the circumcratonic domains. Lessini Mts. and Val d'Adige xenoliths may be ~~the~~ fragments of the ancient SCLM, strongly refertilized by infiltration of asthenosphere-derived melts, rather than newly accreted “off-craton" SCLM. By contrast, Marosticano domain could be interpreted as the vestige of an old (Archean?) SCLM block that underwent depletion via melt extraction and was afterward pervasively metasomatized by CO_2-rich silicate melts, a process, however, was not able to erase fully the original cratonic nature.

7.2 Metasomatic origin of clinopyroxene in Marosticano xenoliths

Despite the general refractory features of MG peridotites, a superimposed metasomatic process is manifested by major and trace element geochemistry of both pyroxenes. Trace-element compositions of Marosticano cpx show variable enrichment characteristics, inconsistent with a residual origin after melt extraction (e.g. Sun et al., 2012). They exhibit a notable LREE-enrichment (Fig. 5c, d), a fractionated REE pattern and a general HFSE depletion (Fig. 5a, b) with respect to C1 model trace element abundances (Sun and McDonough, 1989). Taken together, these signatures confirm that cpx is a phase either formed by a reaction of a residual peridotite with metasomatic melts or it is a new phase directly crystallized from the metasomatic agents.

As nearby VVP districts (Lessini and Val d’Adige) are thought to have been affected by silicatic metasomatism (Beccaluva et al., 2001), we first evaluated whether the MG mantle segment could have been also explained by the same type of metasomatism. Taking into account only those Lessini and Val d’Adige samples that show cpx modal contents and cpx-opx mg# values comparable to those of MG xenoliths, trace element compositions of MG cpx are significantly enriched compared to the primary, spongy and secondary VVP cpx (Fig. 6). This suggests that MG were pervaded by a metasomatic agent that was different from that which affected the rest of the VVP region. However, both group-1 and group-2 cpx are more enriched in LREE (Fig. 5c, d) and depleted in Ti and in HFSE (e.g., Zr, Fig. 5a, b) arguing against a “pure” alkali silicate melt metasomatism and favouring instead the contribution of a carbonatic component. In fact, experimentally produced silica-bearing carbonatite melts crystallize ~~cpx~~ with major element composition similar to both MG group-1 and group-2 ~~cpx~~ (Fig. 3d-f).

Enrichment in LREE accompanied by strong HFSE depletion (Fig. 5a, b) of group-1 and group-2 ~~cpx~~ ~~is~~ notably assigned to an effect of the ~~cpx~~-carbonatite partitioning as shown by experimental and empirical data by Dasgupta et al. (2009), Dixon et al. (2008), Gudfinnsson and Presnall (2005) and Pokhilenko et al. (2015). This geochemical effect has been observed in various carbonatite metasomatized mantle xenoliths from both oceanic and continental settings (i.e: Spitsbergen, Ionov, 1998; North China Craton; Sun et al., 2012; New Zealand, Scott et al., 2016; Comores Archipelago; Coltorti et al, 1999).

~~Cpx group-2~~ mimic~~s~~ the steep M-HREE fractionated pattern, but they have remarkably higher LREE content with respect to ~~cpx~~ formed by a carbonatitic/CO_2-rich silicate melt experimentally obtained at pressure of 6.6 GPa in equilibrium with garnet (Dasgupta et al., 2009~~) (~~Fig. 8). The calculated $^{cpx/carb}D_{La}$ at this pressure is 0.006 but systematically increases with decreasing pressure and with the ~~sp~~ appearance (Dasgupta et al., 2009). Therefore, if we consider REE ~~cpx~~/carbonatite partition coefficients calculated for 2 GPa and 1100-1150°C (e.g., $^{cpx/carb}D_{La}$ of 0.09; Klemme et al., 1995) we can reproduce the general shape of the ~~L- to M-H~~REE pattern of both MG ~~cpx~~ groups (Fig. 8).

The only remarkable difference between group-1 and group-2 ~~cpx~~ is that the former shows a less steep, or flat, HREE pattern indicating ~~that carbonatitic melts migrated and interacted with slightly different peridotitic wallrocks. This could be attributed to a~~ chromatographic fractionation of a metasomatic agent interacting with different peridotitic wallrock (Ionov et al., 2002; Sen et al., 1993). In this scenario, the concentration fronts of the migrating melts are controlled by the ion-exchange with the peridotitic matrix. In general, the fronts of the more incompatible elements (e.g., LREE) travel faster than those of less incompatible ones (e.g., M-HREE) producing enrichments in LREE and depletion or flatness in HREE of the whole rock depending on the original peridotitic matrix (Ionov et al., 2002). In this frame, the ~~cpx~~ group-1 record~~s~~ a continuum feeding of REE from the carbonatitic melt to a possible residual (primary?) ~~cpx~~ (Ionov et a., 2002; Pokhilenko et al., 2015; Sen et al., 1993). On the contrary, the convex-upward REE patterns of ~~cpx~~ group-2 may reflect nearly complete equilibration between the peridotite matrix (mainly ~~ol-opx~~) and the metasomatic melt (Dasgupta et al., 2009; Dixon et al., 2008).

In anhydrous garnet-free peridotites, restitic ~~opx~~ is the counterpart of ~~cpx~~ to incorporate the incoming geochemical budget. The only evidence of metasomatic effects in the MG orthopyroxenes is their high Ti content (up to 281 ppm), not coherent with their low Al_2O_3 (~~Fig. 9;~~ Scott et al., 2016) and in antithesis with the carbonatitic enrichment described for the ~~cpx.~~ This can be explained by the action of CO_2-rich silicate melts which could primarily impart a carbonatite-like trace element signature in ~~cpx~~ (i.e., L-REE) hiding the potential effects of silicate melts (i.e., Ti enrichment), that in turn is magnified in the residual ~~opx~~ (Scott, et al., 2016). Spinel-facies ~~cpx~~ prefers most trace elements, including Ti, compared to ~~opx;~~ however, relative to elements with slightly larger and smaller atomic radii (Eu and Dy), Ti is slightly less favorably partitioned into ~~cpx~~ (Eggins et al., 1998; Scott, et al., 2016). This nuance leads to the formation of small negative Ti anomal~~ies~~ in ~~cpx~~ and a corresponding positive anomaly in ~~opx~~ (Scott et al., 2016). Consequently, both negative and positive Ti anomalies observed in MG ~~opx~~ could be due to a chromatographic fractionation effect during the interaction between carbonatite/CO_2-rich silicate melts and a ~~different~~ peridotitic wallrock where ~~cpx~~ was present or not (Ionov et al., 2002; Scott et al., 2016; Sen et al., 1993).

Though we cannot resolve if this metasomatism initially occurred in the garnet stability field and continued in shallower portions of the MG mantle we can assume that the product of such metasomatism may be stabilized at P conditions of the ~~sp~~ stability field. Accordingly, we interpret the geochemical characteristics (major and trace elements) acquired by MG pyroxenes as consistent with "new" ~~cpx~~ formed by the interaction of a carbonatitic melt with ~~a~~ cratonic flavored ambient peridotite (Griffin et al., 1999; Spengler et al., 2006). Notably, experimental studies (e.g., Dasgupta et al., 2006, 2007; Green, 2015; Hammouda and Keshav, 2015; Hirose, 1997) suggest that a carbon-rich peridotite is necessary to form alkaline and in particular ultra-alkaline mantle melts. Similarly, carbonatitic components have been hypothesized as important contributors to VVP alkaline- to ultra-alkaline magmas, the hosting lavas that ferry VVP mantle xenoliths to the surface (Beccaluva et al., 2007).

7.3 Relationship between carbonatite/CO_2-rich silicate metasomatism and fO_2 conditions

As carbonatitic/CO_2-rich silicate melts contain large amounts of dissolved fluids, they are able to mobilize volatile elements (C-OH-, but also Na and K as lithophile elements); accordingly, their interaction with the peridotite matrix may affect the redox conditions (Dasgupta et al., 2013). MG peridotites represent a cratonic "enclave" of continental mantle of the Adria plate that was later pervaded by carbonatite metasomatism. The high fO_2 (Fig. 7), comparable with the other VVP mantle occurrences and within the range of the subcontinental lithospheric mantle (Foley, 2011), is not compatible with a cratonic origin but requires a late oxidation event, preserved until the xenolith exhumation by Cenozoic host lavas. Volatile mass transport occurs mostly by fluid and silicate (with prevailing H_2O) or carbonate melts (with prevailing CO_2) as function of the redox state of the mantle (Foley, 2008, 2011; Frost and McCammon et al., 2008; Pokhilenko et al., 2015). Assuming the relatively high oxidizing conditions of Marosticano peridotites were affected by CO_2-bearing melts, we calculated CO_2 mole fractions of such melt(s) using the equation of Stagno and Frost (2010). We obtained CO_2 mole fractions close to or slightly higher than 1.0, taking into account the T-fO_2 values independently calculated from the silicate parageneses (Table 2). This is also evident in the diagram of fO_2 as a function of potential T (Goncharov et al., 2012), where almost all the Marosticano peridotites straddle the field for carbonatite and CO_2 fluid (Fig. 10). This may suggest that the Marosticano geothermobarometric conditions record this matrix/carbonatitic melt interaction, rather than the T-fO_2 values of the initial cratonic lithospheric mantle.

The variable redox states of the MG xenolith population may also influence the Eu oxidation state

(Eu^{3+} or Eu^{2+}; Henderson, 1984) and may explain why this element is enriched in group-1 cpx. In oxidized magma Eu is an incompatible element in the trivalent form (Eu^{3+}), while in reduced magma it is preferentially incorporated into plagioclase in its divalent form (Eu^{2+}). This ion-exchange process explains the negative Eu anomaly in many terrestrial basalts showing plagioclase as liquid phase. However, Eu speciation is highly sensitive to small redox variations. Thus the different accommodation of Eu in minerals may change rapidly (McLennan, 2001).

Almost all group-1 cpx have M-HREE flat profiles with evident positive Eu anomaly (Fig. 5a, c). These anomalies are not accompanied by a positive K (not reported) or Sr anomaly, that could be assigned to the melting of pre-existing phlogopite and plagioclase respectively, in the protolith (Marchesi et al., 2013; Tang et al., 2017), neither of which were observed in any Marosticano xenolith. In other xenolith suites, examination of the Eu content in garnet and cpx in eclogites led to the suggestion that the positive Eu anomaly results from the interplay between crystal chemistry and redox conditions during metasomatism (Griffin and O'Reilly, 2007). Karner et al. (2010) determined the Eu partition coefficient between augite and melt (${}^{cpx/melt}D_{Eu}$) in samples crystallized from a highly Eu spiked Martian basalt composition at different fO_2 conditions. These authors observed that D_{Eu} augite/melt steadily increases with fO_2 since Eu^{3+} is more compatible than Eu^{2+} in the pyroxene structure; thus increasing fO_2 leads to greater Eu^{3+}/Eu^{2+} in the melt, allowing for more Eu (total) to partition into the cpx. It is worth noting that positive Eu anomalies are occasionally observed in cpx from metasomatized suboceanic mantle or subcontinental cratonic mantle in both sp and garnet stability field irrespective of the nature of the metasomatic melts (e.g., xenoliths from Loch Roag, North Atlantic Craton, Northern Scotland, Hughes et al., 2015; from Siberian Craton, Pearson et al., 1995; Slave Craton, Heaman et al., 2002; Kaapval craton, Jacob et al., 2003). On the basis of these considerations, we suggest that a small variation of the redox state may induce Eu to modify its solid/solid, solid/melt partitioning behavior, without any change of the large-scale geochemical process.

The interaction between the Marosticano residual mantle with a carbonatite/CO_2 rich silicate melt is explained by a possible chromatographic fractionation effect only in group-1 peridotite. This leads to a "local" variation of fO_2 oxidizing conditions and by consequence to a "local" increase of the Eu^{3+}/Eu^{2+} ratio in the melt and to higher Eu concentration in the newly formed cpx. Group-2 clinopyroxene is suggested to crystallize from the carbonatitic/CO_2-rich silicate melts that control the environmental redox condition.

8 Conclusions

- Petrological and geochemical features of the newly discovered Marosticano peridotite xenoliths indicate that they represent a mantle segment geochemically distinctive from the other VVP peridotites (i.e., Lessini Mts. and Val d'Adige), contributing to enlarge the knowledge of spatial heterogeneity within the mantle of this region.
- MG lherzolites and cpx-bearing harzburgites demonstrate complete sp-facies equilibration. Mineral major and trace elements features are comparable to those observed for on-craton peridotites worldwide.
- Marosticano cpx are secondary in nature and they exhibit a substantive LREE-enrichment, a fractionated REE pattern with positive Eu anomaly, almost flat (cpx group 1) or steep (cpx group 2) HREE patterns, and a remarkable HFSE depletion. These characteristics are attributed to a chromatographic separation of a metasomatic agent with high carbonatitic/CO_2-rich silicatic components.
- Marosticano samples record relatively high oxidation conditions similar to those of the VVP off-craton xenoliths (e.g. Lessini Mts.) but anomalous for a proper cratonic environment. These T-fO_2 relationships are probably due to the oxidizing nature of CO_2-rich circulating fluids.
- The variable, but generally high, redox states of the MG xenolith could be responsible for the positive Eu anomaly in cpx group-1. As higher fO_2 leads to higher Eu^{3+}/Eu^{2+} in the melt increasing the element partitioning in cpx, the positive Eu anomaly could result from the

relatively high redox condition of the Marosticano mantle fragment during the formation of group-1 cpx. On the contrary, group-2 cpx that do not show positive Eu anomalies may show the fingerprint of a carbonatitic/CO_2-rich silicate melt metasomatism, therefore still recording the original redox condition.

- Within the SCLM sampled by VVP magmatism, only Marosticano xenoliths show evidence of carbonatitic metasomatic overprinting of a likely cratonic mantle domain. All the other mantle VVP mantle xenoliths exhibit characteristics of off-craton lithospheric mantle variably affected by Na-alkaline silicatic metasomatism.
- The lithospheric mantle beneath the Adria plate has been affected by complex enrichment and refertilization processes, related to a geodynamic scenario dominated by extension-related magmatism in response to the near active collision between Eurasia and Africa plates (Fig. 11).
- The geochemical features of Marosticano mantle xenoliths introduce a cratonic component in the geodynamic evolution of the Adria plate system in the general frame of the geodynamical reconstruction of the Africa/Eurasia collision. From our current study, together with literature data, we interpret that the cratonic keel is preserved only in the Marosticano district, while Lessini Mts. and Val d'Adige mantle domains could be circumcratonic portions refertilized by infiltration of asthenospheric-derived melts (Fig. 11).

Acknowledgments

R. Carampin (I.G.G-C.N.R. Padova) is thanked for analytical assistance during the EMP analyses. The Italian National Research Program PRIN_2015/prot. 20158A9 (CB-AM) and the IUSS Mobility Research Programme of the University of Ferrara (VB scholarship for Abroad Mobility for Long Period) supported this research. We thank J.M. Scott and an anonymous referee for their constructive comments on a previous version of this paper and Andrew Kerr for his thoughtful suggestions and editorial handling.

References

Ansorge, J., Blundell, D., Müller, S., 1992. Europe's lithospheric structure, in Blundell D., Freeman, R., Müller, S. (Eds.), A Continent Revealed: The European Geotraverse. Cambridge University Press, New York, p. 275.

Arai, S., 1994a. Characterization of spinel peridotites by olivine-spinel compositional relationships; review and interpretation. Chemical Geology 113, 191-204.

Arai, S., 1994b. Compositional variation of olivine chromian spinel in Mg-rich magmas as a guide to their residual spinel peridotites. Journal of Volcanology and Geothermal Research 59, 279-293.

Ballhaus, C., Berry, R., Green, D., 1991. High pressure experimental calibration of the olivine-orthopyroxene-spinel oxygen geobarometer: implications for the oxidation state of the upper mantle. Contributions to Mineralogy and Petrology 107, 27-40.

Barbieri, G., De Zanche, V., Medizza, F., Sedea, R., 1982. Considerazioni sul vulcanesimo terziario del Veneto occidentale e del Trentino meridionale. Rendiconti della Società Geologica Italiana 4, 267-270.

Barbieri, G., De Zanche, V., Sedea, R., 1991. Evoluzione del semigraben paleogenico Alpone-Agno (Monti Lessini). Rendiconti della Società Geologica Italiana 14, 5-12.

Beccaluva, L., Bianchini, G., Bonadiman, C., Coltorti, M., Milani, L., Salvini, L., Siena, F., Tassinari, R., 2007. Intraplate lithospheric and sublithospheric components in the Adriatic domain: Nephelinite to tholeiite magma generation in the Paleogene Veneto Volcanic Province, Southern Alps. Geological Society of America 418, 131-152.

Beccaluva, L., Bianchini, G., Bonadiman, C., Coltorti, Siena, F., 2009. Petrological charactersitics of the Adriatic/North Africa lithospheric mantle: inferences from Cenozoic magmatism and mantle xenoliths. Rendiconti della Società Geologica Italiana 9, 79-84.

Beccaluva, L., Bonadiman, C., Coltorti, M., Salvini, L., Siena, F., 2001. Depletion events, nature of metasomatizing agent and timing of enrichment processes in lithospheric mantle xenoliths from the Veneto Volcanic Province. Journal of Petrology 42, 173-187.

Bernstein, S., Kelemen, P.B., Hanghøj, K., 2007. Consistent olivine Mg# in cratonic mantle reflects Archean mantle melting to the exhaustion of orthopyroxene. Geology 35, 459-462.

Bonadiman, C., Beccaluva, L., Coltorti, M., Siena F., 2005. Kimberlite-like metasomatism and “garnet signature” in spinel-peridotite xenoliths from Sal, Cape Verde Archipelago: relics of a subcontinental mantle domain within the Atlantic Oceanic Lithosphere?. Journal of Petrology 46, 2465-2493.

Boyd, F.R., 1989. Compositional distinction between oceanic and cratonic lithosphere. Earth and Planetary Science Letters 96, 15-26.

Boyd, F.R., Pokhilenko, N.P., Pearson, D.G., Mertzman, S.A., Sobolev, N.V., Finger, L.W., 1997. Composition of the Siberian cratonic mantle: evidence from Udachnaya peridotite xenoliths. Contributions to Mineralogy and Petrology 128, 228-246.

Brey, G.P., Doroshev, A.M., Girnis, A.V., Turkin, A.I., 1999. Garnet-spinel-orthopyroxene equilibria in the FeO-MgO-Al_2O_3-SiO_2-Cr_2O_3 system; I, composition and molar volumes of minerals. European Journal of Mineralogy 11, 599-617.

Brey, G.P., Köhler, T.P., 1990. Geothermobarometry in four-phase lherzolites II. New thermobarometers, and practical assessment of existing thermobarometers. Journal of Petrology 31, 1353-1378.

Caldeira, R., Munhá J.M., 2002. Petrology of ultramafic nodules from Sao Tomé Island, Cameroon Volcanic Line (oceanic sector). Journal of African Earth Sciences 34, 231-246.

Carminati, E., Doglioni, C., 2012. Alps vs Apennines: the paradigm of a tectonically asymmetric Earth. Earth-Science Reviews 112, 67-96.

Catalano, R., Doglioni, C., Merlini, S., 2000. On the Mesozoic Ionian basin. Geophysical Journal International 144, 49-64.

Coltorti, M., Beccaluva, L., Bonadiman, C., Salvini, L., Siena, F., 2000. Glasses in mantle xenoliths as geochemical indicators of metasomatic agents. Earth and Planetary Science Letters 183, 303-320.

Coltorti, M., Bonadiman, C., Hinton, R.W., Siena, F., Upton, B.G.J., 1999. Carbonatite metasomatism of the oceanic upper mantle: evidence from clinopyroxenes and glasses in ultramafic xenoliths of Grande Comore, Indian Ocean. Journal of Petrology 40, 133-165.

Coltorti, M., Bonadiman, C., O'Reilly S.Y., Griffin, W.L., Pearson, N.J., 2010. Buoyant ancient continental mantle embedded in oceanic lithosphere (Sal Island, Cape Verde Archipelago). Lithos 120, 223-233.

Dasgupta, R., Hirschmann, M.M., 2006. Melting in the Earth's deep upper mantle caused by carbon dioxide. Nature 440, 659-662.

Dasgupta, R., Hirschmann, M.M., McDonough, W.F., Spiegelman, M., Withers, A.C., 2009. Trace element partitioning between garnet lherzolite and carbonatite at 6.6 and 8.6 GPa with applications to the geochemistry of the mantle and of mantle-derived melts. Chemical Geology 2009, 57-77.

Dasgupta, R., Hirschmann, M.M., Smith, N.D., 2007. Partial melting experiments of peridotite+CO_2 at 3GPa and genesis of alkali ocean island basalts. Journal of Petrology 48, 2093-2124.

Dasgupta, R., Mallik, A., Tsuno, K., Withers, A.C., Hirth, G., Hirschmann M.M., 2013. Carbon-dioxide-rich silicate melt in the Earth's upper mantle. Nature 493, 211-215.

De Vecchi, G., Gregnanin, A., Piccirillo, E.M., 1976. Tertiary volcanism in the Veneto. Magmatology, petrogenesis and geodynamics implications: Geologische Rundschau 65, 701-710.

De Vecchi, G., Sedea, R., 1995. The Paleogene basalts of the Veneto region (NE Italy). Memorie di Scienze Geologiche 47, 253-374.

Dixon, J., Clague, D.A., Cousens, B., Monsalve, M.L., Uhl, J., 2008. Carbonatite and silicate melt metasomatism of the mantle surrounding the Hawaiian plume: evidence from volatiles, trace elements, and radiogenic isotopes in rejuvenated-stage lavas from Niihau, Hawaii. Geochemistry, Geophysics, Geosystems 9.

Eggins, S.M., Rudnick, R.L., McDonough, W.F., 1998. The composition of peridotites and their minerals: a laser-ablation ICP-MS study. Earth and Planetary Science Letters 3, 247-254.

Eggler, D.H., Furlong, K.P., 1991. Destruction of subcratonic mantle keel: the Wyoming Province. 5^{th} Kimberlite Conference Extended Abstracts, 85-87.

Fan, W.M., Menzies, M.A., 1992. Destruction of aged lower lithosphere and accretion of asthenosphere mantle beneath eastern China. Geotectonica et Metallogenia 16, 171-180.

Foley, S.F., 2008. Rejuvenation and erosion of the cratonic lithosphere. Nature Geoscience 1, 503-510.

Foley, S.F., 2011. A reappraisal of redox melting in the Earth's mantle as a function of tectonic setting and time. Journal of Petrology 52, 1363-1391.

Frost, D.J., McCammon, C.A. 2008. The redox state of Earth's Mantle. Annual Review of Earth and Planetary Sciences 36, 389-420.

Gasperini, D., Bosch, D., Braga, R., Bondi, M., Macera, P., Morten, L., 2006. Ultramafic xenoliths from the Veneto Volcanic Province (Italy): Petrological and geochemical evidence for multiple metasomatism of the SE Alps mantle lithosphere. Geochemical Journal 40, 377-404.

Giese, P., Buness, H., 1992. Moho depth, atlas map 2, in In Blundell, D., Freeman, R., Müller, S., (Eds.), A Continent Revealed: The European Geotraverse. New York, Cambridge University Press, p. 275.

Goncharov, A.G., Ionov, D.A., Doucet, L.S, Pokhilenko, L.N., 2012. Thermal state, oxygen fugacity and C-O-H fluid speciation in cratonic lithospheric mantle: New data on peridotite xenoliths from the Udachnaya kimberlite, Siberia. Earth and Planetary Science Letters 357-358, 99-110.

Green, D.H., 2015. Experimental petrology of peridotites, including effects of water and carbon on melting in the Earth's upper mantle. Physics and Chemistry of Minerals 42, 95-122.

Green, D.H., Hibberson, W., 1970. The instability of plagioclase in peridotite at high pressure. Lithos 3, 209-221.

Green, D.H., Ringwood, A.E., 1970. Mineralogy of peridotitic compositions under upper-mantle conditions. Physics of the Earth and Planetary Interiors 3, 359-371.

Greenfield, A.M.R., Ghent, E.D., Russell, J.K., 2013. Geothermobarometry of spinel peridotites from southern British Columbia: implications for the thermal conditions in the upper mantle. Canadian Journal of Earth Sciences 50, 1019-1032.

Grégoire, M., Bell, D.R., Le Roex A.P., 2003. Garnet lherzolites from the Kaapval Carton (South Africa): trace element evidence for a metasomatic history. Journal of Petrology 44, 629-657.

Griffin, W.L., Doyle, B.J., Ryan, C.G., 1999. Layered mantle lithosphere in the Lac de Gras area, Slave Craton: composition, structure and origin. Journal of Petrology 40, 705-727.

Griffin, W.L., O'Reilly, S.Y., 2007. Cratonic lithospheric mantle: is anything subducted?. Episodes 30, 43-53.

Gudfinnsson, G.H., Presnall, D.C, 2005. Continuous gradations among primary carbonatitic, kimberlitic, melilititic, basaltic, picritic and komatiitic melts in equilibrium with garnet lherzolite at 3-8 GPa. Journal of Petrology 46, 1645-1659.

Hammouda, T., Keshav, S., 2015. Melting in the mantle in the presence of carbon: review of experiments and discussion on the origin of carbonatites. Chemical geology 418, 171-188.

Heaman, L.M., Creaser, R.A., Cookenboo, H.O., 2002. Extreme enrichment of high field strength elements in Jericho eclogite xenoliths: a cryptic record of Paleoproterozoic subduction, partial melting, and metasomatism beneath the Slave Craton, Canada. Geology 30, 507-510.

Hellebrand, E., Snow, J.E., Dick, H.J., Hofmann, A.W., 2001. Coupled major and trace elements as indicators of the extent of melting in mid-ocean-ridge peridotites. Nature 410, 677-681.

Henderson, P., 1984. General geochemical properties and abundances of the rare earth elements, in: Henderson, P. (Ed), Rare Earth Element Geochemistry. Elsevier, Amsterdam, pp. 1-32

Hirose, K., 1997. Partial melt compositions of carbonate peridotites at 3 GPa and role of CO_2 in alkali-basalt magma generation. Geophysical Research Letters 24, 2837-2840.

Hoernle, K., Zhang, Y., Graham, D., 1995. Seismic and geochemical evidence for large-scale mantle upwelling beneath the eastern Atlantic and western and central Europe. Nature 374, 34-39.

Hughes, H.S.R., McDonald, I., Faithfull, J.W., Downes, H., 2015. Trace-element abundances in the shallow lithospheric mantle of the North Atlantic Craton margin: implications for melting and metasomatism beneath Northern Scotland. Mineralogical Magazine 79, 877-907.

Ionov, D.A., 1998. Trace element composition of mantle-derived carbonates and coexisting phases in peridotite xenoliths from alkali basalts. Journal of Petrology 39, 1931-1941.

Ionov, D.A., Bodinier, J-L, Mukasa, S.B., Zanetti, A., 2002. Mechanisms and sources of mantle metasomatism: major and trace element compositions of peridotite xenoliths from Spitsbergen in the context of numerical modelling. Journal of Petrology 43, 2219-2259.

Ionov, D.A., Doucet, L.S., Ashchepkov, I.V., 2010. Composition of the lithospheric mantle in the Siberian Craton: new constraints from fresh peridotites in the Udachnaya-East Kimberlite. Journal of Petrology 51, 2177-2210.

Jacob, D.E., Schimickler, B., Schulze, D.J., 2003. Trace element geochemistry of coesite-bearing eclogites from the Roberts Victor kimberlite, Kaapval Craton. Lithos 71, 337-351.

Karner, J.M., Papike, J.J., Sutton, S.R., Burger, P.V., Shearer, C.K., Le, L., Newville, M., Choi, Y., 2010. American Mineralogist 95, 410-413.

Kelemen, P.B., Hart, S.R., Bernstein, S., 1998. Silica enrichment in the continental upper mantle via melt/rock reaction. Earth and Planetary Science Letters 164, 387-406.

Klemme, S., Vanderlaan, S.R., Foley, S.F., Gunther, D., 1995. Experimentally determined trace and minor element partitioning between clinopyroxene and carbonatite melt under upper-mantle conditions. Earth and Planetary Science Letters 133, 439-448.

Köhler T.P., Brey, G.P., 1990. Calcium exchange between olivine and clinopyroxene calibrated as a geothermobarometer for natural peridotites from 2 to 60 kb with applications. Geochimica et Cosmochimica Acta 54, 2375-2388.

Lenoir, X. Carlos, C.J., Bodinier J-L., Dautria J-M., 2000. Contrasting lithospheric mantle domains beneath the Massif Central (France) revealed by geochemistry of peridotite xenoliths. Earth and Planetary Science Letters 181, 359-375.

Liu, J., Scott, J.M., Martin, C.E., Pearson D.G., 2015. The longevity of Archean mantle residues in the convecting upper mantle and their role in young continent formation. . Earth and Planetary Science Letters 424, 109-118.

Lustrino, M., Duggen, S., Rosenberg, C.L., 2011. The central-western Mediterranean: anomalous igneous activity in an anomalous collisional tectonic setting. Earth-Science Reviews 104, 1-40.

Lustrino, M., Wilson M., 2007. The circum-Mediterranean anorogenic Cenozoic igneous province. Earth-Science Reviews 81, 1-65.

Marchesi, C., Garrido, C.J., Bosch, D., Bodinier, J-L., Gervilla, F., Hidas, K., 2013. Mantle refertilization by melts of crustal-derived garnet pyroxenite: evidence from the Ronda peridotite massif, southern Spain. Earth and Planetary Science Letters 362, 66-75.

McCoy-West, A.J., Bennett, V.C., Puchtel, I.S., Walker, R.J., 2013. Extreme persistence of cratonic lithosphere in the southwest Pacific: Paleoproterozoic Os isotopic signatures in Zealandia. Geology 41, 231-234.

McLennan, S. M., 2001. Relationships between the trace element composition of sedimentary rocks and upper continental crust. Geochemistry Geophysics Geosystems 2, 1021–1024.

Medaris, L.G., 1999. Garnet peridotites in Eurasian high-pressure and ultrahigh-pressure terranes: a diversity of origins and thermal histories. International Geology Review 41, 799-815.

Mercier, J.-C.C., Nicolas, A., 1975. Texture and fabrics of upper-mantle peridotites as illustrated by xenoliths from basalts. Journal of Petrology 16, 454-487.

Milani, L., Beccaluva, L., Coltorti, M., 1999. Petrogenesis and evolution of the Euganean magmatic complex, north eastern Italy. European Journal of Mineralogy 11, 379-399.

Morimoto, N., 1988. Nomenclature of pyroxenes. American Mineralogist 73, 1123-1133.

Morten, L., Taylor, L.A., Durazzo, A., 1989. Spinel in harzburgite and lherzolite inclusions from the San Giovanni Ilarione Quarry, Lessini Mountains, Veneto Region, Italy. Mineralogy and Petrology 40, 73-89.

Muttoni, G., Garzanti, E., Alfonsi, L., Birilli, S., Germani, D., Lowrie, W., 2001. Motion of Africa and Adria since the Permian: paleomagnetic and paleocliamtic constraints from northern Libya. Earth and Planetary Science Letters 192, 159-174.

Niu, Y., 2004. Bulk-rock major and trace element compositions of abyssal peridotites: implications for mantle melting, melt extraction and post-melting processes beneath mid-ocean ridges. Journal of Petrology 45, 2423-2458.

O'Neill, H. St C., Wall, V.J., 1987. The olivine-orthopyroxene-spinel oxygen geobarometer, the nickel curve, and the oxygen fugacity of the Earth's upper mantle. Journal of Petrology, 28, 1169-1191.

O'Reilly, S.Y., Chen, D., Griffin, W.L., Ryan, C.G., 1997. Minor elements in olivine from spinel lherzolite xenoliths: implications for thermobarometry. Mineralogical Magazine, 61, 257-269.

Panza, G.F., Suhaldoc, P., 1990. Properties of the lithosphere in collisional belts in the Mediterranean-A review. Tectonophysics 182, 39-46.

Pearson, D.G., Canil, D., Shirley, S.B., 2003. Mantle samples included in volcanic rocks: xenoliths and diamonds, in: Holland, H.D., Turekian, K.K. (eds) Treatise on Geochemistry-2nd edition, Elsevier, Amsterdam, 171-275.

Pearson, D.G., Shirey, S.B., Carlson, R.W., Boyd, F.R., Pokhilenko, N.P., Shimizu, N., 1995. Re-Os, Sm-Nd, and Rb-Sr isotope evidence for thick Archean lithospheric mantle beneath the

Siberian craton modified by multistage metasomatism. Geochimica et Cosmochimica Acta 59, 959-997.

Pelorosso, B., Bonadiman, C., Coltorti, M., Faccini, B., Melchiorre, M., Nftalos, T., Grégoire M., 2016. Pervasive, tholeiitic refertilisation and heterogeneous metasomatism in Northern Victoria Land lithospheric mantle (Antarctica). Lithos 248-251, 493-505.

Piccoli, G., 1966. Studio geologico del vulcanesimo paleogenico veneto. Memorie degli Istituti di Geologia e Mineralogia dell'Università di Padova 26, 100 pp.

Pokhilenko, N.P., Agashev, A.M., Litasov, K.D., Pokhilenko, L.N., 2015. Carbonatite metasomatism of peridotite lithospheric mantle: implications for diamond formation and carbonatite-kimberlite magmatism. Russian Geology and Geophysics 56, 280-295.

Schmid, S.M., Bernoulli, D., Fugenschuh, B., Matenco, L., Schefer, S., Schuster, R., Tschler, M., Ustaszewski, K., 2008. The Alpine-Carpathian-Dinaridic orogenic system: correlation and evolution of tectonic units. Swiss Journal of Geosciences 101, 139-183.

Schmid, S.M., Pfiffer, O.A., Schoenborn, G., Froitzheim, N., Kissling, E., 1997. Integrated cross section and tectonic evolution of the Alps along the eastern traverse. Results of NRP20; Deep Structure of the Swiss Alps (Eds.), 289-304.

Scott, J.M., Hodgkinson, A., Palin, J.M, Waight, T.E., van der Meer, Q.H.A., Cooper, A.F., 2014b. Ancient melt depletion overprinted by young carbonatitic meatsomatism in the New Zealand lithospheric mantle. Contributions to Mineralogy and Petrology 167, 1-17.

Scott, J.M., Waight, T.E., van der Meer, Q.H.A., Palin, J.M., Cooper, A.F., Münker, C., 2014a. Metasomatized ancient lithospheric mantle beneath the young Zealandia microcontinent and its role in HIMU-like intraplate magmatism. Geochemistry, Geophysics, Geosystems 15, 3477, 3501.

Scott, J.M., Liu, J., Pearson, D.G., Waight, T.E., 2016. Mantle depletion and metasomantism recorded in orthopyroxene in highly depleted peridotites. Chemical Geology 441, 280-291.

Sen, G., Frey, F.A., Schimizu, N., Leeman, W.P., 1993. Evolution of the lithosphere beneath Oahu, Hawaii: rare earth element abundances in mantle xenoliths. Earth and Planetary Science Letters 119, 53-69.

Siena, F., Coltorti, M., 1989. Lithospheric mantle evolution: evidences from ultramafic xenoliths in the Lessinean volcanics (Northern Itlay). Chemical Geology 77, 347-364.

Siena, F., Coltorti, M., 1993. Thermobarometric evolution and metasomatic processes of upper mantle in different tectonic settings: evidence from spinel peridotite xenoliths. European Journal of Mineralogy 5, 1073-1090.

Simon, N.S.C., Carlson R. W., Pearson, D.G., Davies G.R., 2007. The origin and the evolution of the Kaapval cratonic lithospheric mantle. Journal of Petrology 48, 589-625.

Simon, N.S.C., Irvine, G.J., Davies, G.R., Pearson, D.G., Carlson, R.W., 2003. The origin of garnet and clinopyroxene in "depleted" Kaapval peridotites. Lithos, 71, 289-322.

Spengler, D., Van Roermund, H.L.M., Drury, M.R., Ottolini, L., Mason, P.R.D., Davies, G.R., 2006. Deep origin and hot melting of an Archaean orogenic peridotite massif in Norway. Nature 440, 913-917.

Stagno, V., Frost, D.J., 2010. Carbon speciation in the asthenosphere: experimental measurements of the redox conditions at which carbonate-bearing melts coexist with graphite or diamond in peridotite assemblages. Earth and Planetary Science Letters 300, 72-84.

Streckeisen, A., 1974. Classification and nomenclature of plutonic rocks recommendations of the IUGS subcommission on the systematics of Igneous Rocks. Geologische Rundschau 63, 773-786.

Sun, J., Liu C-Z., Wu F-Y., Yang Y-H., Chu Z-Y., 2012. Metasomatic origin of clinopyroxene in Archean mantle xenoliths from Hebi, North China Craton: trace-element and Sr-isotope constraints. Chemical Geology 328, 123-136.

Sun, C., Liang, Y., 2014. An assessment of sub-solidus re-equilibration on REE distribution among mantle minerals olivine, orthopyroxene, clinopyroxene, and garnet in peridotites. Chemical Geology 372, 80-91.

Sun, S.S., McDonough, W.F., 1989. Chemical and isotopic systematics of oceanic basalts: implications for mantle composition and processes. In: Saunders, A.D, Norry, M.J. (Eds). Magmatism in the Oceanic Basins. Geological Society London, Special Publications 42, 313-346.

Takahashi, E., 1987. Origin of basaltic magmas-implications from peridotite melting experiments and an olivine fractionation model. Bulletin of the Volcanological Society of Japan 30, 17-40.

Taylor, W.R., 1998. An experimental test of some geothermometer and geobarometer formulations for upper mantle peridotites with application to the thermobarometry of fertile lherzolite and garnet websterite. Neues Jahrbuch für Mineralogie-Abhandlungen 172, 381-408.

Tang, Y.J., Zhang, H.F., Deloule, E., Su, B.X., Ying, J.F., Xiao, Y., Hu., Y., 2012. Slab-derived lithium isotopic signatures in mantle xenoliths from northeastern North China Craton. Lithos 149, 79-90.

Tang, Y.J., Zhang, H.F., Ying, J.F., Su, B.X., 2013. Widespread refertilization of cratonic and circum-cratonic lithospheric mantle. Earth-Science Reviews 118, 45-68.

Tang, Y.J., Zhang, H.F., Ying, J.F., Zhang, J., Liu, X.M., 2008. Refertilization of ancient lithospheric mantle beneath the central North China Craton: evidence from petrology and geochemistry of peridotite xenoliths. Lithos 101. 435-452.

Tang, M., McDonough, W.F., Ash, R.D., 2017. Europium and strontium anomalies in the MORB source mantle. Geochimica et Cosmochimica Acta 197, 132-141.

von Blankenburg, F., Davies, J.H., 1995. Slab breakoff: amodel for syncollisional magmatism and tectonics in the Alps. Tectonics 14, 120-131.

Walter, M.J., 2003. Melt extraction and compositional variability in mantle lithosphere. The Mantle & Core. Treatise of Geochemistry-2nd edition. Elsevier, Amsterdam, 363-394.

Wells, P.R.A., 1977. Pyroxene thermometry in simple and complex systems. Contributions to Mineralogy and Petrology 62, 129-139.

Wilson, M., Patterson, R., 2001. Intraplate magmatism related to short-wavelength convective instabilities in the upper mantle: evidence from the Tertiary Quaternary volcanic province of western and central Europe. Geological Society of America Special Paper 352, 37-58.

Wood, B.J., Banno, S., 1973. Garnet-orthopyroxene and orthopyroxene-clinopyroxene relationship in simple and complex system. Contributions to Mineralogy and Petrology 42, 109-124.

Zampieri, D., 1995. Tertiary extension in the southern Trento Platform, southern Alps, Italy. Tectonics 14, 645-657.

Zhang, H.F., Goldstein, S.L., Zhou, X.H., Sun, M., Cai, Y., 2009a. Comprehensive refertilization of lithospheric mantle beneath the North China Craton: further Os-Sr-Nd isotopic constraints. Journal of the Geological Society, London 166, 249-259.

Zhang, H.F., Sun, Y.L., Tang, Y.J., Xiao, Y., Zhang, W.H., Zhao, X.M., Santosh, M., Menzies, M.A., 2012. Melt-peridotite interaction in the Pre-Cambrian mantle beneath the western North China Craton: petrology, geochemistry and Sr, Nd and Re isotopes. Lithos 149, 100-114.

Figure captions

Fig. 1. Geological map of the Veneto Volcanic Province (De Vecchi and Sedea, 1995), showing the location of Monte Gloso, xenolith site ~~in Marosticano volcanic district~~. Inset a) Locations of VVP in the Italian peninsula, European, African and Adria Plates. The white arrows show the subduction directions (modified ~~after~~ Carminati and Doglioni, 2012 ~~modified~~).

Fig. 2. Photomicrographs of representative ~~microstructures in the~~ MG xenoliths. (a) ~~clinopyroxene with cloudy, spongy rims near a kinked olivine;~~ (b) clinopyroxene with cloudy, spongy rims; (c) reaction areas surrounding ~~a~~ spinel, constituted by small crystals of olivine, clinopyroxene, spinel and rare glass; (d) orthopyroxene ~~crystals showing a~~ reaction rim composed of secondary clinopyroxene and olivine.

Fig. 3. Compositional variations vs mg# [=MgO/(MgO+FeO)mol%] for MG xenoliths, Lessini Mts. peridotites (from Beccaluva et al., 2001; Gasperini et al., 2006; Morten et al., 1989; Siena and Coltorti, 1989), Val d'Adige xenoliths (from Gasperini et al., 2006): (a) modal olivine compositional variation (wt.%) vs Fo, the "oceanic trend" (from Boyd, 1989) is also shown (b) olivine compositional variation in terms of Ni (ppm) vs. Fo; fields of olivines from Archean craton peridotites, both garnet and spinel facies (Kelemen et al., 1998) and Phanerozoic mantle array (Takahashi, 1987) are also plotted; (c) orthopyroxene compositional variation in terms of Al_2O_3 vs. mg#; (d) clinopyroxene compositional variation in terms of Al_2O_3 vs. mg#; (e) clinopyroxene compositional variation in terms of Na_2O vs. mg#; (f) clinopyroxene compositional variation in terms of TiO_2 vs. mg#; (g) spinel compositional variation in terms of Cr_2O_3 vs. mg# . In b, d, e, f hypothetical trend of interaction with M. Gloso host lava is shown. In d, e, f black crosses represent average major element compositions of cpx crystallized from silica-bearing carbonatite melts (from Dasgupta et al., 2009), they are plotted for defining metasomatic agents of MG xenoliths. Filled and open symbols are for lherzolite (Lh) and harzburgite (Hz), respectively.

Fig. 4. Chondrite-normalized (Sun and McDonough, 1989) incompatible trace elements diagrams for opx in MG lherzolites (a) and harzburgites (b).

Fig. 5. Chondrite-normalized (Sun and McDonough, 1989) incompatibile trace elements diagrams of cpx group-1 (a) and cpx group-2 (b). Chondrite-normalized (Sun and McDonough, 1989) REE patterns of cpx group-1 (c) and cpx group-2 (d).

Fig. 6. Comparison of chondrite-normalized (Sun and McDonough, 1989) trace element distributions of MG cpx (this study) and primary, spongy, secondary cpx from VVP xenoliths

(Beccaluva et al., 2001) that exhibit comparable cpx modal contents and cpx-opx mg# values. Patterns of VVP cpx (Beccaluva et al., 2001) are represented with shadowed areas.

Fig. 7. Temperatures and ΔlogfO_2 relative to the buffer reaction fayalite-quartz-magnetite (ΔlogfO_2 FQM). Temperatures are calculated using the approach of Brey and Köhler (1990). ΔlogfO_2 estimates are calculated with the method of Ballhaus et al., 1991. P is fixed at 1.5 GPa. Filled and open symbols are for lherzolite (Lh) and harzburgite (Hz), respectively. T-fO_2 conditions of Lessini and Val d'Adige lherzolites are calculated using EMP data from Gasperini et al., 2006. Shadowed area represents the T-fO_2 range of highly metasomatized Lessini xenoliths previously reported in Siena and Coltorti (1989).

Fig. 8. Comparison of chondrite-normalized REE patterns of MG cpx (this study), carbonatitic/CO_2-rich silicate melt experimentally obtained at pressure 6.6GPa in equilibrium with garnet (Dasgupta et al., 2009) and modeled cpx formed by a carbonatitic/CO_2-rich silicate melt applying ${}^{cpx/carb}D$ calculated at 2 GPa 1100-1150°C (Klemme et al., 1995) (shadowed area). Chondrite compositions for the normalisation of all compositions are from Sun and McDonough (1989).

Fig. 9. Orthopyroxene Ti (ppm) and Al_2O_3 (wt.%) contents are consistent with depletion due to melt extraction followed by Ti enrichment due to and CO_2-rich silicatic metasomatism (from Scott el al., 2016).

Fig. 10. Oxygen fugacity (ΔlogfO_2) vs. temperature for MG xenoliths. Stability fields of diamond, graphite and carbonates are delineated by the graphite/diamond transition and the EMOD/G and D/GCO oxygen buffers (Goncharov et al., 2012 and references therein). Almost all the Marosticano peridotites straddle the fields for carbonatite and CO_2 fluid suggesting that the Marosticano

geothermobarometric conditions record the interaction between matrix and carbonatite/CO_2-rich silicate metasomatic melts.

Fig. 11. Summary sketch of the model presented of the processes significant in the VVP mantle during the European/Adria collision. Purple denotes the cratonic keel preserved beneath the Marosticano district, and blue represents the refertilized cratonic portions due to the infiltration of asthenospheric-derived melts beneath the Lessini Mts. and Val d'Adige districts.

Supplementary material

1. **Analytical methods**

Major element compositions of minerals from xenoliths and host lavas were analyzed at the Istituto di Geoscienze e Georisorse, CNR, Padua (Italy) on Electron MicroProbe (EMP), using ZAF on-line data reduction and matrix correction procedure. An acceleration voltage of 20 keV and sample currents of 20 nA with 10-20 s counting time on peak position was used. Synthetic oxide standards (MgO, FeO, MnO, ZnO, NiO, Al_2O_3, Cr_2O_3, TiO_2 and SiO_2) were used. Analytical precision is better than ±2% for elements in the range of >10 wt.%, better than 5% for elements in the range 2-10 wt.%, and better than 10% for elements in the range 0.5-2 wt.%.

Trace element concentrations in cpx and opx were obtained by Laser Ablation Inductively Coupled Plasma Mass Spectrometry (LA-ICP-MS) at the Department of Earth Sciences, University of New Hampshire (USA) using an Analyte Excite 193 nm excimer laser plumbed into a Nu instruments AttoM high resolution inductively coupled plasma mass spectrometer. Typical spot size was 65 μm, and laser operating conditions were 6.0 mJ at 80% output, fluence of 8.1 J/cm^2 and repetition rate of 5 Hz. Silicate glass MPI-Ding standard, ML3B-G (Jochum et al., 2006), was used as the calibration standard every four sample spots to correct for within-run instrumental drift. Resulting data were then processed with the Iolite software package, using calcium data from EMPA as an internal standard. Precision and accuracy were assessed to be within 10% for ppm-level concentrations by repeated measurements of KH-1 and KL2-G as independent standards. Results of the repeated "blind" standard results are present in Supplementary material Table G.

Two out of five samples only were suitable for bulk rock analyses. Major elements were determined by Wavelength Dispersive X-Ray Fluorescence Spectrometry (WDXRF) on pressed powder pellets at the Dipartimento di Fisica e di Scienze della Terra, Università di Ferrara (Italy), using an ARL Advant-XP spectrometer, following the full matrix correction method proposed by Traill and Lachance (1966). Accuracy is generally lower than 2% for major oxides.

References

Jochum, K.P., Stoll, B., Herwig, K., Willbold, M., Hofmann, A.W., et al., 2006. MPI-DING reference glasses for in situ microanalysis: new reference values for element concentrations and isotope ratios. Geochemistry Geophysics Geosystems 7.

Traill, R.J., Lachance, G.R., 1966. A practical solution to the matrix problem in X-ray analysis. Canadian Journal of Spectroscopy 11, 43-48.

On-line Supplementary material (Excel file)

Major (wt.%) abundances of representative olivine (Table A), orthopyroxenes (Table B), clinopyroxenes (Table C) and spinel (Table D) in MG spinel peridotite xenoliths. Trace element (ppm) abundances of representative orthopyroxenes (Table E), clinopyroxenes (Table F) in MG spinel peridotite xenoliths. Table G: Standard used for LA-ICP-MS analyses. The values are in ppm.

Refertilized mantle keel below the Southern Alps domain (North-East Italy): ~~evidence~~ Evidence from Marosticano refractory mantle peridotites

Formatted: Centered

Valentina Brombin[a]*, Costanza Bonadiman[a], Massimo Coltorti[a], M. Florencia Fahnestock[b], Julia G. Bryce[b], Andrea Marzoli[c]

[a] *Dipartimento di Fisica e di Scienze della Terra, Università di Ferrara, Italy; brmvnt@unife.it*

[b] *Department of Earth Science, University of New Hampshire, USA; julie.bryce@unh.edu; florencia.fahnestock@unh.edu*

[c] *Dipartimento di Geoscienze e IGG-CNR, Università di Padova, Italy; andrea.marzoli@unipd.it*

ABSTRACT

The Veneto Volcanic Province (VVP), a ~~Tertiary~~ Cenozoic magmatic province in northeastern Italy, is one of the widest volcanic areas of the Adria p~~P~~late. It consists of five main volcanic districts, ~~with the~~ and its most primitive products common~~ly~~ host~~ing~~ mantle xenoliths. In this study, we present a newly discovered ~~found~~ xenolith suite from the Marosticano district that ~~consists of~~contains peridotites ~~revealing~~ with compositional characteristics of mineral assemblages that ~~allow to depict~~provide insight into an unexpected nature for the sub-continental lithospheric mantle (SCLM) of the Adria plate. In contrast to xenoliths from other VVP sites previously studied ~~the majority of VVP xenolith population~~ (i.e.: Val d'Adige and Lessini Mts.), Marosticano xenoliths exhibit highly refractory compositions typical of on-craton peridotites. In particular, high olivine forsteritic contents (Fo: 91-93) indicate high degrees of partial melting (>25%) that should lead to the complete consumption of clinopyroxene. Major and trace element compositions further link these peridotite fragments to ~~Early~~ early Proterozoic cratonic mantle, and the juxtaposition of clinopyroxene within these rocks suggests like most on-craton clinopyroxene, Marosticano clinopyroxene have a metasomatic legacy. The i) LREE-enrichments of ~~these~~ Marosticano clinopyroxene~~s~~ and ii) the dissolved CO_2 mole fractions (up to 1.0) for the inferred clinopyroxene-forming melt ~~speak in favor of~~are consistent with carbonatite/CO_2-rich silicatic melts as ~~the~~ metasomatic agents. The latter could be responsible for the equilibrium temperatures (1033-1117 °C) and oxidizing conditions ($\Delta logfO_2$ (FMQ)=-0.6 - +1.1), anomalously high for a ~~proper~~ cratonic environment but similar to the off-craton VVP xenoliths.

The cratonic signature and carbonatite/CO_2-rich silicate ~~metasomatic~~ metasomatism ~~evidences~~ found together in the Marosticano mantle xenoliths reveal ~~how SCLM can preserve~~that ancient features can be preserved even in SCLM~~,~~ ~~even if drawn~~ in a young, active geodynamic ~~scenario~~ setting as the Adria plate boundary. In this framework Lessini Mts. and Val d'Adige xenoliths could be interpreted as the typical features of circumcratonic reminiscent domains affected by refertilization due to infiltration of asthenosphere-derived melts, rather than newly accreted "off-craton" SCLM. These new interpretations could be useful for completing the reconstruction of the Africa/Eurasia interplay during the Alpine collision.

HIGHLIGHTS

Petrology and geochemistry of newly discovered Adria ~~Plate~~ plate mantle xenoliths present~~s~~ unexpected cratonic features.

Xenolith c~~C~~linopyroxene~~s~~ record metasomatic overprinting of restitic peridotite from carbonatite/CO_2-rich silicate melts.

Cratonic keel is preserved only in the Marosticano district, while the rest of VVP mantle domains are interpreted as circumcratonic portions ~~liable~~ subject to rejuvenation ~~due to~~from asthenospheric-derived melts.

KEYWORDS

Veneto Volcanic Province, cratonic mantle xenoliths, carbonatite metasomatism, rejuvenation.

1. Introduction

The stability of continents is intimately linked to the underlying sub-continental lithospheric mantle (SCLM). Peridotite xenoliths hosted in intraplate basaltic rocks provide a useful way to evaluate the petrological features and evolution of the SCLM in terms of mineral compositions, modal abundance and to ~~evidence~~ fluid modification~~s by fluids~~ (Liu et al., 2015).

The mantle xenoliths occurring in Veneto Volcanic Province ~~Together with mantle xenoliths of Sardinia and Iblei Mts. (Sicily) (Beccaluva et al., 2009), the relevant number of xenolith sites occurring in Veneto Volcanic Province~~ (VVP; SE Alps, NE Italy, Fig. 1) depict~~s~~ the "big" picture of the SCLM beneath the Adria plate, the African promontory of the central-western Mediterranean area. ~~During~~ In the Cretaceous ~~this region~~the VVP region was involved in a convergence between Africa and Eurasia plates, inducing subduction processes of the latter southeastward (Schmid et al., 1997; von Blanckenburg and Davies, 1995). ~~Despite~~ In spite of the immense quantity of seismic, structural, petrologic, and geochemical data compiled over at least five decades, the Adria microplate (Fig. 1, inset) remains an enigmatic aspect in the geodynamic evolution of the Africa-Eurasia collision system (Carminati and Doglioni, 2012; Lustrino, et al., 2011). It has been considered either to be in crustal continuity with the African mainland or separated from the latter by an oceanic plate (Catalano et al., 2000; Lustrino et al., 2011; Muttoni et al., 2001; Schmid et al., 2008).

Mantle xenoliths from a few VVP localities ~~were already~~previously investigated (Lessini Mts. and Val d'Adige localities; Fig. 1) reveal~~ing~~ variably depleted mantle domains, which were subsequently enriched by one or more episodes of metasomatism as recorded by widespread interstitial recrystallized glassy patches (Beccaluva et al., 2001; Gasperini et al., 2006; Morten et al., 1989; Siena and Coltorti, 1989). In this paper, we describe results from a

~~The~~ petrological and geochemical study of ~~the new~~a newly discovered occurrence of mantle xenoliths from the Marostica Hills, ~~that constituted~~ in the Marosticano district of the VVP. ~~, may help to better~~We then interpret our findings to constrain the mantle domain underlying the northern (continental) sector of the Adria ~~Plate~~plate, with the ultimate goal of shedding insight into dynamic processes at work during plate boundary interaction ~~and ultimately to understand its relative plate motion~~ (Carminati and Doglioni, 2012).

2. Geological setting

The Central-Western Mediterranean area is a geologically young area, mostly developed during the last 30 Ma. G~~The g~~eological structures and the igneous activity ~~developed~~ within this ~~area~~ region are intimately linked with the relative movements of two large plates (Africa and Europe) plus a number of smaller continental and oceanic plates (e.g., Lustrino et al., 2011). A key smaller plate, likely ~~Between them, of particular relevance is the existence of~~ an African promontory, is the ~~called~~ Adria (or Apulia) plate in which ~~where~~ the VVP (Fig. 1) constitutes one of the largest and most important magmatic provinces. ~~In fact, d~~During the ~~Tertiary~~Cenozoic, the Veneto and Trentino regions were affected by extensive volcanic activity, mainly basic-ultrabasic in composition that took place intermittently from the l~~L~~ate Paleocene to the l~~L~~ate Oligocene (Barbieri et al., 1982, 1991; De Vecchi et al., 1976; De Vecchi and Sedea, 1995; Piccoli, 1966). Most of the VVP products are spread over a NNW to SSE elongated area of about 1,500 km^2. Five main volcanic districts can be defined from west to east (Fig. 1): (1) the Val d'Adige district, between Arco and Rovereto; (2) the Lessini Mts. district between Val d'Adige and the Schio-Vicenza tectonic line; (3) the Marosticano district, east of the Schio-Vicenza line; (4) the Berici Hills district, which is separated from (5) the Euganean Hills, the southernmost district, by the Riviera dei Berici line (Beccaluva et al., 2007). Most VVP volcanic products are relatively undifferentiated lavas, and range in composition from nephelinites to quartz (Qz)-normative tholeiitic basalts. They tend to be spatially and temporally distributed, becoming gradually younger and less alkaline toward SE. Differentiated products only occur in the Euganean district, where quartz-trachytes and rhyolites predominate (Milani et al., 1999, and references therein). Nephelinites and basanites commonly carry spinel-peridotite mantle xenoliths (Beccaluva et al., 2001; 2007).

The mafic volcanism in the VVP is thought to be related to extensional tectonics in the Southern Alps foreland as response to Alpine orogenesis (De Vecchi and Sedea, 1995; Milani et al., 1999; Zampieri, 1995). Geophysical data (Ansorge et al., 1992; Giese and Buness, 1992) indicate a rather normal thickness of the continental crust under the VVP, with a NW-SE elliptical mantle dome culminating at about 28 ~~Km~~ km beneath the Lessini Mts., while the lithosphere-asthenosphere boundary has been detected at a depth of ~100 ~~km~~ km (Panza and Suhadolc, 1990).

Isotopic signatures, notably $^{206}Pb/^{204}Pb$ and $^{87}Sr/^{86}Sr$ ratios (18.8-19.8 and 0.703-0.704, respectively) led Beccaluva et al. (2001, 2007) to argue that the SCLM beneath the Adria plate has been enriched by metasomatizing agents, likely including FOZO or HIMU components. This signature may be related to the European Asthenospheric Reservoir (EAR; Hoernle et al., 1995), a large mantle upwelling extending from the eastern Atlantic to Europe and the Mediterranean area.

Alternatively, Wilson and Patterson (2001), and more recently Lustrino and Wilson (2007) argued that this Tertiary-Quaternary volcanism is related to diapiric upwelling of small-scale, finger-like, convective instabilities from the base of the upper mantle.

3. Petrography

The Marosticano xenoliths were sampled in the quarry of Monte Gloso (MG), a few kilometers east of Marostica (Fig. 1). The basanitic host lavas show a porphyritic texture with phenocrysts of olivine, clinopyroxene, and magnetite set in a fine-grained groundmass composed of clinopyroxene, plagioclase, and oxides. The xenoliths are generally subrounded or (more rarely) angular, ranging in size from a few centimeters up to 10 cm. Heavy fracturing and alteration are present throughout of the suite. Only five samples were sufficiently fresh to permit a complete petrological characterization. These samples also showed no evidence of host magma infiltration.

The Marosticano xenoliths are peridotites with complete spinel-facies equilibration. They display a coarse-grained protogranular texture following the nomenclature of Mercier and Nicholas (1975). Two of the five investigated xenoliths are harzburgites with 4% clinopyroxene (cpx), one is low-cpx (6%) lherzolite and two are lherzolites with 9-13% cpx (Table 1). In two out of three lherzolites, orthopyroxene (opx) is modally scarce (12-14%) as compared to typical peridotites (e.g., Streckeisen, 1974). All Marosticano peridotites are ~~characterised~~ characterized by large crystals of olivine (ol) and opx (up to 2 mm across) with smaller grains of cpx (0.5-1 mm in size) and spinel (sp) (up to 1 mm across). These latter show a typical holly-leaf or lobate shape, while ol and pyroxene crystals display curvilinear grain boundaries. Kinking is common in ol, while opx display exsolution lamellae and, rarely, show sieved rims. Cpx are always smaller in size with respect to opx and show large cloudy portions (spongy cpx).

Several types of pyrometamorphic textures are superimposed on these features. They consist of (1) cloudy, spongy cpx crystals: the recrystallized portion generally replaces the whole crystal, in rare cases it covers only the rim zones (Fig. 2a, b); (2) reaction areas involving primary opx, cpx and sp, with a secondary assemblage made up of small crystals of ol, cpx, vermicular sp and rare glass (Fig. 2c, d); (3) brown to pale yellow glassy patches containing secondary crystals of ol, cpx and sp. The secondary paragenesis is generally too small to be ~~analysed~~ analyzed by Electron MicroProbe (EMP) and therefore was not considered for *in-situ* analysis.

4. Analytical methods

The modal composition of Marosticano samples was estimated by point counting with more than 1000 points for each thin section. Major element compositions of minerals from xenoliths and host lavas were determined by Electron Microprobe (EMP), using a Cameca SX50 instrument at the

Istituto di Geoscienze e Georisorse, CNR, Padova (Italy). Trace element concentrations in cpx and opx were obtained by Laser Ablation Inductively Coupled Plasma Mass Spectrometry (LA-ICP-MS) at the Department of Earth Sciences, University of New Hampshire (USA) using an Analyte Excite 193 nm excimer laser plumbed into a Nu instruments AttoM high-resolution inductively coupled plasma mass spectrometer. Two out of five samples only were sufficiently unaltereted so as to be suitable for bulk rock analysis, that which was performed on powder pellets using an ARL Advant-XP spectrometer at the Dipartimento di Fisica e di Scienze della Terra, Università di Ferrara (Italy). More extensive descriptions of the analytical procedures, together with the standards supporting the analyses, are reported in the on-line Supplementary material.

5. Mineral Chemistry

Within each xenolith, minerals are generally homogeneous in composition with no significant chemical variation between core and rims of the same crystal. The latter is observed only for spongy crystals and grains close to reaction areas (Fig. 2). When these areas are near the contact with host basanites, ol and cpx core and rim analyses were performed and compared with ol and cpx phenocrysts in order to check if they could be the result of the host magma infiltration. Representative analyses of ol, opx, cpx, and sp are reported in Tables A-D of the Supplementary online material.

5.1 Major element composition

Olivine is chemically unzoned in Monte Gloso (MG) lherzolites and harzburgites. It shows a narrow compositional range with Fo content [=100 x Mg/(Mg+Fe)$_{mol}$] varying from 91.3 to 92.2 for lherzolites and from 90.5 to 92.5 for harzburgites (Fig. 3a), with high Ni contents (2600-3620 ppm and 2670-3540 ppm in lherzolites and harzburgites, respectively). Though conspicuous variability

Formatted: Subscript

of Ni in ol within individual samples may suggest a potential interaction between MG xenoliths and the host magma, the invariant Fo contents for each sample are inconsistent with melt-xenolith reaction explaining the variable Ni contents. Specifically, it is noteworthy, that ol phenocrysts from the host lavas have Fo content ranging from 86.1 to 87.2 and Ni contents from 2240 to 2251 ppm, suggesting that melt-xenolith reaction may explain only a small component of the variable Ni contents found in the MG xenolith suite (Fig. 3b).

Opx from unreacted core to reacted rims is chemically unzoned and frequently contains elongate oriented rods of exsolved cpx. Opx mg# [=100 x Mg/(Mg+Fe)$_{mol}$] values vary from 91.2 to 92.8 for both lherzolites and harzburgites, like the coexisting ol grains. Contents of Al_2O_3 in opx are highly variable in lherzolite (1.68-4.18 wt.%) whereas a more restricted range is shown by harzburgites (1.78-2.60 wt.%), reflecting a common "harzburgitic" melting degree, or limited temperature-dependent subsolidus exchange with sp (Brey et al., 1999) (Fig. 3c). Contents of TiO_2 in lherzolites are more variable (0-0.07 wt.%) than those of harzburgites (0-0.03 wt.%).

By texture the most reactive phase, cpx bears evident compositional heterogeneity within each individual sample for most compositional features but mg#. Along with the coexisting ol and opx, mg#$_{cpx}$ ranges from 91.0 to 93.3 across all lithologies. By contrast, the Al_2O_3, Cr_2O_3 and to lesser extent Na_2O are highly variable in both lherzolite and harzburgite cpx. Lherzolites generally show a larger range in Al_2O_3 (1.73-4.53 wt.%), Cr_2O_3 (0.72-1.64 wt.%) and Na_2O (0.49-1.89 wt.%) compared to harzburgites (Al_2O_3= 0.63 to 3.79 wt.%; Cr_2O_3= 0.89-1.52 wt.%; Na_2O= 0.35-1.18 wt.%; Fig. 3). The high chromium contents classify these crystals as chromiferous cpx (Morimoto, 1988) with TiO_2 being always less than 0.60 wt.% (Fig. 3f). Mg# values in cpx for both lherzolite and harzburgite are not correlated with Al_2O_3, Na_2O, and TiO_2 distribution as would be expected for a mantle residual trend or, in turn, for alkaline basic-ultrabasic magma fractionation lines (Fig. 3d-f). Accordingly, we interpret negligible, if any interactions between peridotites and basanitic host lavas.

Large compositional variations are exhibited in sp cr# [=100 x Cr /(Cr+Al)$_{mol}$] and mg#, with overlapping values for both lherzolite and harzburgite. However, cr# and mg# are homogenous

Formatted: Subscript

Formatted: Font color: Auto, Subscript within each individual sample with the exception of harzburgite MG13 (Fig. 3g). Across the samples, cr# and mg# vary from Cr-rich in harzburgite (cr#: 38.3-67.2; mg#: 56.2-69.6) to Al-rich types in lherzolite (cr#: 30.4-52.7; mg#: 62.2-75.9).

5.2 Pyroxene trace elements

Representative *in situ* (LA-ICP-MS) trace element analyses of pyroxenes are reported in Tables E-F of the on-line Supplementary material. The values are shown in chondrite-normalized incompatible trace elements (Fig. 4a, b; 5a, b) and rare earth element (REE) diagrams (Fig. 5c, d). In order to characterise characterize the "original" features of the MG lithospheric domain prior to the metasomatic event trace element contents of the cores of both opx and unreacted cpx core were considered. One sample (harzburgite MG13) has only opx with rare cpx crystals occurring in reaction areas, where their small size (<30 μm) prevent high resolved quantitative analysis.

Both lherzolite and harzburgite bear opx with heavy REE (HREE) contents in a narrow range ($(Tb/Lu)_N$ in lherzolites= 0.05-0.44; in harzburgites= 0.13-0.47) but large light (L)- middle (M)REE variability between grains and samples (e.g., Eu_N). MG16 lherzolite shows distinctive opx REE contents with nearly flat M-HREE ($(Dy/Lu)_N$=0.39-0.49) and LREE downward convex enrichments ($(La/Nd)_N$=0.27-0.79) (Fig. 4a). MG1, MG6 lherzolite and MG14 harzburgite preserve residual M-HREE signatures ($(Dy/Lu)_N$=0.18-0.37; Fig. 4a, b) typical of the sp-stability field after melt extraction co-existing with an apparent LREE enrichment ($(La/Nd)_N$=1.05-13.1). In turn, opx of MG13 harzburgite shows an overall M-HREE enrichment ($(Dy/Lu)_N$=0.41-0.42; Fig. 4b). Finally, Ti shows both positive and negative anomalies in both xenolith rock types.

Across all lithologies MG cpx have an overall high REE content (ΣREE=185-621 ppm) and distinctive LREE enrichment relative to HREE (La_N up to 100 times chondritic; $(La/Yb)_N$ in lherzolites = 9.58-26.68; $(La/Yb)_N$ in harzburgites = 13.88-19.24).

The geochemical data, taken together, allow for two groups of cpx compositions to be defined. Group-1 includes cpx of lherzolites MG1, MG6 and harzburgites MG13, MG14, which shows an almost flat M-HREE pattern ($(Sm/Lu)_N$= 1.31-4.76) with abrupt (more than one order of magnitude) LREE-enrichment ($(La/Nd)_N$= 1.53-6.18). Almost all these cpx display a positive Eu anomaly ($\{Eu_N/[(Sm+Gd)_N/2]\}$= 1.07-1.68) (Fig. 5c). In turn, group-2 is constituted by cpx of MG16 lherzolite only, which show distinctive convex upward REE pattern with a steep negative slope from Nd to Lu ($(Nd/Lu)_N$=14.0-18.0) and a maximum at Pr_N (114-143) (Fig. 5d).

The entire MG cpx population has variable high Th and U content (Th and U up to 3.03 and 0.63 ppm, respectively) with negative anomalies in Ti and HFSE (e.g. Nb, Ta, Zr, and Hf), the most evident being the Zr anomaly in harzburgite with Zr* ($Zr_N/[(Nd+Hf)_N/2]$)=0.09-0.24 (Fig. 5a, b). It should be noted that MG unreacted cpx have trace elements contents similar or even higher than those of primary and secondary cpx from mantle xenoliths of the Lessini Mts. (Beccaluva et al., 2001; Fig. 6).

6. Geothermobarometry

To estimate the temperature conditions under which the MG sp lherzolites and harzburgites were equilibrated, we used the two-pyroxene geothermometer based on Fe/Mg exchange of Brey and Köhler (1990) which we will denote as T_{BK}. Ol-sp geothermometers of Wells (1977) and Taylor (1998) were also applied for comparative purposes and are denoted as T_W and T_T, respectively. For the thermo-barometric calculations, we considered only cores of unreacted opx and cpx grains that were in close contact.

Though some studies provide barometry, mainly based on the Ca distribution of ol and cpx (e.g., Köhler and Brey, 1990), determining appropriate barometry in sp-bearing peridotites (Medaris, 1999; O'Reilly et al., 1997) is challenging. Therefore, we assume the equilibrium pressure from experimental stability phase relationships (Caldeira and Munhá, 2002). Taking into account the absence of amphiboles (which could modify the peridotite mineral stability fields) and the presence of sp as the sole aluminum-bearing phase, an upper limit of 2.1 GPa and a lower limit of 0.9 GPa are set (Caldeira and Munhá, 2002; Green and Hibberson, 1970; Green and Ringwood, 1970; O'Neill and Wall, 1987; Siena and Coltorti, 1989). This pressure approximation agrees with the maximum depth of the local SCLM, constrained by seismic profiles (Carminati and Doglioni, 2012) to fall within the 1.5-2.0 GPa range. The pyroxene Fe/Mg exchange is largely dependent on temperature (Brey and Köhler, 1990; Wells, 1977; Wood and Banno, 1973) and is relatively insensitive to pressure; temperatures calculated at 1.0 GPa and 2.0 GPa show only minor variations (<10°C). Accordingly, primarily for comparative purposes, temperature calculations were made at a fixed pressure of 1.5 GPa.

6.1 Equilibration temperatures

MG sp-lherzolites record residual temperatures in the range of 923-1058°C. The highest value (MG16) is comparable with those recorded by the two MG harzburgites (MG13: 1117 ± 20°; MG14: 1033 ± 30°C; Table 2). This is in agreement with its low cpx content (6%), which could reflect a residual character analogous to harzburgites. We compared MG peridotites equilibration temperatures with those from the nearby districts of Lessini Mts. and Val d'Adige calculated with the Wells (1977) and Taylor (1998) geothermometers (Gasperini et al., 2006).

For comparison, equilibration temperature of a few Lessini Mts. and Val d'Adige peridotites were recalculated together with MG samples of this work applying the three thermobarometric models (Table 2). We observed that: i) as seen in other geothermobarometric studies (e.g., Greenfield et al., 2013), T_T values are always lower than T_{BK} and T_W; ii) with the exception of one sample from Lessini Mts., differences between T_{BK} and T_W within each sample are negligible (<20°C); iii) T_T diverges from T_{BK} by 2 to 78°C and diverges from T_W from by 19 to 78°C.

Taking this into account, the temperature range of 923-1117°C recorded by MG peridotites is higher than most of Val d'Adige (T_{BK}: 896-902°C) and of Lessini Mts. (T_{BK}: 885-975°C) xenoliths. Looking at the entire VVP mantle domain, the high equilibration temperatures recorded for MG mantle xenoliths are only comparable to the highly metasomatized Lessini Mts. peridotites (1130 ± 60°C) studied by Siena and Coltorti (1989) (Fig. 7).

6.2 Oxygen fugacity

Oxygen fugacities for Marosticano peridotites were estimated using the method of Ballhaus et al. (1991) using temperatures provided by the Brey-Köhler thermometer (T_{BK}). Calculated fO_2 values are plotted in Fig. 7 in logarithmic units with respect to the fayalite-magnetite-quartz (FMQ) buffer ($\Delta\log fO_2$). Estimates for the two sp-harzburgites range from +0.6 to +0.9, while for the sp-lherzolites the range is wider (-0.6 to +1.1), with MG6 lherzolite being the most reduced sample. With the exception of the latter xenolith, MG peridotites are more oxidized than Val d'Adige lherzolites (Table 2 and Fig. 7, $\Delta\log fO_2$ (FMQ) from +0.2 to +0.3 as calculated for compositions from Gasperini et al., 2006 and T_{BK} from Table 2). The Lessini Mts. peridotites also yield more variability in the recorded redox conditions ($\Delta\log fO_2$ (FMQ) from -1 to +1, calculated from data of Gasperini et al., 2006 and Siena and Coltorti, 1993; Table 2) encompassing the entire range of Marosticano and Val d'Adige samples (Fig. 7).

7. Discussion

7.1. A cratonic origin?

The highly refractory bulk composition of lherzolites (Al_2O_3 <1.03 wt.%, mg# 90.3-91.6; Table 3), associated with low Al_2O_3 contents, high mg# values in both pyroxenes and sp of MG peridotites (Fig. 3c-d and Tables B-D in the on-line Supplementary material) testify for a large extraction of basaltic melts from the Marosticano mantle domain which appears the most residual of the entire VVP (e.g., Lessini Mts. lherzolites: Al_2O_3 >2.52 wt.% and mg# 85.8-89.9).

Peridotites with refractory composition are expected in Phanerozoic and Proterozoic off craton mantle and ophiolites. They generally follow the so-called "residual or oceanic trend", explained as an extraction of basaltic components, resulting in an increase of Fo content in ol accompanied by increased ol modal content (Boyd, 1989). Refractory peridotites characterize also the cratonic mantle, but they rarely follow the oceanic trend (Bernstein et al, 2007; Boyd, 1989; Boyd et al., 1997; Ionov et al., 2010). They are characterized by ol with a range of high Fo content (~91-94) at extremely variable modal ol content (~40-75%). In particular, the high Fo of ol in sp-bearing (shallow) cratonic peridotites with relatively low opx modal content (<20%) (e.g., Tanzanian, Greenland, and Slave Cratons) are indicative of high degrees (~30 to 50%) of partial melting in thermal regime active only till Archean/~~Early~~ early Proterozoic time (Ionov et al., 2010; Walter, 2003).

MG ol plotted (Fig. 3a) in the Boyd diagram (Boyd, 1989; Boyd et al., 1997) plot off the oceanic trend, and follow the general behavior of cratonic ol (i.e. Kapvaal, Tanzanian, Greenland and Slave Cratons). While most of the Val d'Adige and Lessini Mts. exhibit lower ol modal contents at lower Fo following the oceanic trend (Fig. 3a). In addition Marosticano ol have also Ni values higher than those of Lessini Mts. but similar to those of Val d'Adige (Fig. 3b).

In association with high-Fo ol, MG peridotites show high Mg-opx in the range of 30-12% modal contents (Table 1), out of any "ideal" Phanerozoic (abyssal, oceanic and continental) off-craton melting trend (Niu, 2004; Pelorosso et al., 2016). Instead, they recall a general ol-opx behavior recorded in "shallow" (garnet-free) cratonic mantle and interpreted as physical segregation of ol and opx in high-pressure melting residuum and polybaric re-equilibration (Bernstein et al., 2007; Ionov et al., 2010). In addition, trace element distributions in opx from MG16 lherzolite and MG13 harzburgite show almost flat M-HREE profiles (i.e. $(Dy/Yb)_N$), consistent with an original subsolidus equilibrium with garnet (Bonadiman et al., 2005). In garnet-bearing lherzolites at progressively decreasing sub-solidus T (1300-900°C), opx decreases the total REE contents with equal M-HREE solid-solid partition coefficient (Sun and Liang, 2014). In turn opx of MG1, MG6 and MG14 seem to be originally equilibrated in the sp stability field showing the typical steep slope for M-HREE at comparable subsolidus temperature (1000-900°C) (Sun and Liang, 2014) (Fig. 4a, b).

Spinel, the distinctive phase of the great majority of off-craton mantle xenoliths, has cr# (30-67) which suggests a residual component neither coherent with the oceanic residual trend (i.e. "OSMA"; Arai, 1994a, 1994b) nor with the more fertile VVP-mantle fragment (cr# 9-12). On the other hand, Marosticano sp mimic the tendency observed for sp coexisting with ol in shallow on-craton (garnet-free) xenoliths (Bernstein et al., 2007).

In this refractory P-T system, ol Fo of 91.5 and sp cr# of 60.0 would suggest strong (or complete) cpx consumption by high degrees of partial melting (>25%; Bernstein et al., 2007; Bonadiman et al., 2005; Hellebrand et al., 2001; Scott et al., 2016; Walter, 2003) that are typical of the Archean or ~~Early~~ early Proterozoic mantle (Walter, 2003). Therefore, we suggest that the partial melting occurred at high melting T and thus more likely in an old mantle thermal regime. Subsequently, the Marosticano mantle was enriched, forming the observed cpx (cpx modal contents 4-13%) in MG xenolith. These are thus secondary in nature in accordance with several studies demonstrating that most cpx in on-craton mantle may have a metasomatic legacy (Grégoire et al., 2003; Pearson et al., 2003; Simon et al., 2003; 2007).

To sum up, Marosticano xenoliths are characterized by cratonic fingerprints (Fig. 3a), according to major and trace element compositions of the peridotite phases, and Re-Os geochronological modeling (T model age: 2.1-2.9; Brombin et al., in prep.). These geochemical characteristics are evident only for the Marosticano mantle fragments, whereas the rest of the VVP mantle is, as expected, off-craton SCLM. The sole, intriguing link between on-craton and off-craton VVP mantle is the similarity of the Re-Os ages, ranging between 1.9 to 2.1 Ga, with a unique value at 3.1 Ga for the entire VVP domain. These results speak in favor for a continuum geodynamic set which includes on-craton and off-craton mantle portions, as more frequently reported.

Cratonic signatures in off-craton sp-bearing mantle xenoliths derived from intra-plate volcanic areas are recognized in a few mantle xenolith populations, e.g. in the Massif Central (France; Lenoir et al., 2000), West Otago (New Zealand; Liu et al., 2015; Scott et al., 2014, 2016) and Cape Verde (Bonadiman et al., 2005; Coltorti et al., 2010).

In the Massif Central, two contrasting shallow lithospheric domains are faced. Relatively refractory (i.e., Al_2O_3 <2.0 wt.%) and highly fertile (i.e., Al_2O_3 >4.0 wt.%) lherzolites and harzburgites are interpreted as reminiscent of cratonic and circumcratonic SCLM domains, respectively (Lenoir, 2000). West Otago sp-peridotites with high variable Re depletion Os model ages (0.5-2.7 Ga) would represent relicts of Archean depleted mantle residues recycled through the asthenosphere over Ga timescales along with more fertile convecting mantle (Liu et al., 2015; McCoy-West et al., 2013). Therefore, different remnants of shallow lithospheric domains are incorporated within the young (<300 Ma) Zealandia microplate.

It is important to note that "shallow" (garnet-free) cratonic mantle is not exclusive of continental setting. Cape Verde Islands lie in the Atlantic Ocean, in a clearly oceanic setting. Here Archean sp-bearing mantle xenoliths, record garnet precursor and K-rich metasomatism (Bonadiman et al., 2005), suggesting the involvement of ancient geochemical reservoir also for the genesis of oceanic basalts (Coltorti et al., 2010).

Although Archean cratons are considered ancient continental nuclei characterized by tectonic inactivity for at least the past 2 Ga and low heat flow, recent studies show that their highly refractory mantle roots are intensively ~~modify~~ modified over ~~the~~ time by mechanical destructions (lithospheric thinning and incipient rifting) and by episodic rejuvenation events (Foley, 2008; Tang et al., 2013; Zhang et al., 2009a; Zhang et al., 2012).

The Wyoming Craton and North China Craton are well-known examples of complete chemical rejuvenation by varying degrees of refertilization (Eggler and Furlong, 1991; Fan and Menzies, 1992; Tang et al., 2008, 2012, 2013). In turn, other cratons might have not yet suffered large-scale removal of their ancient keels but they are in the early stages of disruption due to the efficiency of extensive regime (Foley, 2008). We recall that Lessini Mts. and Val d'Adige xenoliths are generally fertile lherzolites with cpx and opx coherently showing the typical LREE-depleted, M-REE flat and steep H-LREE fractionated patterns respectively (Beccaluva et al., 2001; Lenoir et al., 2000). These features are chemically contrasting with the refractory nature and the LREE enrichments of Marosticano xenolith population.

These differences could be interpreted in terms of compositional rejuvenation of the circumcratonic domains. Lessini Mts. and Val d'Adige xenoliths may be the fragments of the ancient SCLM, strongly refertilized by infiltration of asthenosphere-derived melts, rather than newly accreted "off-craton" SCLM. By contrast, Marosticano domain could be interpreted as the vestige of an old (Archean?) SCLM block that underwent depletion via melt extraction and was afterward pervasively metasomatized by CO_2-rich silicate melts, a process, ~~that~~ however, was not able to erase fully the original cratonic nature.

7.2 Metasomatic origin of clinopyroxene in Marosticano xenoliths

Despite the general refractory features of MG peridotites, a superimposed metasomatic process is manifested by major and trace element geochemistry of both pyroxenes. Trace-element compositions of Marosticano cpx show variable enrichment characteristics, inconsistent with a residual origin after melt extraction (e.g Sun et al., 2012). They exhibit a notable LREE-enrichment (Fig. 5c, d), a fractionated REE pattern and a general HFSE depletion (Fig. 5a, b) with respect to C1 model trace element abundances (Sun and McDonough, 1989). Taken together, these signatures confirm that cpx is a phase either formed by a reaction of a residual peridotite with metasomatic melts or it is a new phase directly ~~crystallised~~ crystallized from the metasomatic agents.

As nearby VVP districts (Lessini and Val d'Adige) are thought to have been affected by silicatic metasomatism (Beccaluva et al., 2001), we first evaluated whether the MG mantle segment could have been also explained by the same type of metasomatism. Taking into account only those Lessini and Val d'Adige samples that show cpx modal contents and cpx-opx mg# values comparable to those of MG xenoliths, trace element compositions of MG cpx are significantly enriched compared to the primary, spongy and secondary VVP cpx (Fig. 6). This suggests that MG were pervaded by a metasomatic agent that was different from that which affected the rest of the VVP region. However, both group-1 and group-2 cpx are more enriched in LREE (Fig. 5c, d) and depleted in Ti and in HFSE (e.g., Zr. Fig. 5a, b) arguing against a "pure" alkali silicate melt metasomatism and favouring instead the contribution of a carbonatic component. In fact, experimentally produced silica-bearing carbonatite melts crystallize cpx with major element composition similar to both MG group-1 and group-2 cpx (Fig. 3d-f).

Enrichment in LREE accompanied by strong HFSE depletion (Fig. 5a, b) of group-1 and group-2 cpx is notably assigned to an effect of the cpx-carbonatite partitioning as shown by experimental and empirical data by Dasgupta et al. (2009), Dixon et al. (2008), Gudfinnsson and Presnall (2005) and Pokhilenko et al. (2015). This geochemical effect has been observed in various carbonatite ~~metasomatised~~ metasomatized mantle xenoliths from both oceanic and continental settings (i.e: Spitsbergen, Ionov, 1998; North China Craton; Sun et al., 2012; New Zealand, Scott et al., 2016; Comores Archipelago; Coltorti et al, 1999).

Cpx group-2 mimics the steep M-HREE fractionated pattern, but they have remarkably higher LREE content with respect to cpx formed by a carbonatitic/CO_2-rich silicate melt experimentally obtained at pressure of 6.6 GPa in equilibrium with garnet (Dasgupta et al., 2009) (Fig. 8). The calculated $^{cpx/carb}D_{La}$ at this pressure is 0.006 but systematically increases with decreasing pressure and with the sp appearance (Dasgupta et al., 2009). Therefore, if we consider REE cpx/carbonatite partition coefficients calculated for 2 GPa and 1100-1150°C (e.g., $^{cpx/carb}D_{La}$ of 0.09; Klemme et al.,

1995) we can reproduce the general shape of the L- to M-HREE pattern of both MG cpx groups (Fig. 8).

The only remarkable difference between group-1 and group-2 cpx is that the former shows a less steep, or flat, HREE pattern indicating that carbonatitic melts migrated and interacted with slightly different peridotitic wallrocks. This could be attributed to a chromatographic fractionation of a metasomatic agent interacting with different peridotitic wallrock~~s~~ (Ionov et al., 2002; Sen et al., 1993). In this scenario, the concentration fronts of the migrating melts are controlled by the ion-exchange with the peridotitic matrix. In general, the fronts of the more incompatible elements (e.g., LREE) travel faster than those of less incompatible ones (e.g., M-HREE) producing enrichments in LREE and depletion or flatness in HREE of the whole rock depending on the original peridotitic matrix (Ionov et al., 2002). In this frame, the cpx group-1 records a continuum feeding of REE from the carbonatitic melt to a possible residual (primary?) cpx (Ionov et a., 2002; Pokhilenko et al., 2015; Sen et al., 1993). On the contrary, the convex-upward REE patterns of cpx group-2 may reflect nearly complete equilibration between the peridotite matrix (mainly ol-opx) and the metasomatic melt (Dasgupta et al., 2009; Dixon et al., 2008).

In anhydrous garnet-free peridotites, restitic opx is the counterpart of cpx to incorporate the incoming geochemical budget. The only evidence of metasomatic effects in the MG orthopyroxenes is their high Ti content (up to 281 ppm), not coherent with their low Al_2O_3 (Fig. 9; Scott et al., 2016) and in antithesis with the carbonatitic enrichment described for the cpx. This can be explained by the action of CO_2-rich silicate melts which could primarily impart a carbonatite-like trace element signature in cpx (i.e., L-REE) hiding the potential effects of silicate melts (i.e., Ti enrichment), that in turn is magnified in the residual opx (Scott, et al., 2016). Spinel-facies cpx prefers most trace elements, including Ti, compared to opx; however, relative to elements with slightly larger and smaller atomic radii (Eu and Dy), Ti is slightly less favorably partitioned into cpx (Eggins et al., 1998; Scott, et al., 2016). This nuance leads to the formation of small negative Ti anomalies in cpx and a corresponding positive anomaly in opx (Scott et al., 2016). Consequently, both negative and positive Ti anomalies observed in MG opx could be due to a chromatographic fractionation effect during the interaction between carbonatite/CO_2-rich silicate melts and a different peridotitic wallrock where cpx was present or not (~~Scott et al, 2016;~~ Ionov et al., 2002; Scott et al, 2016; Sen et al., 1993).

Though we cannot resolve if this metasomatism initially occurred in the garnet stability field and continued in shallower portions of the MG mantle we can assume that the product of such metasomatism may be stabilized at P conditions of the sp stability field. Accordingly, we interpret the geochemical characteristics (major and trace elements) acquired by MG pyroxenes as consistent with "new" cpx formed by the interaction of a carbonatitic melt with a cratonic flavored ambient peridotite (Griffin et al., 1999; Spengler et al., 2006). Notably, experimental studies (e.g., Dasgupta et al., 2006, 2007; Green, 2015; Hammouda and Keshav, 2015; Hirose, 1997) suggest that a carbon-rich peridotite is necessary to form alkaline and in particular ultra-alkaline mantle melts. Similarly, carbonatitic components have been hypothesized as important contributors to VVP alkaline- to ultra-alkaline magmas, the hosting lavas that ferry VVP mantle xenoliths to the surface (Beccaluva et al., 2007).

7.3 Relationship between carbonatite/CO_2-rich silicate metasomatism and fO_2 conditions

As carbonatitic/CO_2-rich silicate melts contain large amounts of dissolved fluids, they are able to mobilize volatile elements (C-OH-, but also Na and K as lithophile elements); accordingly, their interaction with the peridotite matrix may affect the redox conditions (Dasgupta et al., 2013). MG peridotites represent a cratonic "enclave" of continental mantle of the Adria ~~Plate~~ plate that was later pervaded by carbonatite metasomatism. The high fO_2 (Fig. 7), comparable with the other VVP mantle occurrences and within the range of the subcontinental lithospheric mantle (Foley, 2011), is not compatible with a cratonic origin but requires a late oxidation event, preserved until the xenolith exhumation by Cenozoic host lavas. Volatile mass transport occurs mostly by fluid and silicate (with prevailing H_2O) or carbonate melts (with prevailing CO_2) as function of the redox state of the mantle (Foley, 2008, 2011; Frost and McCammon et al., 2008; Pokhilenko et al., 2015). Assuming the relatively high ~~oxidising~~ oxidizing conditions of Marosticano peridotites were affected by CO_2-bearing melts, we calculated CO_2 mole fractions of such melt~~/~~(s) using the equation of Stagno and Frost (2010). We obtained CO_2 mole fractions close to or slightly higher than 1.0, taking into account the T-fO_2 values independently calculated from the silicate parageneses (Table 2). This is also evident in the diagram of fO_2 as a function of potential T (Goncharov et al., 2012), where almost all the Marosticano peridotites straddle the field for carbonatite and CO_2 fluid (Fig. 10). This may suggest that the Marosticano geothermobarometric conditions record this matrix/carbonatitic melt interaction, rather than the T-fO_2 values of the initial cratonic lithospheric mantle.

The variable redox states of the MG xenolith population may also influence the Eu oxidation state (Eu^{3+} or Eu^{2+}; Henderson, 1984) and may explain why this element is enriched in group-1 cpx. In oxidized magma Eu is an incompatible element in the trivalent form (Eu^{3+}), while in reduced magma it is preferentially incorporated into plagioclase in its divalent form (Eu^{2+}). This ion-exchange process explains the negative Eu anomaly in many terrestrial basalts showing plagioclase as liquid phase. However, Eu speciation is highly sensitive to small redox variations. Thus the different accommodation of Eu in minerals may change rapidly (McLennan, 2001).

Almost all group-1 cpx have M-HREE flat profiles with evident positive Eu anomaly (Fig. 5a, c). These anomalies are not accompanied by a positive K (not reported) or Sr anomaly, that could be assigned to the melting of pre-existing phlogopite and plagioclase respectively, in the protolith (Marchesi et al., 2013; Tang et al., 2017), neither of which were observed in any Marosticano xenolith. In other xenolith suites, examination of the Eu content in garnet and cpx in eclogites led to the suggestion that the positive Eu anomaly results from the interplay between crystal chemistry and redox conditions during metasomatism (Griffin and O'Reilly, 2007). Karner et al. (2010) determined the Eu partition coefficient between augite and melt (${}^{cpx/melt}D_{Eu}$) in samples ~~crystallised~~ crystallized from a highly Eu spiked Martian basalt composition at different fO_2 conditions. These authors observed that D_{Eu} augite/melt steadily increases with fO_2 since Eu^{3+} is more compatible than Eu^{2+} in the pyroxene structure; thus increasing fO_2 leads to greater Eu^{3+}/Eu^{2+} in the melt, allowing for more Eu (total) to partition into the cpx. It is worth noting that positive Eu anomalies are occasionally observed in cpx from metasomatized suboceanic mantle or subcontinental cratonic mantle in both sp and garnet stability field irrespective of the nature of the metasomatic melts (e.g., xenoliths from Loch Roag, North Atlantic Craton, Northern Scotland, Hughes et al., 2015; from Siberian Craton, Pearson et al., 1995; Slave Craton, Heaman et al., 2002; Kaapval craton, Jacob et al., 2003). On the basis of these considerations, we suggest that a small variation of the redox state may induce Eu to modify its solid/solid, solid/melt partitioning behavior, without any change of the large-scale geochemical process.

The interaction between the Marosticano residual mantle with a carbonatite/CO_2 rich silicate melt is explained by a possible chromatographic fractionation effect only in group-1 peridotite. This leads to a "local" variation of fO_2 ~~oxidising~~ oxidizing conditions and by consequence to a "local" increase of the Eu^{3+}/Eu^{2+} ratio in the melt and to higher Eu concentration in the newly formed cpx. Group-2 clinopyroxene is suggested to ~~crystallise~~ crystallize from the carbonatitic/CO_2-rich silicate melts that control the environmental redox condition.

8 Conclusions

- Petrological and geochemical features of the newly discovered Marosticano peridotite xenoliths indicate that they represent a mantle segment geochemically distinctive from the other VVP peridotites (i.e., Lessini Mts. and Val d'Adige), contributing to enlarge the knowledge of spatial heterogeneity within the mantle of this region.
- MG lherzolites and cpx-bearing harzburgites demonstrate complete sp-facies equilibration. Mineral major and trace elements features are comparable to those observed for on-craton peridotites worldwide.

- Marosticano cpx are secondary in nature and they exhibit a substantive LREE-enrichment, a fractionated REE pattern with positive Eu anomaly, almost flat (cpx group 1) or steep (cpx group 2) HREE patterns, and a remarkable HFSE depletion. These characteristics are attributed to a chromatographics separation of a metasomatic agent with high carbonatitic/CO_2-rich silicatic components.
- Marosticano samples record relatively high oxidation conditions similar to those of the VVP off-craton xenoliths (e.g. Lessini Mts.) but anomalous for a proper cratonic environment. These T-fO_2 relationships are probably due to the action oxidizing nature of CO_2-rich circulating fluids playing an oxidizing role.
- The variable, but generally high, redox states of the MG xenolith could be responsible for the positive Eu anomaly in cpx group-1. As higher fO_2 leads to higher Eu^{3+}/Eu^{2+} in the melt increasing the element partitioning in cpx, the positive Eu anomaly could result from the relatively high redox condition of the Marosticano mantle fragment during the formation of group-1 cpx. On the contrary, group-2 cpx that do not show positive Eu anomalies may show the fingerprint of a carbonatitic/CO_2-rich silicate melt metasomatism, therefore still recording the original redox condition.
- Within the SCLM sampled by VVP magmatism, only Marosticano xenoliths show evidence of carbonatitic metasomatic overprinting of a likely cratonic mantle domain. All the other mantle VVP mantle xenoliths exhibit characteristics of off-craton lithospheric mantle variably affected by Na-alkaline silicatic metasomatism.
- The lithospheric mantle beneath the Adria Plate plate has been affected by complex enrichment and refertilization processes, related to a geodynamic scenario dominated by extension-related magmatism in response to the near active collision between Eurasia and Africa plates (Fig. 11).
- The geochemical features of Marosticano mantle xenoliths introduce a cratonic component in the geodynamic evolution of the Adria Plate plate system in the general frame of the geodynamical reconstruction of the Africa/Eurasia collision. From our current study, together

with literature data, we interpret that the cratonic keel is preserved only in the Marosticano district, while Lessini Mts. and Val d'Adige mantle domains could be circumcratonic portions refertilized by infiltration of asthenospheric-derived melts (Fig. 11).

Acknowledgments

R. Carampin (I.G.G-C.N.R. Padova) is thanked for analytical assistance during the EMP analyses. The Italian National Research Program PRIN_2015/prot. 20158A9 (CB-AM) and the IUSS Mobility Research Programme of the University of Ferrara (VB scholarship for Abroad Mobility for Long Period) supported this research. We thank J.M. Scott and an anonymous referee for their constructive comments on a previous version of this paper and Andrew Kerr for his thoughtful suggestions and editorial handling.

References

Ansorge, J., Blundell, D., Müller, S., 1992. Europe's lithospheric structure, in Blundell D., Freeman, R., Müller, S. (Eds.), A Continent Revealed: The European Geotraverse. Cambridge University Press, New York, p. 275.

Arai, S., 1994a. Characterization of spinel peridotites by olivine-spinel compositional relationships; review and interpretation. Chemical Geology 113, 191-204.

Arai, S., 1994b. Compositional variation of olivine chromian spinel in Mg-rich magmas as a guide to their residual spinel peridotites. Journal of Volcanology and Geothermal Research 59, 279-293.

Ballhaus, C., Berry, R., Green, D., 1991. High pressure experimental calibration of the olivine-orthopyroxene-spinel oxygen geobarometer: implications for the oxidation state of the upper mantle. Contributions to Mineralogy and Petrology 107, 27-40.

Barbieri, G., De Zanche, V., Medizza, F., Sedea, R., 1982. Considerazioni sul vulcanesimo terziario del Veneto occidentale e del Trentino meridionale. Rendiconti della Società Geologica Italiana 4, 267-270.

Barbieri, G., De Zanche, V., Sedea, R., 1991. Evoluzione del semigraben paleogenico Alpone-Agno (Monti Lessini). Rendiconti della Società Geologica Italiana 14, 5-12.

Beccaluva, L., Bianchini, G., Bonadiman, C., Coltorti, M., Milani, L., Salvini, L., Siena, F., Tassinari, R., 2007. Intraplate lithospheric and sublithospheric components in the Adriatic domain: Nephelinite to tholeiite magma generation in the Paleogene Veneto Volcanic Province, Southern Alps. Geological Society of America 418, 131-152.

Beccaluva, L., Bianchini, G., Bonadiman, C., Coltorti, Siena, F., 2009. Petrological charactersitics of the Adriatic/North Africa lithospheric mantle: inferences from Cenozoic magmatism and mantle xenoliths. Rendiconti della Società Geologica Italiana 9, 79-84.

Beccaluva, L., Bonadiman, C., Coltorti, M., Salvini, L., Siena, F., 2001. Depletion events, nature of metasomatizing agent and timing of enrichment processes in lithospheric mantle xenoliths from the Veneto Volcanic Province. Journal of Petrology 42, 173-187.

Bernstein, S., Kelemen, P.B., Hanghøj, K., 2007. Consistent olivine Mg# in cratonic mantle reflects Archean mantle melting to the exhaustion of orthopyroxene. Geology 35, 459-462.

Bonadiman, C., Beccaluva, L., Coltorti, M., Siena F., 2005. Kimberlite-like metasomatism and "garnet signature" in spinel-peridotite xenoliths from Sal, Cape Verde Archipelago: relics of a subcontinental mantle domain within the Atlantic Oceanic Lithosphere?. Journal of Petrology 46, 2465-2493.

Boyd, F.R., 1989. Compositional distinction between oceanic and cratonic lithosphere. Earth and Planetary Science Letters 96, 15-26.

Boyd, F.R., Pokhilenko, N.P., Pearson, D.G., Mertzman, S.A., Sobolev, N.V., Finger, L.W., 1997. Composition of the Siberian cratonic mantle: evidence from Udachnaya peridotite xenoliths. Contributions to Mineralogy and Petrology 128, 228-246.

Brey, G.P., Doroshev, A.M., Girnis, A.V., Turkin, A.I., 1999. Garnet-spinel-orthopyroxene equilibria in the FeO-MgO-Al_2O_3-SiO_2-Cr_2O_3 system; I, composition and molar volumes of minerals. European Journal of Mineralogy 11, 599-617.

Brey, G.P., Köhler, T.P., 1990. Geothermobarometry in four-phase lherzolites II. New thermobarometers, and practical assessment of existing thermobarometers. Journal of Petrology 31, 1353-1378.

Caldeira, R., Munhá J.M., 2002. Petrology of ultramafic nodules from Sao Tomé Island, Cameroon Volcanic Line (oceanic sector). Journal of African Earth Sciences 34, 231-246.

Carminati, E., Doglioni, C., 2012. Alps vs Apennines: the paradigm of a tectonically asymmetric Earth. Earth-Science Reviews 112, 67-96.

Catalano, R., Doglioni, C., Merlini, S., 2000. On the Mesozoic Ionian basin. Geophysical Journal International 144, 49-64.

Coltorti, M., Beccaluva, L., Bonadiman, C., Salvini, L., Siena, F., 2000. Glasses in mantle xenoliths as geochemical indicators of metasomatic agents. Earth and Planetary Science Letters 183, 303-320.

Coltorti, M., Bonadiman, C., Hinton, R.W., Siena, F., Upton, B.G.J., 1999. Carbonatite metasomatism of the oceanic upper mantle: evidence from clinopyroxenes and glasses in ultramafic xenoliths of Grande Comore, Indian Ocean. Journal of Petrology 40, 133-165.

Coltorti, M., Bonadiman, C., O'Reilly S.Y., Griffin, W.L., Pearson, N.J., 2010. Buoyant ancient continental mantle embedded in oceanic lithosphere (Sal Island, Cape Verde Archipelago). Lithos 120, 223-233.

Dasgupta, R., Hirschmann, M.M., 2006. Melting in the Earth's deep upper mantle caused by carbon dioxide. Nature 440, 659-662.

Dasgupta, R., Hirschmann, M.M., McDonough, W.F., Spiegelman, M., Withers, A.C., 2009. Trace element partitioning between garnet lherzolite and carbonatite at 6.6 and 8.6 GPa with

applications to the geochemistry of the mantle and of mantle-derived melts. Chemical Geology 2009, 57-77.
Dasgupta, R., Hirschmann, M.M., Smith, N.D., 2007. Partial melting experiments of peridotite+CO_2 at 3GPa and genesis of alkali ocean island basalts. Journal of Petrology 48, 2093-2124.
Dasgupta, R., Mallik, A., Tsuno, K., Withers, A.C., Hirth, G., Hirschmann M.M., 2013. Carbon-dioxide-rich silicate melt in the Earth's upper mantle. Nature 493, 211-215.
De Vecchi, G., Gregnanin, A., Piccirillo, E.M., 1976. Tertiary volcanism in the Veneto. Magmatology, petrogenesis and geodynamics implications: Geologische Rundschau 65, 701-710.
De Vecchi, G., Sedea, R., 1995. The Paleogene basalts of the Veneto region (NE Italy). Memorie di Scienze Geologiche 47, 253-374.
Dixon, J., Clague, D.A., Cousens, B., Monsalve, M.L., Uhl, J., 2008. Carbonatite and silicate melt metasomatism of the mantle surrounding the Hawaiian plume: evidence from volatiles, trace elements, and radiogenic isotopes in rejuvenated-stage lavas from Niihau, Hawaii. Geochemistry, Geophysics, Geosystems 9.
Eggins, S.M., Rudnick, R.L., McDonough, W.F., 1998. The composition of peridotites and their minerals: a laser-ablation ICP-MS study. Earth and Planetary Science Letters 3, 247-254.
Eggler, D.H., Furlong, K.P., 1991. Destruction of subcratonic mantle keel: the Wyoming Province. 5th Kimberlite Conference Extended Abstracts, 85-87.
Fan, W.M., Menzies, M.A., 1992. Destruction of aged lower lithosphere and accretion of asthenosphere mantle beneath eastern China. Geotectonica et Metallogenia 16, 171-180.
Foley, S.F., 2008. Rejuvenation and erosion of the cratonic lithosphere. Nature Geoscience 1, 503-510.
Foley, S.F., 2011. A reappraisal of redox melting in the Earth's mantle as a function of tectonic setting and time. Journal of Petrology 52, 1363-1391.

Frost, D.J., McCammon, C.A. 2008. The redox state of Earth's Mantle. Annual Review of Earth and Planetary Sciences 36, 389-420.

Gasperini, D., Bosch, D., Braga, R., Bondi, M., Macera, P., Morten, L., 2006. Ultramafic xenoliths from the Veneto Volcanic Province (Italy): Petrological and geochemical evidence for multiple metasomatism of the SE Alps mantle lithosphere. Geochemical Journal 40, 377-404.

Giese, P., Buness, H., 1992. Moho depth, atlas map 2, in In Blundell, D., Freeman, R., Müller, S., (Eds.), A Continent Revealed: The European Geotraverse. New York, Cambridge University Press, p. 275.

Goncharov, A.G., Ionov, D.A., Doucet, L.S, Pokhilenko, L.N., 2012. Thermal state, oxygen fugacity and C-O-H fluid speciation in cratonic lithospheric mantle: New data on peridotite xenoliths from the Udachnaya kimberlite, Siberia. Earth and Planetary Science Letters 357-358, 99-110.

Green, D.H., 2015. Experimental petrology of peridotites, including effects of water and carbon on melting in the Earth's upper mantle. Physics and Chemistry of Minerals 42, 95-122.

Green, D.H., Hibberson, W., 1970. The instability of plagioclase in peridotite at high pressure. Lithos 3, 209-221.

Green, D.H., Ringwood, A.E., 1970. Mineralogy of peridotitic compositions under upper-mantle conditions. Physics of the Earth and Planetary Interiors 3, 359-371.

Greenfield, A.M.R., Ghent, E.D., Russell, J.K., 2013. Geothermobarometry of spinel peridotites from southern British Columbia: implications for the thermal conditions in the upper mantle. Canadian Journal of Earth Sciences 50, 1019-1032.

Grégoire, M., Bell, D.R., Le Roex A.P., 2003. Garnet lherzolites from the Kaapval Carton (South Africa): trace element evidence for a metasomatic history. Journal of Petrology 44, 629-657.

Griffin, W.L., Doyle, B.J., Ryan, C.G., 1999. Layered mantle lithosphere in the Lac de Gras area, Slave Craton: composition, structure and origin. Journal of Petrology 40, 705-727.

Griffin, W.L., O'Reilly, S.Y., 2007. Cratonic lithospheric mantle: is anything subducted?. Episodes 30, 43-53.

Gudfinnsson, G.H., Presnall, D.C, 2005. Continuous gradations among primary carbonatitic, kimberlitic, melilititic, basaltic, picritic and komatiitic melts in equilibrium with garnet lherzolite at 3-8 GPa. Journal of Petrology 46, 1645-1659.

Hammouda, T., Keshav, S., 2015. Melting in the mantle in the presence of carbon: review of experiments and discussion on the origin of carbonatites. Chemical geology 418, 171-188.

Heaman, L.M., Creaser, R.A., Cookenboo, H.O., 2002. Extreme enrichment of high field strength elements in Jericho eclogite xenoliths: a cryptic record of Paleoproterozoic subduction, partial melting, and metasomatism beneath the Slave Craton, Canada. Geology 30, 507-510.

Hellebrand, E., Snow, J.E., Dick, H.J., Hofmann, A.W., 2001. Coupled major and trace elements as indicators of the extent of melting in mid-ocean-ridge peridotites. Nature 410, 677-681.

Henderson, P., 1984. General geochemical properties and abundances of the rare earth elements, in: Henderson, P. (Ed), Rare Earth Element Geochemistry. Elsevier, Amsterdam, pp. 1-32

Hirose, K., 1997. Partial melt compositions of carbonate peridotites at 3 GPa and role of CO_2 in alkali-basalt magma generation. Geophysical Research Letters 24, 2837-2840.

Hoernle, K., Zhang, Y., Graham, D., 1995. Seismic and geochemical evidence for large-scale mantle upwelling beneath the eastern Atlantic and western and central Europe. Nature 374, 34-39.

Hughes, H.S.R., McDonald, I., Faithfull, J.W., Downes, H., 2015. Trace-element abundances in the shallow lithospheric mantle of the North Atlantic Craton margin: implications for melting and metasomatism beneath Northern Scotland. Mineralogical Magazine 79, 877-907.

Ionov, D.A., 1998. Trace element composition of mantle-derived carbonates and coexisting phases in peridotite xenoliths from alkali basalts. Journal of Petrology 39, 1931-1941.

Ionov, D.A., Bodinier, J-L, Mukasa, S.B., Zanetti, A., 2002. Mechanisms and sources of mantle metasomatism: major and trace element compositions of peridotite xenoliths from Spitsbergen in the context of numerical modelling. Journal of Petrology 43, 2219-2259.

Ionov, D.A., Doucet, L.S., Ashchepkov, I.V., 2010. Composition of the lithospheric mantle in the Siberian Craton: new constraints from fresh peridotites in the Udachnaya-East Kimberlite. Journal of Petrology 51, 2177-2210.

Jacob, D.E., Schimickler, B., Schulze, D.J., 2003. Trace element geochemistry of coesite-bearing eclogites from the Roberts Victor kimberlite, Kaapval Craton. Lithos 71, 337-351.

Karner, J.M., Papike, J.J., Sutton, S.R., Burger, P.V., Shearer, C.K., Le, L., Newville, M., Choi, Y., 2010. American Mineralogist 95, 410-413.

Kelemen, P.B., Hart, S.R., Bernstein, S., 1998. Silica enrichment in the continental upper mantle via melt/rock reaction. Earth and Planetary Science Letters 164, 387-406.

Klemme, S., Vanderlaan, S.R., Foley, S.F., Gunther, D., 1995. Experimentally determined trace and minor element partitioning between clinopyroxene and carbonatite melt under upper-mantle conditions. Earth and Planetary Science Letters 133, 439-448.

Köhler T.P., Brey, G.P., 1990. Calcium exchange between olivine and clinopyroxene calibrated as a geothermobarometer for natural peridotites from 2 to 60 kb with applications. Geochimica et Cosmochimica Acta 54, 2375-2388.

Lenoir, X. Carlos, C.J., Bodinier J-L., Dautria J-M., 2000. Contrasting lithospheric mantle domains beneath the Massif Central (France) revealed by geochemistry of peridotite xenoliths. Earth and Planetary Science Letters 181, 359-375.

Liu, J., Scott, J.M., Martin, C.E., Pearson D.G., 2015. The longevity of Archean mantle residues in the convecting upper mantle and their role in young continent formation. . Earth and Planetary Science Letters 424, 109-118.

Lustrino, M., Duggen, S., Rosenberg, C.L., 2011. The central-western Mediterranean: anomalous igneous activity in an anomalous collisional tectonic setting. Earth-Science Reviews 104, 1-40.

Lustrino, M., Wilson M., 2007. The circum-Mediterranean anorogenic Cenozoic igneous province. Earth-Science Reviews 81, 1-65.

Marchesi, C., Garrido, C.J., Bosch, D., Bodinier, J-L., Gervilla, F., Hidas, K., 2013. Mantle refertilization by melts of crustal-derived garnet pyroxenite: evidence from the Ronda peridotite massif, southern Spain. Earth and Planetary Science Letters 362, 66-75.

McCoy-West, A.J., Bennett, V.C., Puchtel, I.S., Walker, R.J., 2013. Extreme persistence of cratonic lithosphere in the southwest Pacific: Paleoproterozoic Os isotopic signatures in Zealandia. Geology 41, 231-234.

McLennan, S. M., 2001. Relationships between the trace element composition of sedimentary rocks and upper continental crust. Geochemistry Geophysics Geosystems 2, 1021–1024.

Medaris, L.G., 1999. Garnet peridotites in Eurasian high-pressure and ultrahigh-pressure terranes: a diversity of origins and thermal histories. International Geology Review 41, 799-815.

Mercier, J.-C.C., Nicolas, A., 1975. Texture and fabrics of upper-mantle peridotites as illustrated by xenoliths from basalts. Journal of Petrology 16, 454-487.

Milani, L., Beccaluva, L., Coltorti, M., 1999. Petrogenesis and evolution of the Euganean magmatic complex, north eastern Italy. European Journal of Mineralogy 11, 379-399.

Morimoto, N., 1988. Nomenclature of pyroxenes. American Mineralogist 73, 1123-1133.

Morten, L., Taylor, L.A., Durazzo, A., 1989. Spinel in harzburgite and lherzolite inclusions from the San Giovanni Ilarione Quarry, Lessini Mountains, Veneto Region, Italy. Mineralogy and Petrology 40, 73-89.

Muttoni, G., Garzanti, E., Alfonsi, L., Birilli, S., Germani, D., Lowrie, W., 2001. Motion of Africa and Adria since the Permian: paleomagnetic and paleoclimatic constraints from northern Libya. Earth and Planetary Science Letters 192, 159-174.

Niu, Y., 2004. Bulk-rock major and trace element compositions of abyssal peridotites: implications for mantle melting, melt extraction and post-melting processes beneath mid-ocean ridges. Journal of Petrology 45, 2423-2458.

O'Neill, H. St C., Wall, V.J., 1987. The olivine-orthopyroxene-spinel oxygen geobarometer, the nickel curve, and the oxygen fugacity of the Earth's upper mantle. Journal of Petrology, 28, 1169-1191.

O'Reilly, S.Y., Chen, D., Griffin, W.L., Ryan, C.G., 1997. Minor elements in olivine from spinel lherzolite xenoliths: implications for thermobarometry. Mineralogical Magazine, 61, 257-269.

Panza, G.F., Suhaldoc, P., 1990. Properties of the lithosphere in collisional belts in the Mediterranean-A review. Tectonophysics 182, 39-46.

Pearson, D.G., Canil, D., Shirley, S.B., 2003. Mantle samples included in volcanic rocks: xenoliths and diamonds, in: Holland, H.D., Turekian, K.K. (eds) Treatise on Geochemistry-2nd edition, Elsevier, Amsterdam, 171-275.

Pearson, D.G., Shirey, S.B., Carlson, R.W., Boyd, F.R., Pokhilenko, N.P., Shimizu, N., 1995. Re-Os, Sm-Nd, and Rb-Sr isotope evidence for thick Archean lithospheric mantle beneath the Siberian craton modified by multistage metasomatism. Geochimica et Cosmochimica Acta 59, 959-997.

Pelorosso, B., Bonadiman, C., Coltorti, M., Faccini, B., Melchiorre, M., Nftalos, T., Grégoire M., 2016. Pervasive, tholeiitic refertilisation and heterogeneous metasomatism in Northern Victoria Land lithospheric mantle (Antarctica). Lithos 248-251, 493-505.

Piccoli, G., 1966. Studio geologico del vulcanesimo paleogenico veneto. Memorie degli Istituti di Geologia e Mineralogia dell'Università di Padova 26, 100 pp.

Pokhilenko, N.P., Agashev, A.M., Litasov, K.D., Pokhilenko, L.N., 2015. Carbonatite metasomatism of peridotite lithospheric mantle: implications for diamond formation and carbonatite-kimberlite magmatism. Russian Geology and Geophysics 56, 280-295.

Schmid, S.M., Bernoulli, D., Fugenschuh, B., Matenco, L., Schefer, S., Schuster, R., Tschler, M., Ustaszewski, K., 2008. The Alpine-Carpathian-Dinaridic orogenic system: correlation and evolution of tectonic units. Swiss Journal of Geosciences 101, 139-183.

Schmid, S.M., Pfiffer, O.A., Schoenborn, G., Froitzheim, N., Kissling, E., 1997. Integrated cross section and tectonic evolution of the Alps along the eastern traverse. Results of NRP20; Deep Structure of the Swiss Alps (Eds.), 289-304.

Scott, J.M., Hodgkinson, A., Palin, J.M, Waight, T.E., van der Meer, Q.H.A., Cooper, A.F., 2014b. Ancient melt depletion overprinted by young carbonatitic meatsomatism in the New Zealand lithospheric mantle. Contributions to Mineralogy and Petrology 167, 1-17.

Scott, J.M., Waight, T.E., van der Meer, Q.H.A., Palin, J.M., Cooper, A.F., Münker, C., 2014a. Metasomatized ancient lithospheric mantle beneath the young Zealandia microcontinent and its role in HIMU-like intraplate magmatism. Geochemistry, Geophysics, Geosystems 15, 3477, 3501.

Scott, J.M., Liu, J., Pearson, D.G., Waight, T.E., 2016. Mantle depletion and metasomantism recorded in orthopyroxene in highly depleted peridotites. Chemical Geology 441, 280-291.

Sen, G., Frey, F.A., Schimizu, N., Leeman, W.P., 1993. Evolution of the lithosphere beneath Oahu, Hawaii: rare earth element abundances in mantle xenoliths. Earth and Planetary Science Letters 119, 53-69.

Siena, F., Coltorti, M., 1989. Lithospheric mantle evolution: evidences from ultramafic xenoliths in the Lessinean volcanics (Northern Itlay). Chemical Geology 77, 347-364.

Siena, F., Coltorti, M., 1993. Thermobarometric evolution and metasomatic processes of upper mantle in different tectonic settings: evidence from spinel peridotite xenoliths. European Journal of Mineralogy 5, 1073-1090.

Simon, N.S.C., Carlson R. W., Pearson, D.G., Davies G.R., 2007. The origin and the evolution of the Kaapval cratonic lithospheric mantle. Journal of Petrology 48, 589-625.

Simon, N.S.C., Irvine, G.J., Davies, G.R., Pearson, D.G., Carlson, R.W., 2003. The origin of garnet and clinopyroxene in "depleted" Kaapval peridotites. Lithos, 71, 289-322.

Spengler, D., Van Roermund, H.L.M., Drury, M.R., Ottolini, L., Mason, P.R.D., Davies, G.R., 2006. Deep origin and hot melting of an Archaean orogenic peridotite massif in Norway. Nature 440, 913-917.

Stagno, V., Frost, D.J., 2010. Carbon speciation in the asthenosphere: experimental measurements of the redox conditions at which carbonate-bearing melts coexist with graphite or diamond in peridotite assemblages. Earth and Planetary Science Letters 300, 72-84.

Streckeisen, A., 1974. Classification and nomenclature of plutonic rocks recommendations of the IUGS subcommission on the systematics of Igneous Rocks. Geologische Rundschau 63, 773-786.

Sun, J., Liu C-Z., Wu F-Y., Yang Y-H., Chu Z-Y., 2012. Metasomatic origin of clinopyroxene in Archean mantle xenoliths from Hebi, North China Craton: trace-element and Sr-isotope constraints. Chemical Geology 328, 123-136.

Sun, C., Liang, Y., 2014. An assessment of sub-solidus re-equilibration on REE distribution among mantle minerals olivine, orthopyroxene, clinopyroxene, and garnet in peridotites. Chemical Geology 372, 80-91.

Sun, S.S., McDonough, W.F., 1989. Chemical and isotopic systematics of oceanic basalts: implications for mantle composition and processes. In: Saunders, A.D, Norry, M.J. (Eds). Magmatism in the Oceanic Basins. Geological Society London, Special Publications 42, 313-346.

Takahashi, E., 1987. Origin of basaltic magmas-implications from peridotite melting experiments and an olivine fractionation model. Bulletin of the Volcanological Society of Japan 30, 17-40.

Taylor, W.R., 1998. An experimental test of some geothermometer and geobarometer formulations for upper mantle peridotites with application to the thermobarometry of fertile lherzolite and garnet websterite. Neues Jahrbuch für Mineralogie-Abhandlungen 172, 381-408.

Tang, Y.J., Zhang, H.F., Deloule, E., Su, B.X., Ying, J.F., Xiao, Y., Hu., Y., 2012. Slab-derived lithium isotopic signatures in mantle xenoliths from northeastern North China Craton. Lithos 149, 79-90.

Tang, Y.J., Zhang, H.F., Ying, J.F., Su, B.X., 2013. Widespread refertilization of cratonic and circum-cratonic lithospheric mantle. Earth-Science Reviews 118, 45-68.

Tang, Y.J., Zhang, H.F., Ying, J.F., Zhang, J., Liu, X.M., 2008. Refertilization of ancient lithospheric mantle beneath the central North China Craton: evidence from petrology and geochemistry of peridotite xenoliths. Lithos 101. 435-452.

Tang, M., McDonough, W.F., Ash, R.D., 2017. Europium and strontium anomalies in the MORB source mantle. Geochimica et Cosmochimica Acta 197, 132-141.

von Blankenburg, F., Davies, J.H., 1995. Slab breakoff: amodel for syncollisional magmatism and tectonics in the Alps. Tectonics 14, 120-131.

Walter, M.J., 2003. Melt extraction and compositional variability in mantle lithosphere. The Mantle & Core. Treatise of Geochemistry-2nd edition. Elsevier, Amsterdam, 363-394.

Wells, P.R.A., 1977. Pyroxene thermometry in simple and complex systems. Contributions to Mineralogy and Petrology 62, 129-139.

Wilson, M., Patterson, R., 2001. Intraplate magmatism related to short-wavelength convective instabilities in the upper mantle: evidence from the Tertiary Quaternary volcanic province of western and central Europe. Geological Society of America Special Paper 352, 37-58.

Wood, B.J., Banno, S., 1973. Garnet-orthopyroxene and orthopyroxene-clinopyroxene relationship in simple and complex system. Contributions to Mineralogy and Petrology 42, 109-124.

Zampieri, D., 1995. Tertiary extension in the southern Trento Platform, southern Alps, Italy. Tectonics 14, 645-657.

Zhang, H.F., Goldstein, S.L., Zhou, X.H., Sun, M., Cai, Y., 2009a. Comprehensive refertilization of lithospheric mantle beneath the North China Craton: further Os-Sr-Nd isotopic constraints. Journal of the Geological Society, London 166, 249-259.

Zhang, H.F., Sun, Y.L., Tang, Y.J., Xiao, Y., Zhang, W.H., Zhao, X.M., Santosh, M., Menzies, M.A., 2012. Melt-peridotite interaction in the Pre-Cambrian mantle beneath the western North China Craton: petrology, geochemistry and Sr, Nd and Re isotopes. Lithos 149, 100-114.

Figure captions

Fig. 1. Geological map of the Veneto Volcanic Province (De Vecchi and Sedea, 1995), showing the location of Monte Gloso, xenolith site in Marosticano volcanic district. Inset a) Locations of VVP in the Italian peninsula, European, African and Adria Plates. The white arrows show the subduction directions (modified after Carminati and Doglioni, 2012-modified).

Fig. 2. Photomicrographs of representative microstructures in the MG xenoliths. (a) clinopyroxene with cloudy, spongy rims near a kinked olivine; (b) clinopyroxene with cloudy, spongy rims; (c) reaction areas surrounding a spinel, constituted by small crystals of olivine, clinopyroxene, spinel and rare glass; (d) orthopyroxene crystals showing a reaction rim composed of secondary clinopyroxene and olivine.

Fig. 3. Compositional variations vs mg# [=MgO/(MgO+FeO)mol%] for MG xenoliths, Lessini Mts. peridotites (from Beccaluva et al., 2001; Gasperini et al., 2006; Morten et al., 1989; Siena and Coltorti, 1989), Val d'Adige xenoliths (from Gasperini et al., 2006): (a) modal olivine compositional variation (wt.%) vs Fo, the "oceanic trend" (from Boyd, 1989) is also shown (b) olivine compositional variation in terms of Ni (ppm) vs. Fo; fields of olivines from Archean craton peridotites, both garnet and spinel facies (Kelemen et al., 1998) and Phanerozoic mantle array (Takahashi, 1987) are also plotted; (c) orthopyroxene compositional variation in terms of Al_2O_3 vs. mg#; (d) clinopyroxene compositional variation in terms of Al_2O_3 vs. mg#; (e) clinopyroxene compositional variation in terms of Na_2O vs. mg#; (f) clinopyroxene compositional variation in terms of TiO_2 vs. mg#; (g) spinel compositional variation in terms of Cr_2O_3 vs. mg# . In b, d, e, f hypothetical trend of interaction with M. Gloso host lava is shown. In d, e, f black crosses represent average major element compositions of cpx ~~crystallised~~ crystallized from silica-bearing carbonatite

melts (from Dasgupta et al., 2009), they are plotted for defining metasomatic agents of MG xenoliths. Filled and open symbols are for lherzolite (Lh) and harzburgite (Hz), respectively.

Fig. 4. Chondrite-normalized (Sun and McDonough, 1989) incompatible trace elements diagrams for opx in MG lherzolites (a) and harzburgites (b).

Fig. 5. Chondrite-normalized (Sun and McDonough, 1989) incompatibile trace elements diagrams of cpx group-1 (a) and cpx group-2 (b). Chondrite-normalized (Sun and McDonough, 1989) REE patterns of cpx group-1 (c) and cpx group-2 (d).

Fig. 6. Comparison of chondrite-normalized (Sun and McDonough, 1989) trace element distributions of MG cpx (this study) and primary, spongy, secondary cpx from VVP xenoliths (Beccaluva et al., 2001) that exhibit comparable cpx modal contents and cpx-opx mg# values. Patterns of VVP cpx (Beccaluva et al., 2001) are represented with shadowed areas.

Fig. 7. Temperatures and $\Delta \log fO_2$ relative to the buffer reaction fayalite-quartz-magnetite ($\Delta \log fO_2$ FQM). Temperatures are calculated using the approach of Brey and Köhler (1990). $\Delta \log fO_2$ estimates are calculated with the method of Ballhaus et al., 1991. P is fixed at 1.5 GPa. Filled and open symbols are for lherzolite (Lh) and harzburgite (Hz), respectively. T-fO_2 conditions of Lessini and Val d'Adige lherzolites are calculated using EMP data from Gasperini et al., 2006. Shadowed area represents the T-fO_2 range of highly metasomatized Lessini xenoliths previously reported in Siena and Coltorti (1989).

Fig. 8. Comparison of chondrite-normalized REE patterns of MG cpx (this study), carbonatitic/CO_2-rich silicate melt experimentally obtained at pressure 6.6GPa in equilibrium with

garnet (Dasgupta et al., 2009) and modeled cpx formed by a carbonatitic/CO_2-rich silicate melt applying $^{cpx/carb}D$ calculated at 2 GPa 1100-1150°C (Klemme et al., 1995) (shadowed area). Chondrite compositions for the normalisation of all compositions are from Sun and McDonough (1989).

Fig. 9. Orthopyroxene Ti (ppm) and Al_2O_3 (wt.%) contents are consistent with depletion due to melt extraction followed by Ti enrichment due to and CO_2-rich silicatic metasomatism (from Scott el al., 2016).

Fig. 10. Oxygen fugacity ($\Delta \log fO_2$) vs. temperature for MG xenoliths. Stability fields of diamond, graphite and carbonates are delineated by the graphite/diamond transition and the EMOD/G and D/GCO oxygen buffers (Goncharov et al., 2012 and references therein). Almost all the Marosticano peridotites straddle the fields for carbonatite and CO_2 fluid suggesting that the Marosticano geothermobarometric conditions record the interaction between matrix and carbonatite/CO_2-rich silicate metasomatic melts.

Fig. 11. Summary sketch of the model presented of the processes significant in the VVP mantle during the European/Adria collision. Purple denotes the cratonic keel preserved beneath the Marosticano district, and blue represents the refertilized cratonic portions due to the infiltration of asthenospheric-derived melts beneath the Lessini Mts. and Val d'Adige districts.

Supplementary material

1. **Analytical methods**

Major element compositions of minerals from xenoliths and host lavas were analyzed at the Istituto di Geoscienze e Georisorse, CNR, Padua (Italy) on Electron MicroProbe (EMP), using ZAF on-line data reduction and matrix correction procedure. An acceleration voltage of 20 keV and sample currents of 20 nA with 10-20 s counting time on peak position was used. Synthetic oxide standards (MgO, FeO, MnO, ZnO, NiO, Al_2O_3, Cr_2O_3, TiO_2 and SiO_2) were used. Analytical precision is better than ±2% for elements in the range of >10 wt.%, better than 5% for elements in the range 2-10 wt.%, and better than 10% for elements in the range 0.5-2 wt.%.

Trace element concentrations in cpx and opx were obtained by Laser Ablation Inductively Coupled Plasma Mass Spectrometry (LA-ICP-MS) at the Department of Earth Sciences, University of New Hampshire (USA) using an Analyte Excite 193 nm excimer laser plumbed into a Nu instruments AttoM high resolution inductively coupled plasma mass spectrometer. Typical spot size was 65 µm, and laser operating conditions were 6.0 mJ at 80% output, fluence of 8.1 J/cm^2 and repetition rate of 5 Hz. Silicate glass MPI-Ding standard, ML3B-G (Jochum et al., 2006), was used as the calibration standard every four sample spots to correct for within-run instrumental drift. Resulting data were then processed with the Iolite software package, using calcium data from EMPA as an internal standard. Precision and accuracy were assessed to be within 10% for ppm-level concentrations by repeated measurements of KH-1 and KL2-G as independent standards. Results of the repeated "blind" standard results are present in Supplementary material Table G.

Two out of five samples only were suitable for bulk rock analyses. Major elements were determined by Wavelength Dispersive X-Ray Fluorescence Spectrometry (WDXRF) on pressed powder pellets at the Dipartimento di Fisica e di Scienze della Terra, Università di Ferrara (Italy), using an ARL Advant-XP spectrometer, following the full matrix correction method proposed by Traill and Lachance (1966). Accuracy is generally lower than 2% for major oxides.

References

Jochum, K.P., Stoll, B., Herwig, K., Willbold, M., Hofmann, A.W., et al., 2006. MPI-DING reference glasses for in situ microanalysis: new reference values for element concentrations and isotope ratios. Geochemistry Geophysics Geosystems 7.

Traill, R.J., Lachance, G.R., 1966. A practical solution to the matrix problem in X-ray analysis. Canadian Journal of Spectroscopy 11, 43-48.

On-line Supplementary material (Excel file)

Formatted: Justified

Major (wt.%) abundances of representative olivine (Table A), orthopyroxenes (Table B), clinopyroxenes (Table C) and spinel (Table D) in MG spinel peridotite xenoliths. Trace element (ppm) abundances of representative orthopyroxenes (Table E), clinopyroxenes (Table F) in MG spinel peridotite xenoliths. Table G: Standard used for LA-ICP-MS analyses. The values are in ppm.

Figure 1

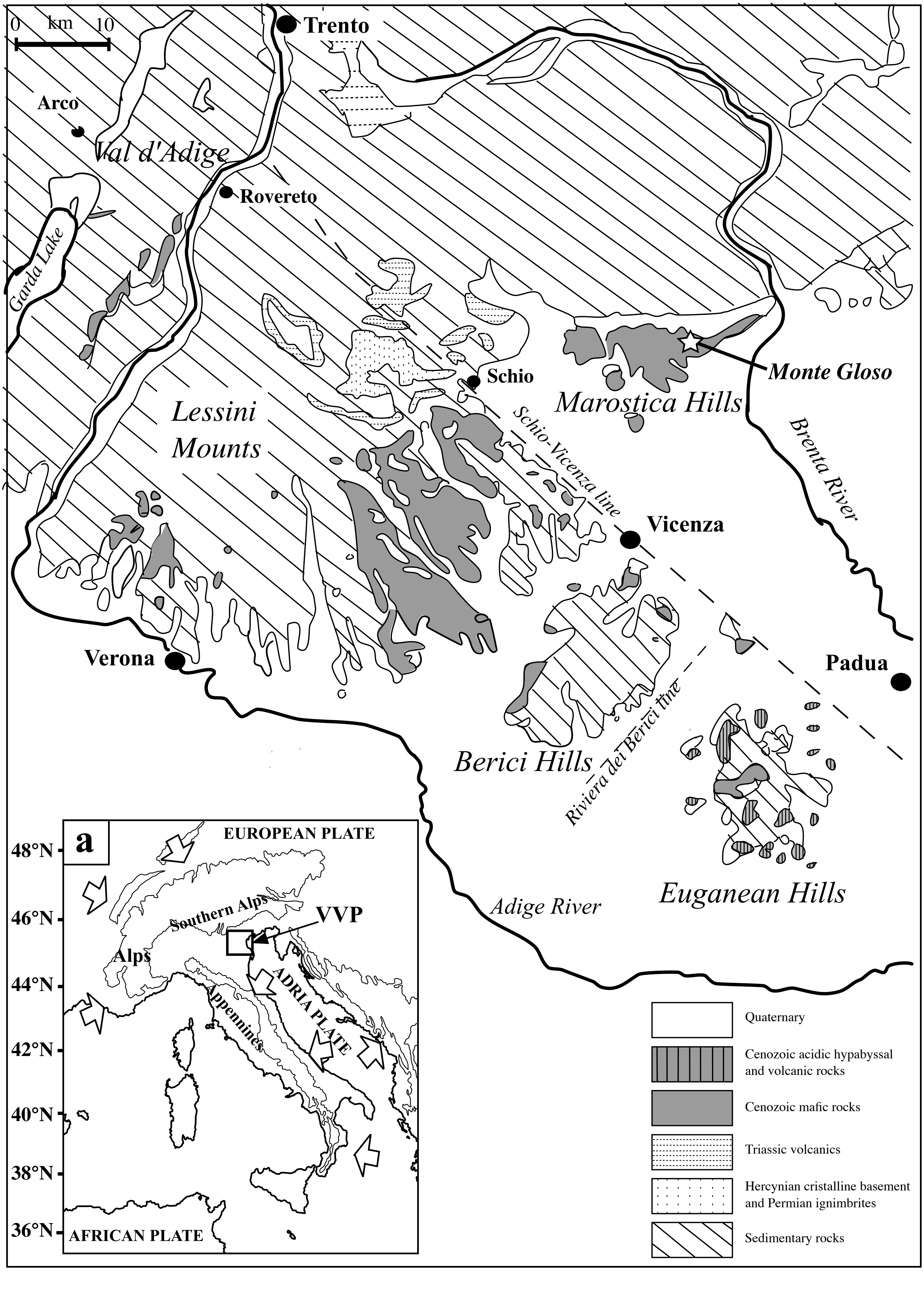
0 km 10
Trento
Arco
Val d'Adige
Rovereto
Garda Lake
Schio
Monte Gloso
Marostica Hills
Lessini
Mounts
Schio-Vicenza line
Brenta River
Vicenza
Verona
Padua
Berici Hills
Riviera dei Berici line
Euganean Hills
Adige River
a
EUROPEAN PLATE
48°N
46°N
44°N
42°N
40°N
38°N
36°N
Southern Alps
VVP
Alps
ADRIA PLATE
Appennines
AFRICAN PLATE
Quaternary
Cenozoic acidic hypabyssal and volcanic rocks
Cenozoic mafic rocks
Triassic volcanics
Hercynian cristalline basement and Permian ignimbrites
Sedimentary rocks

Figure 2

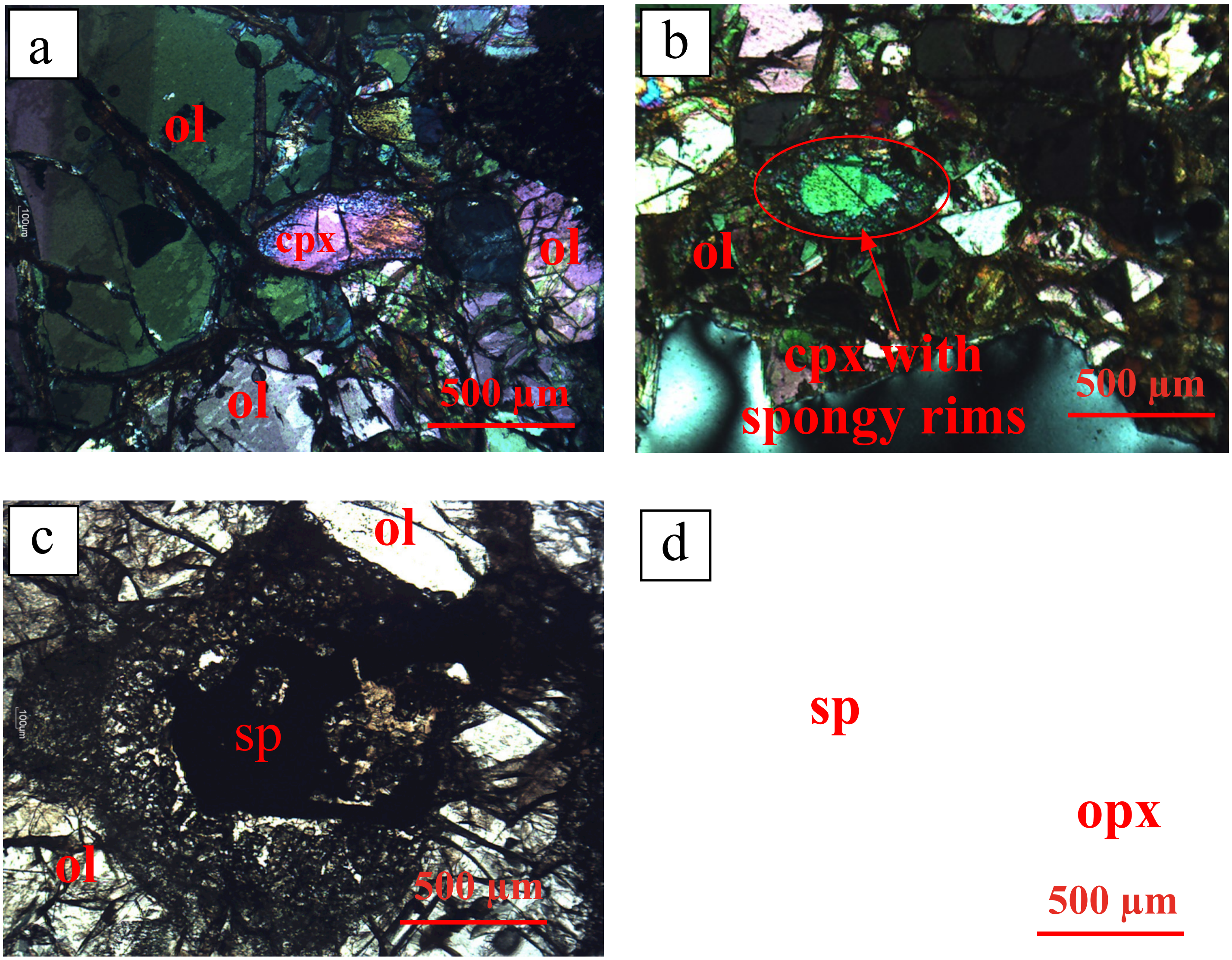

a
ol
cpx
ol
ol
500 µm
b
ol
cpx with
spongy rims
500 µm
c
ol
sp
ol
500 µm
d
sp
opx
500 µm

Figure 3

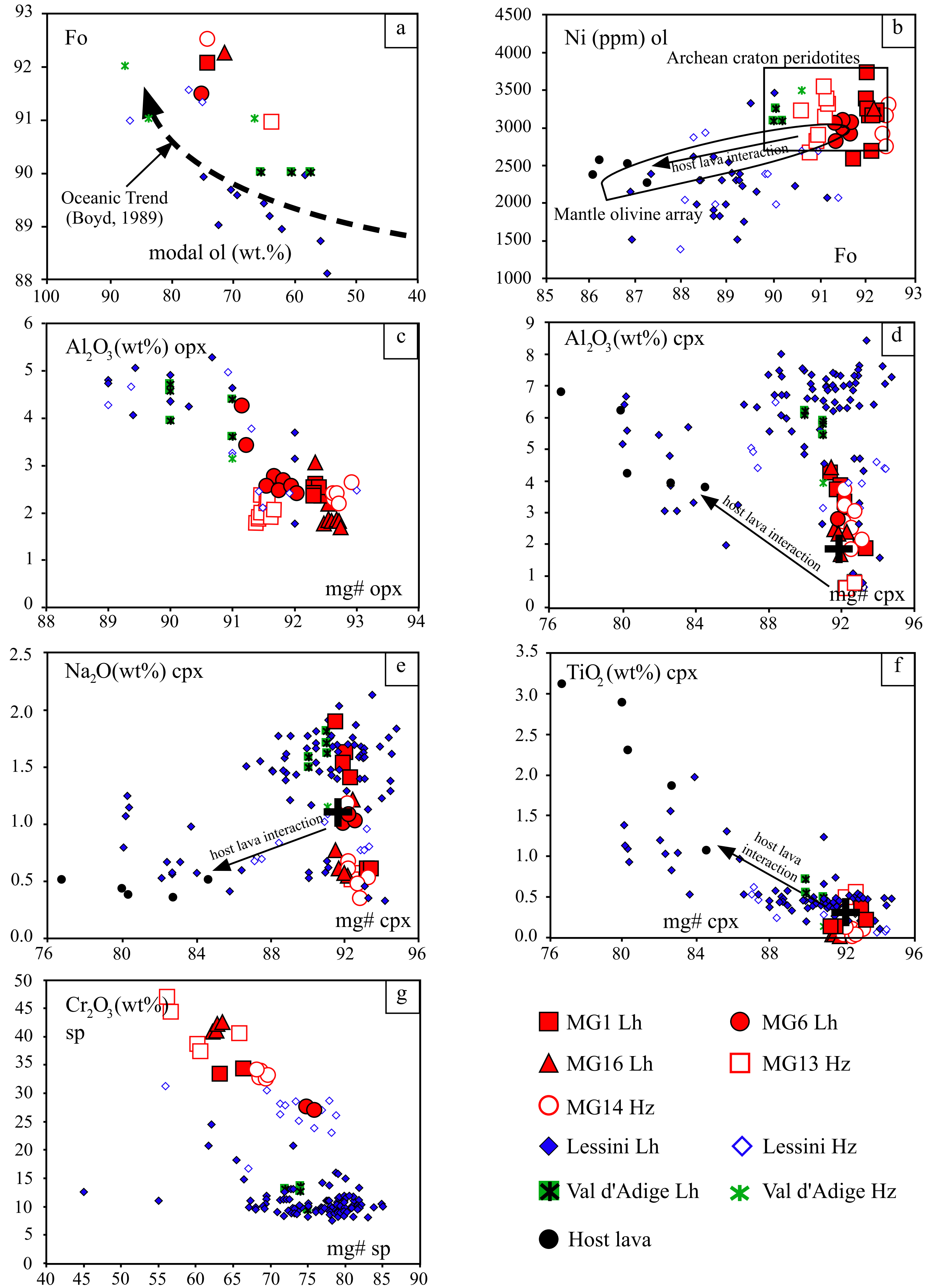

a
Fo
Oceanic Trend
(Boyd, 1989)
modal ol (wt.%)
b
Ni (ppm) ol
Archean craton peridotites
host lava interaction
Mantle olivine array
Fo
c
Al_2O_3(wt%) opx
mg# opx
d
Al_2O_3(wt%) cpx
host lava interaction
mg# cpx
e
Na_2O(wt%) cpx
host lava interaction
mg# cpx
f
TiO_2 (wt%) cpx
host lava interaction
mg# cpx
g
Cr_2O_3(wt%) sp
mg# sp
MG1 Lh
MG6 Lh
MG16 Lh
MG13 Hz
MG14 Hz
Lessini Lh
Lessini Hz
Val d'Adige Lh
Val d'Adige Hz
Host lava

Figure 4

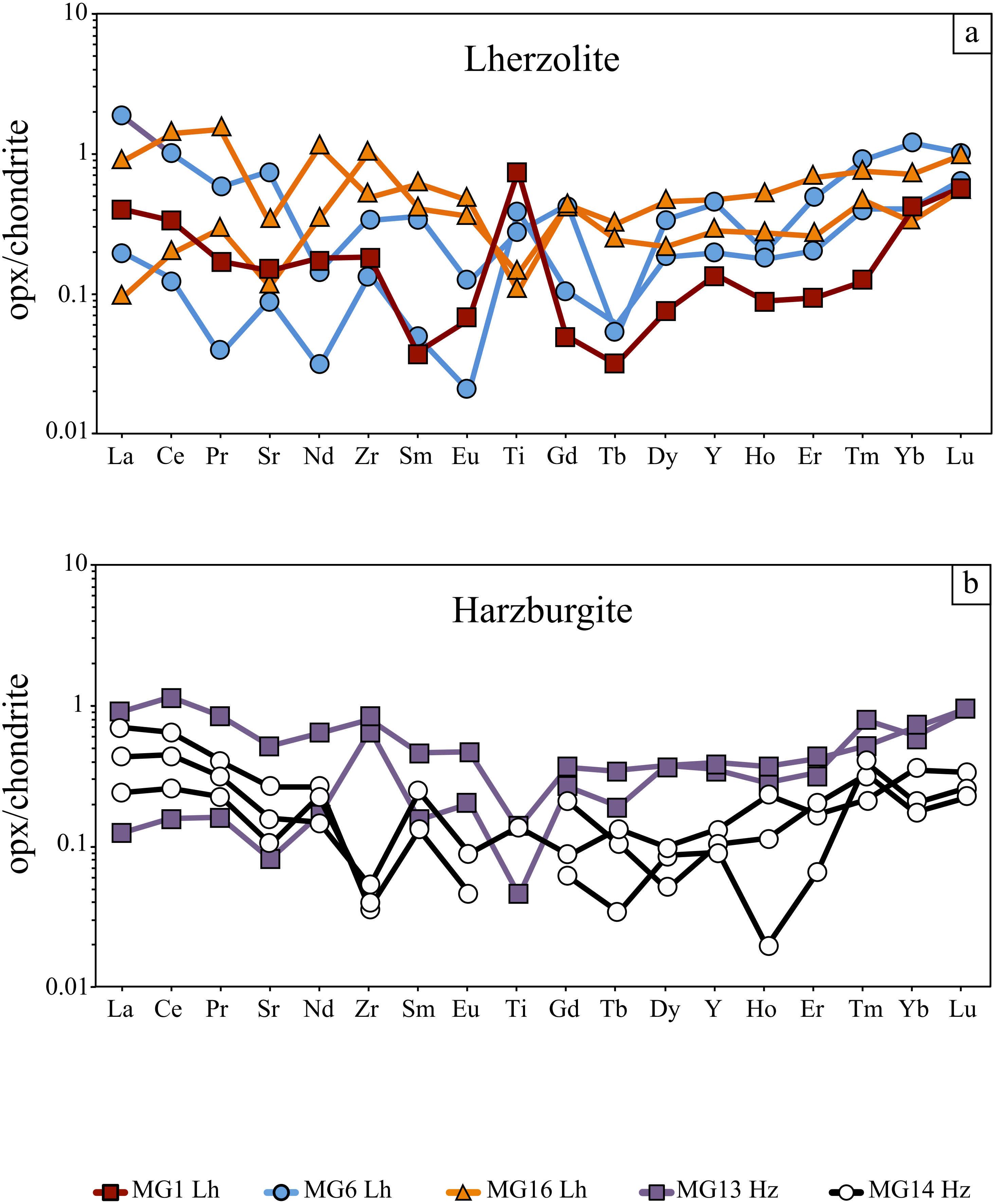
10
1
0.1
0.01
opx/chondrite
Lherzolite
a
La Ce Pr Sr Nd Zr Sm Eu Ti Gd Tb Dy Y Ho Er Tm Yb Lu
10
1
0.1
0.01
opx/chondrite
Harzburgite
b
La Ce Pr Sr Nd Zr Sm Eu Ti Gd Tb Dy Y Ho Er Tm Yb Lu
MG1 Lh
MG6 Lh
MG16 Lh
MG13 Hz
MG14 Hz

Figure 5

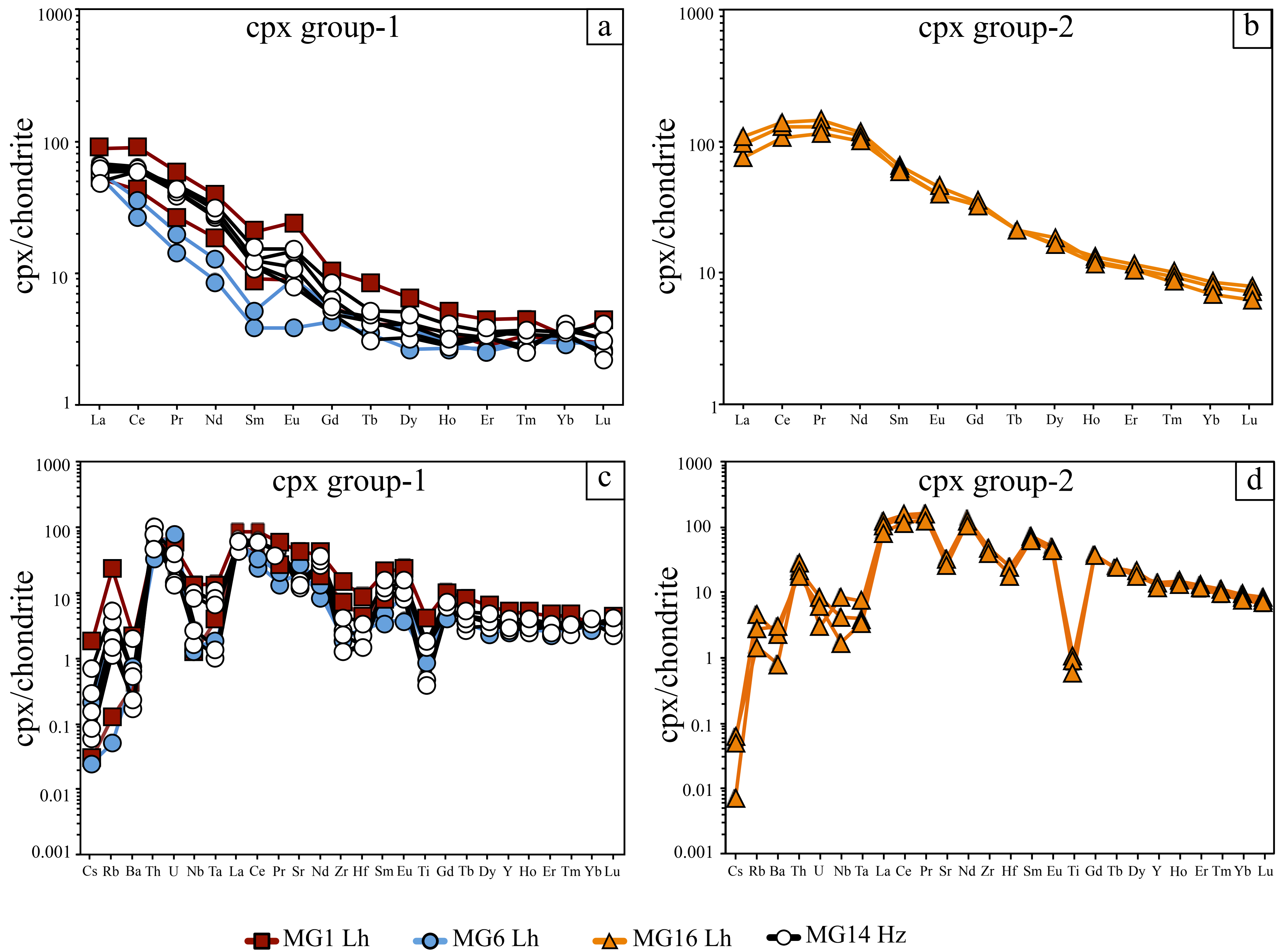
cpx group-1
a
cpx group-2
b
cpx group-1
c
cpx group-2
d
cpx/chondrite
1000
100
10
1
0.1
0.01
0.001
La Ce Pr Nd Sm Eu Gd Tb Dy Ho Er Tm Yb Lu
Cs Rb Ba Th U Nb Ta La Ce Pr Sr Nd Zr Hf Sm Eu Ti Gd Tb Dy Y Ho Er Tm Yb Lu
MG1 Lh
MG6 Lh
MG16 Lh
MG14 Hz

Figure 6

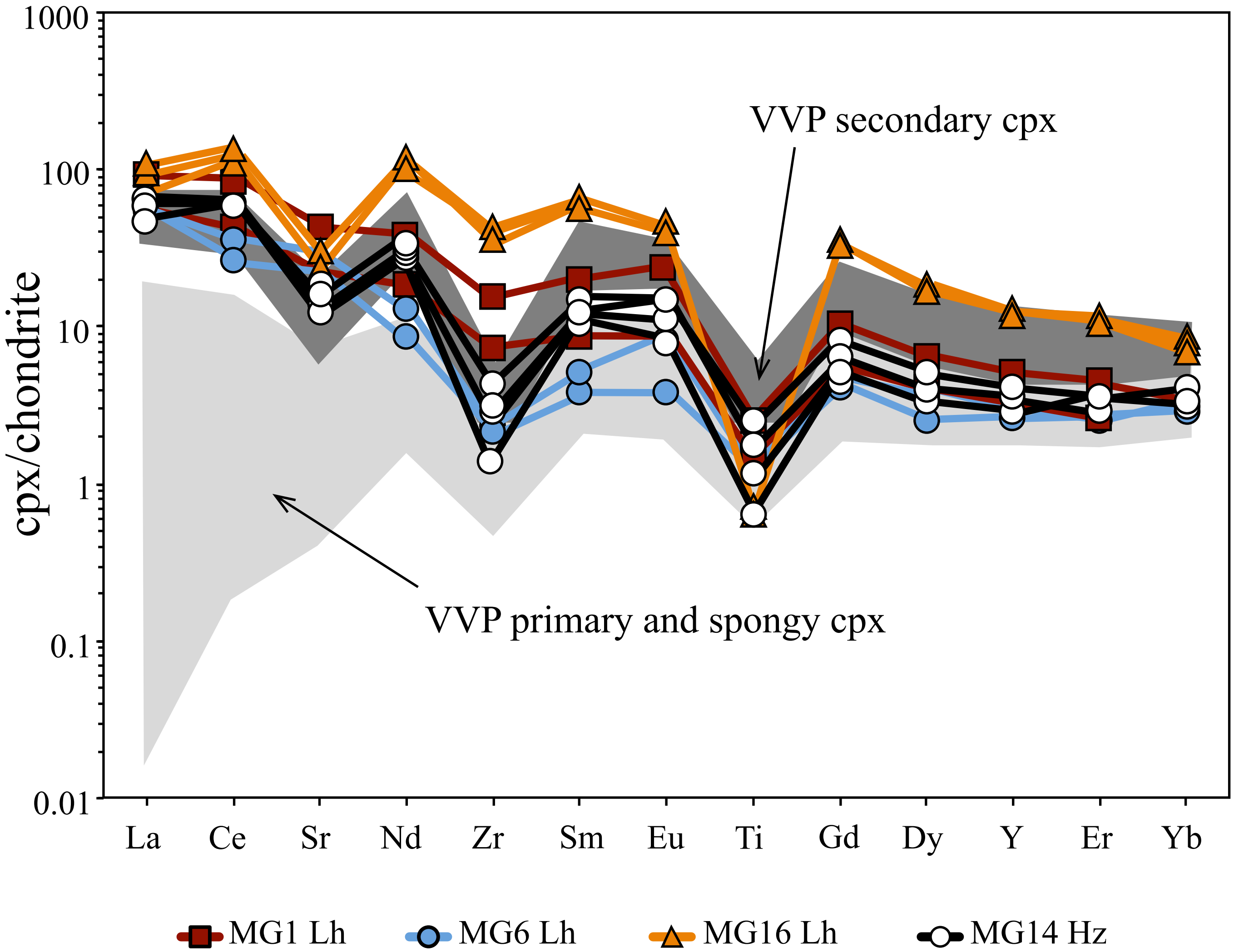

1000
100
10
1
0.1
0.01
cpx/chondrite
VVP secondary cpx
VVP primary and spongy cpx
La
Ce
Sr
Nd
Zr
Sm
Eu
Ti
Gd
Dy
Y
Er
Yb
MG1 Lh
MG6 Lh
MG16 Lh
MG14 Hz

Figure 7

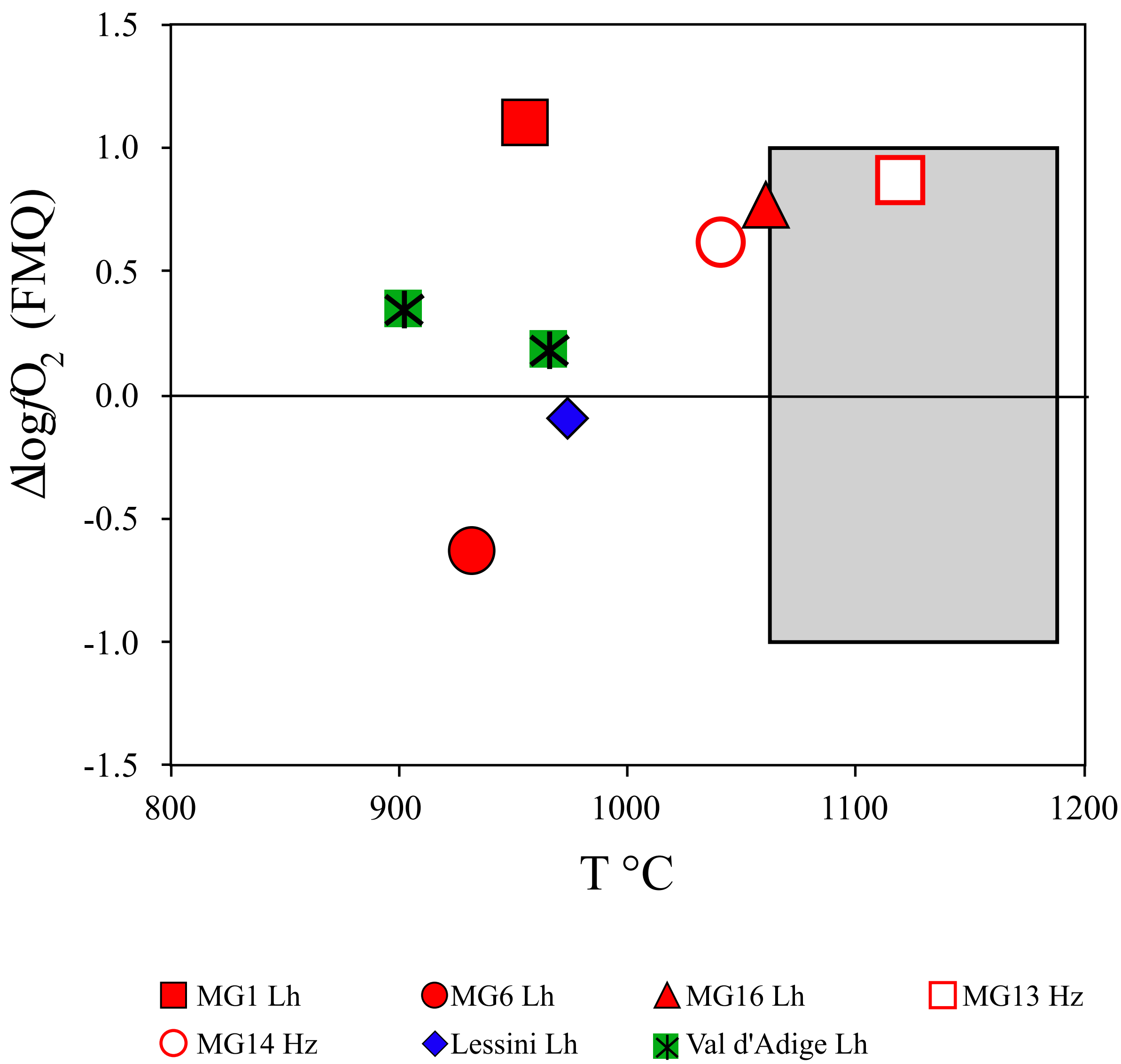

1.5
1.0
0.5
0.0
-0.5
-1.0
-1.5
ΔlogfO2 (FMQ)
800
900
1000
1100
1200
T °C
MG1 Lh
MG6 Lh
MG16 Lh
MG13 Hz
MG14 Hz
Lessini Lh
Val d'Adige Lh

Figure 8

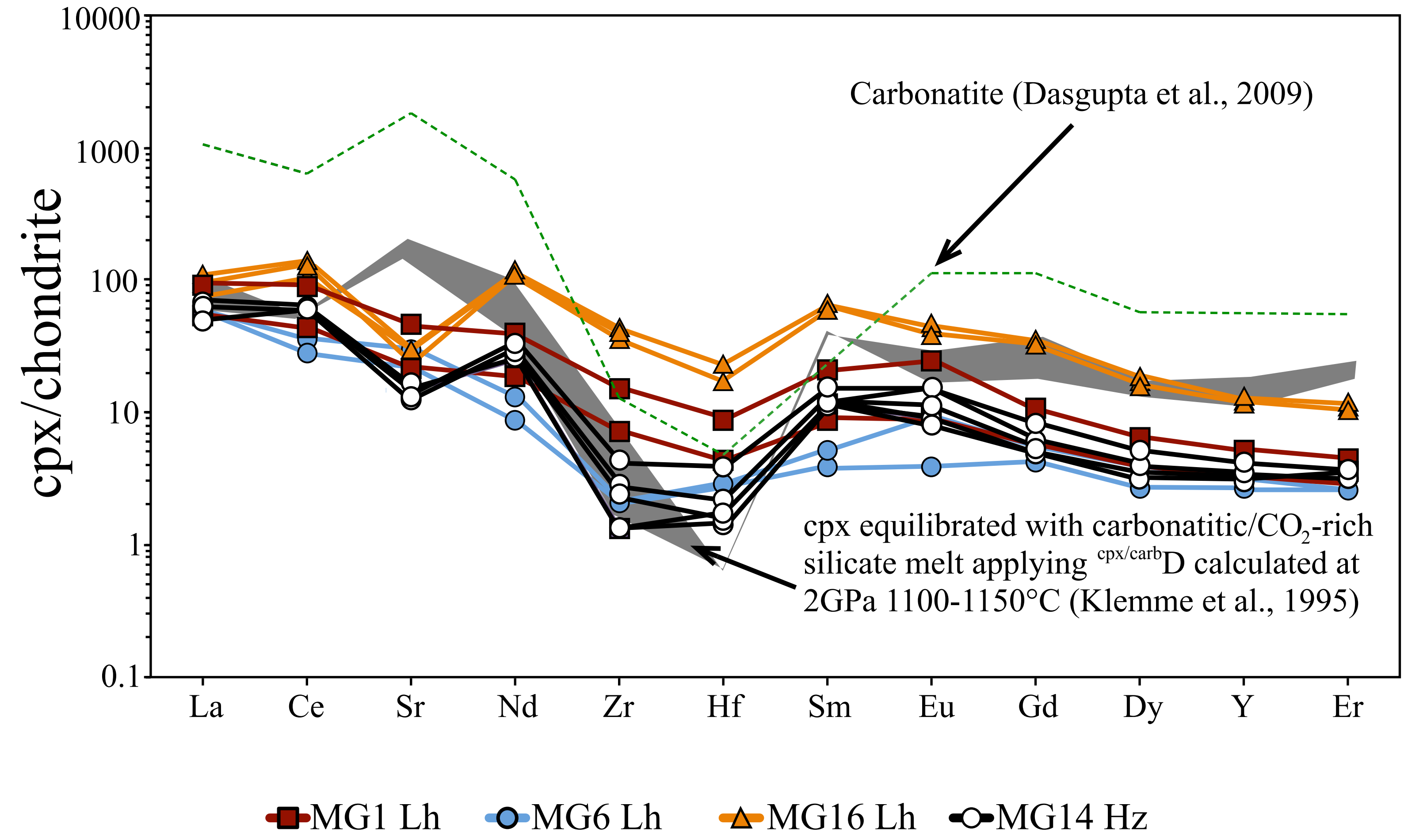

Carbonatite (Dasgupta et al., 2009)
cpx equilibrated with carbonatitic/CO2-rich silicate melt applying cpx/carbD calculated at 2GPa 1100-1150°C (Klemme et al., 1995)
cpx/chondrite
10000
1000
100
10
1
0.1
La
Ce
Sr
Nd
Zr
Hf
Sm
Eu
Gd
Dy
Y
Er
MG1 Lh
MG6 Lh
MG16 Lh
MG14 Hz

Figure 9

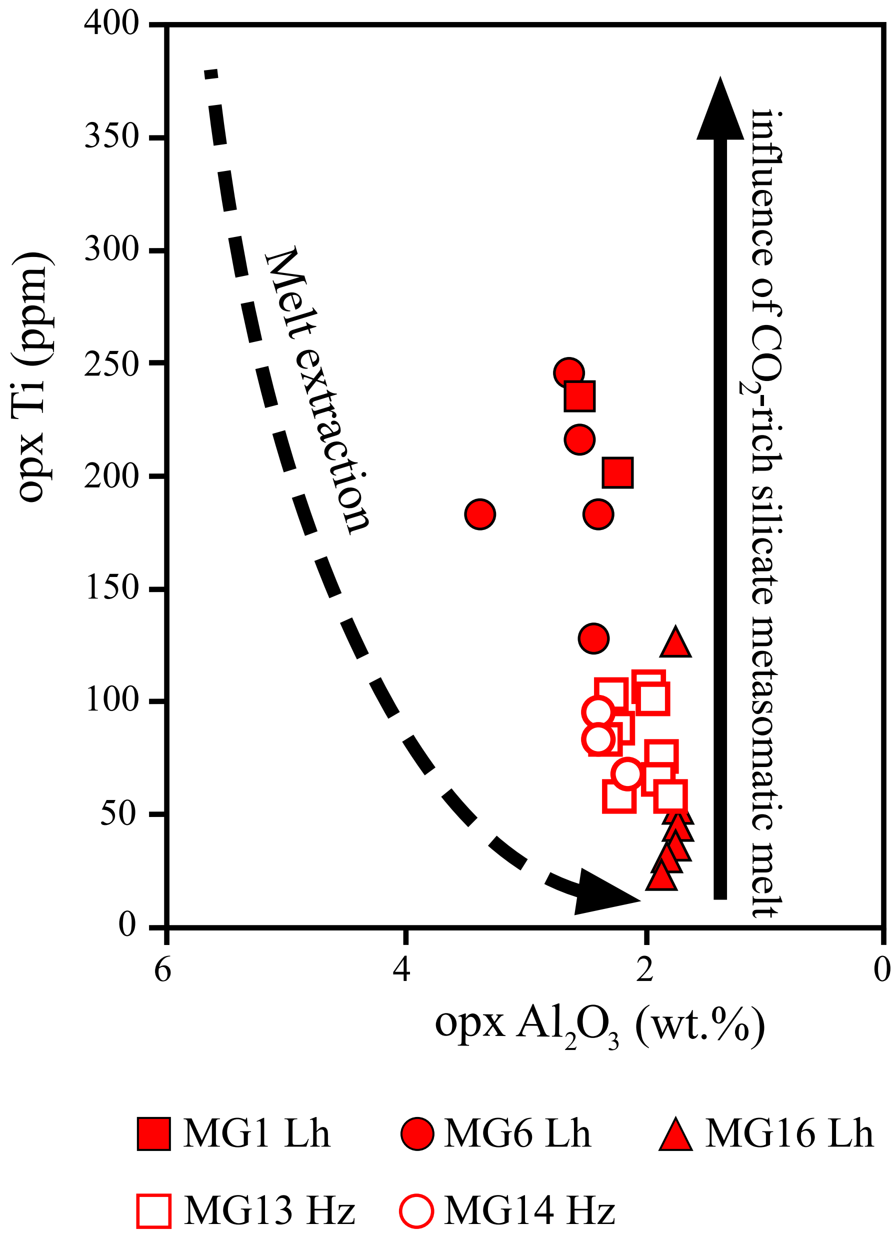

400
350
300
250
200
150
100
50
0
opx Ti (ppm)
6
4
2
0
opx Al_2O_3 (wt.%)
Melt extraction
influence of CO_2-rich silicate metasomatic melt
MG1 Lh
MG6 Lh
MG16 Lh
MG13 Hz
MG14 Hz

Figure 10

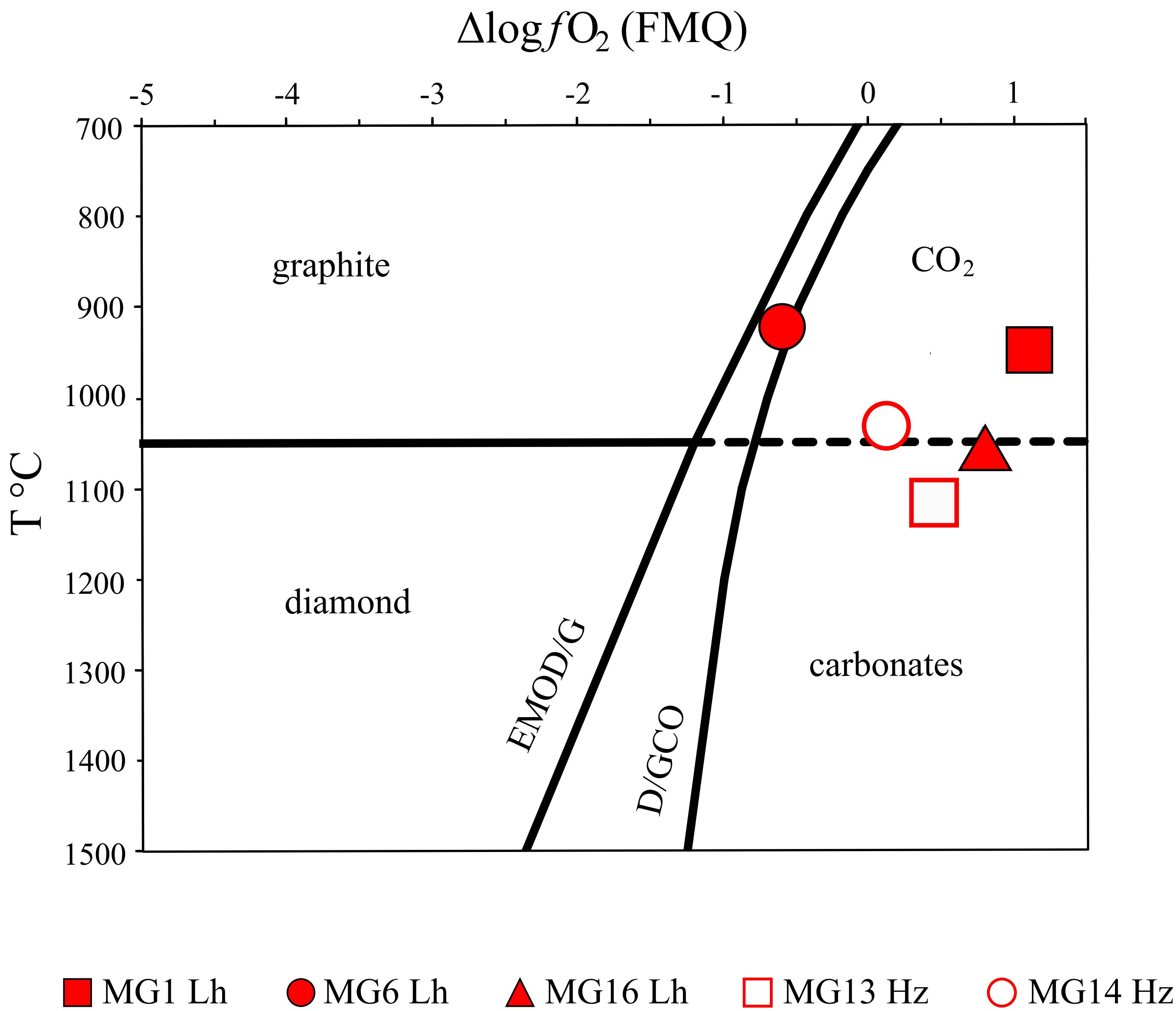

Δlog fO2 (FMQ)
-5
-4
-3
-2
-1
0
1
700
800
900
1000
1100
1200
1300
1400
1500
T °C
graphite
CO2
diamond
carbonates
EMOD/G
D/GCO
MG1 Lh
MG6 Lh
MG16 Lh
MG13 Hz
MG14 Hz

Figure

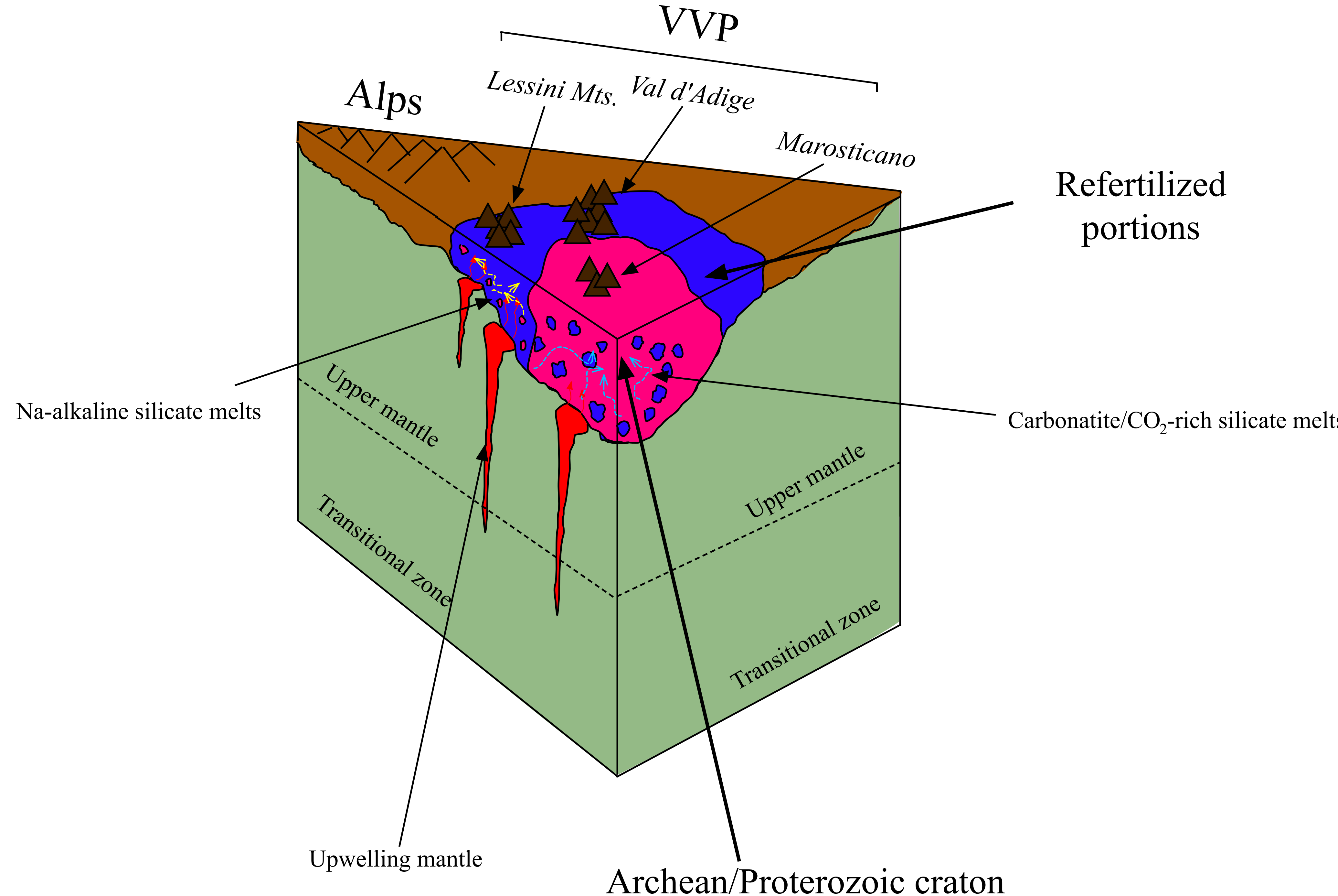

VVP
Alps
Lessini Mts.
Val d'Adige
Marosticano
Refertilized portions
Na-alkaline silicate melts
Carbonatite/CO2-rich silicate melts
Upper mantle
Transitional zone
Upper mantle
Transitional zone
Upwelling mantle
Archean/Proterozoic craton

Table 1: Modal composition (%) of MG spinel peridotite xenoliths.

	Lherzolites			Harzburgites	
Samples	MG1	MG6	MG16	MG13	MG14
Ol	73	74	70	63	73
Opx	12	14	20	31	19
Cpx	13	9	6	4	4
Sp	2	3	4	2	4
Gl	trace	trace		trace	trace
Alteration	trace	trace	trace	trace	trace

Ol= olivine; Opx= orthopyroxene; Cpx= clinopyroxene; Sp= spinel; Gl= glass.

Table
Click here to download Table: Brombin-REVISION 3 Table 2.docx

Table 2: Average temperature (T) and oxygen fugacity ~~(ΔlogfO_2)~~ for MG spinel-peridotites from Marosticano, ~~spinel-peridotites from~~ Val d'Adige and ~~spinel-lherzolites from~~ Lessini, calculated at 1.5 GPa. Estimated ~~Ts~~ are from geothermometers of Brey & Köhler (1990; T_{BK}), ~~of~~ Taylor (1998; T_T) and ~~of~~ Wells (1977; T_W). ~~Estimated~~ ΔlogfO_2 (FMQ) is ~~provided~~ from the method of Ballhaus et al. (1991) using T_{BK} ~~and a uniform equilibration pressure of 1.5 GPa~~. T_{BK} and ΔlogfO_2 (FMQ) of spinel-peridotites from Val d'Adige and Lessini were calculated ~~using EMP~~ data ~~from~~ Gasperini et al. (2006). CO_2 mole fractions are ~~calculated~~ by equation of Stagno and Frost (2010) using the estimated T_{BK} and ΔlogfO_2 (FMQ).

	n	**Average T_{BK} (°C)**	**2σ uncertainty T_{BK} (°C)**	**Average T_T (°C)**	**2σ uncertainty T_T (°C)**	**Average T_W (°C)**	**2σ uncertainty T_W (°C)**	**Average ΔlogfO_2 (FMQ)**	**2σ uncertainty ΔlogfO_2 (FMQ)**	**CO_2 mole fractions**
Sp-lherzolite (Marosticano)										
MG1	2	949	*36*	912	*60*	954	*46*	1.1	*0.00*	1.19
MG6	2	923	*25*	898	*12*	940	*12*	-0.6	*0.08*	0.02
MG16	2	1058	*21*	1022	*19*	1041	*10*	0.8	*0.08*	1.03
Sp-harzburgite (Marosticano)										
MG13	2	1117	*20*	1069	*22*	1109	*22*	0.9	*0.44*	1.85
MG14	3	1033	*30*	1010	*28*	1029	*29*	0.6	*0.12*	0.65
Sp-lherzolite (Val d'Adige)										
56B	1	902		836		914		0.3		
F56-7	1	966		888		956		0.2		
Sp-harzburgite (Val d'Adige)										
F56-5	1	896		842		909				
Sp-lherzolite (Lessini)										
25	1	975		969		998		-0.1		
25C	1	885		883		926				

n= number of analyses per sample.

Table 3: Major oxide (wt.%) abundances of MG lherzolites (Lh).

Sample	**MG 1**	**MG 6**
Host Rock	Lh	Lh
SiO_2	44.66	46.94
TiO_2	0.02	0.02
Al_2O_3	0.41	1.03
Fe_2O_3	0.00	0.00
FeO	7.44	8.15
MnO	0.11	0.12
MgO	45.72	42.61
CaO	1.57	1.12
Na_2O	0.00	0.00
K_2O	0.07	0.02
P_2O_5	0.00	0.00
Tot	100.00	100.00
mg#	91.64	90.31

Table
Click here to download Table: Brombin-REVISION 3-Supplementary material-.xlsx

Table A: Major oxide (wt.%) abundances of representative olivine in MG spinel peridotite xenolit

Sample	**MG1**	**MG1**	**MG1**	**MG1**	**MG1**	**MG1**
Lithology	Lh	Lh	Lh	Lh	Lh	Lh
SiO_2	40.87	41.08	41.04	39.82	40.19	40.71
FeO	7.83	7.84	8.28	8.08	7.95	7.91
MnO	0.15	0.09	0.12	0.12	0.14	0.11
MgO	51.58	51.25	51.07	51.84	51.74	51.08
CaO	0.04	0.06	0.05	0.05	0.09	0.07
NiO	0.41	0.46	0.33	0.43	0.34	0.4
Tot	100.96	100.83	100.92	100.42	100.61	100.44
Si	0.99	0.99	0.99	0.97	0.98	0.99
Fe	0.16	0.16	0.17	0.16	0.16	0.16
Mn	0.00	0.00	0.00	0.00	0.00	0.00
Mg	1.86	1.84	1.84	1.88	1.87	1.85
Ni	0.01	0.01	0.01	0.01	0.01	0.01
Fo	92.15	92.09	91.66	91.96	92.06	92.01

Abbreviations: Lh= lherzolite; Hz= harzburgite; b.d.l.= below detection limit.